NOAA OAR Special Report

PMEL Tsunami Forecast Series: Vol. 1
A Tsunami Forecast Model for Hilo, Hawaii

Liujuan Tang
Vasily V. Titov
Christopher D. Chamberlin

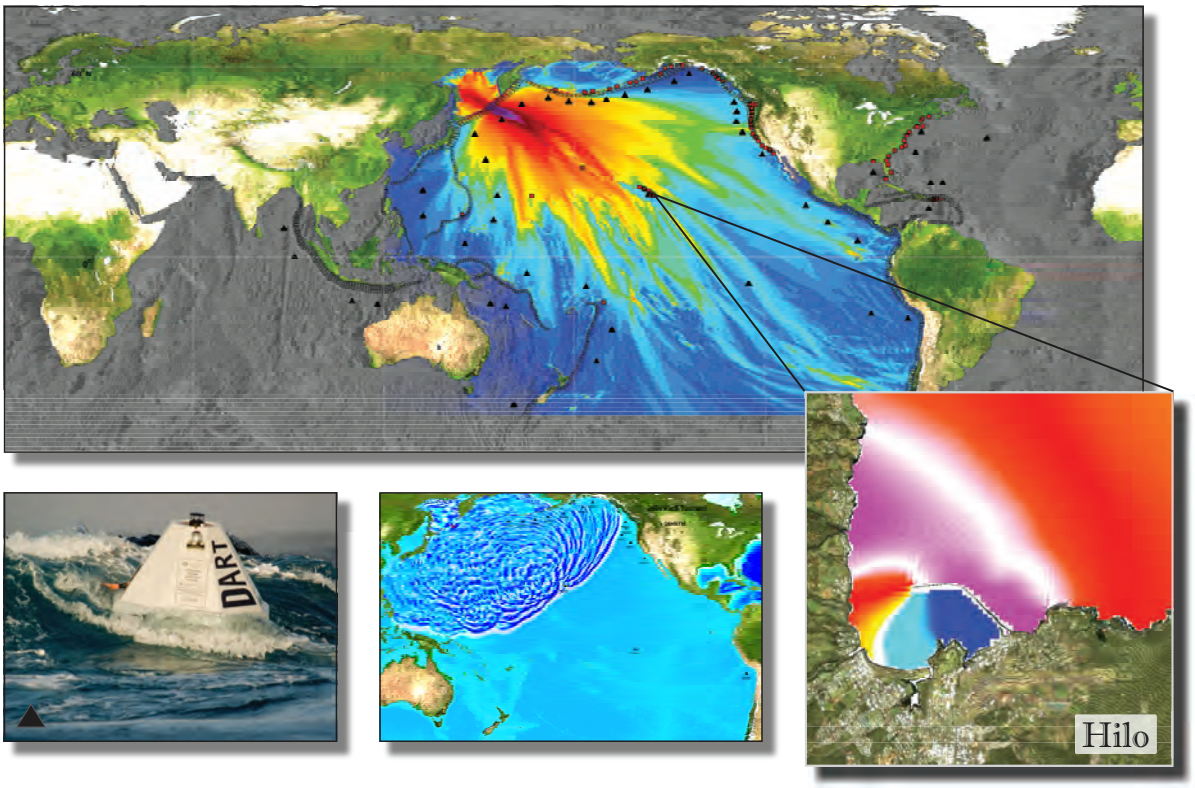

NOAA Center for Tsunami Research (NCTR)
Pacific Marine Environmental Laboratory

Front cover image: Overview of NOAA tsunami forecast system. Top frame illustrates components of the tsunami forecast using the 15 November 2006 Kuril Islands tsunami as an example: DART systems (black triangles), pre-computed tsunami source function database (unfilled black rectangles) and high-resolution forecast models in the Pacific, Atlantic, and Indian oceans (red squares). Colors show computed maximum tsunami amplitudes of the off-shore forecast. Black contour lines indicate tsunami travel times in hours. Lower panels show the forecast process sequence left to right: tsunami detection with the DART system (third generation DART ETD is shown); model propagation forecast based on DART observations; coastal forecast with high-resolution tsunami inundation model.

PDF versions of the PMEL Tsunami Forecast Series reports are available at
`http://nctr.pmel.noaa.gov/forecast_reports`

NOAA OAR Special Report

PMEL Tsunami Forecast Series: Vol. 1
A Tsunami Forecast Model for Hilo, Hawaii

Liujuan Tang[1,2], Vasily V. Titov[2], and Christopher D. Chamberlin[1,2]

[1]Joint Institute for the Study of the Atmosphere and Ocean (JISAO), University of Washington, Seattle, WA
[2]NOAA/Pacific Marine Environmental Laboratory (PMEL), Seattle, WA

March 2010

UNITED STATES DEPARTMENT OF COMMERCE

Gary Locke
Secretary

NATIONAL OCEANIC AND ATMOSPHERIC ADMINISTRATION

Jane Lubchenco
Under Secretary for Oceans and Atmosphere/Administrator

Office of Oceanic and Atmospheric Research

Craig McLean
Assistant Administrator

NOTICE from NOAA

Mention of a commercial company or product does not constitute an endorsement by NOAA/OAR. Use of information from this publication concerning proprietary products or the tests of such products for publicity or advertising purposes is not authorized. Any opinions, findings, and conclusions or recommendations expressed in this material are those of the authors and do not necessarily reflect the views of the National Oceanic and Atmospheric Administration.

Contribution No. 3340 from NOAA/Pacific Marine Environmental Laboratory
Contribution No. 1766 from Joint Institute for the Study of the Atmosphere and Ocean (JISAO)

Also available from the National Technical Information Service (NTIS)
(http://www.ntis.gov)

Contents

List of Figures

List of Tables

Foreword

Tsunamis have been recognized as a potential hazard to United States coastal communities since the mid-twentieth century, when multiple destructive tsunamis caused damage to the states of Hawaii, Alaska, California, Oregon, and Washington. In response to these events, the United States, under the auspices of the National Oceanic and Atmospheric Administration (NOAA), established the Pacific and Alaska Tsunami Warning Centers, dedicated to protecting United States interests from the threat posed by tsunamis. NOAA also created a tsunami research program at the Pacific Marine Environmental Laboratory (PMEL) to develop improved warning products.

The scale of destruction and unprecedented loss of life following the December 2004 Sumatra tsunami served as the catalyst to refocus efforts in the United States on reducing tsunami vulnerability of coastal communities, and on 20 December 2006, the United States Congress passed the "Tsunami Warning and Education Act" under which education and warning activities were thereafter specified and mandated. A "tsunami forecasting capability based on models and measurements, including tsunami inundation models and maps…" is a central component for the protection of United States coastlines from the threat posed by tsunamis. The forecasting capability for each community described in the *PMEL Tsunami Forecast Series* is the result of collaboration between the National Oceanic and Atmospheric Administration office of Oceanic and Atmospheric Research, National Weather Service, National Ocean Service, National Environmental Satellite, Data, and Information Service, the University of Washington's Joint Institute for the Study of the Atmosphere and Ocean, National Science Foundation, and United States Geological Survey.

NOAA Center for Tsunami Research

PMEL Tsunami Forecast Series: Vol. 1
A Tsunami Forecast Model for Hilo, Hawaii

L. Tang[1,2], V.V. Titov[2], and C.D. Chamberlin[1,2]

Abstract. This study describes the development, validation, and testing of a tsunami forecast model for Hilo, Hawaii. Based on the Method of Splitting Tsunamis (MOST) model, the forecast model is capable of simulating 4 hr of tsunami wave dynamics at a resolution of 2 arc sec (~60 m) in 10 min of computational time. A reference inundation model at a higher resolution of 1/3 arc sec (~10 m) was also developed in parallel, to provide modeling references for the forecast model. Both models were tested for 16 past tsunamis and a set of 18 simulated magnitude 9.3 tsunamis.

The error of the maximum wave height computed by the forecast model is within 35% when the observation is greater than 0.5 m; when the observation is below 0.5 m the error is less than 0.3 m. The error of the modeled arrival time of the first peak is within ±3% of the travel time. The good agreement between the model computations and observations, along with the numerical consistency between the model results for the maximum amplitude and velocity, provide a quantitative validation and reliable robustness and stability testing of the forecast model.

The validated Hilo forecast model was further applied to hazard assessment from 1435 scenarios of simulated tsunami events based on subduction zone earthquakes of magnitude 7.5, 8.2, 8.7, and 9.3 in the Pacific Ocean basin. The results show an impressive local variability of tsunami amplitudes even for far-field tsunamis, and indicate the complexity of forecasting tsunami amplitudes at a coastal location. It is essential to use high-resolution models in order to provide accuracy that is useful for the practical guidance of coastal tsunami forecasts.

1. Background and Objectives

The National Oceanic and Atmospheric Administration (NOAA) Center for Tsunami Research at NOAA's Pacific Marine Environmental Laboratory (PMEL) has developed a tsunami forecasting system for operational use by NOAA's two Tsunami Warning Centers, located in Hawaii and Alaska (Titov *et al.*, 2005; Titov, 2009). The forecast system combines real-time deep-ocean tsunami measurements from Deep-ocean Assessment and Reporting of Tsunami (DART) buoys (González *et al.*, 2005; Bernard *et al.*, 2006; Bernard and Titov, 2007) with the Method of Splitting Tsunami (MOST) model, a suite of finite difference numerical codes based on nonlinear long-wave approximation (Titov and Synolakis, 1998; Titov and González, 1997; Synolakis *et al.*, 2008) to produce real-time forecasts of tsunami arrival time, heights, periods, and inundation. To achieve an accurate and detailed forecast of tsunami impact for specific sites, high-resolution tsunami forecast models are under development for United States coastal communities at risk (Tang *et al.*, 2008b; 2009). The resolution of these models has to be high enough to resolve the dynamics of a tsunami inside a particular harbor, including influences of major harbor structures such as breakwaters. These models have been integrated as crucial components into the forecast system.

[1]Joint Institute for the Study of the Atmosphere and Ocean (JISAO), University of Washington, Seattle, WA

[2]NOAA/Pacific Marine Environmental Laboratory (PMEL), Seattle, WA

Hilo, Hawaii's history of tsunami inundation (Dudley and Stone, 2000; Pararas-Carayannis, 1969) concentrated population density, year-round tourism, and transportation infrastructure all contribute to making it a crucial forecast model for tsunami inundation (**Figure 1**). Hilo is often impacted by tsunamis generated in many tectonic regions of the Pacific Ocean Basin. The city downtown was devastated when the 1946 Unimak tsunami generated south of Unimak Island along the Aleutian Trench struck the Hawaiian Islands. It was again badly damaged when, in 1960, a tsunami generated off the coast of Chile traversed the Pacific Ocean. Hilo was chosen as the pilot site for testing of coastal tsunami forecasting beginning in the late 1990s. The 17 November 2003 Rat Island tsunami provided the first real-time test of the Hilo forecast model, along with NOAA's forecast methodology, which became the proof of concept for the development of the tsunami forecast system (Titov *et al.*, 2005). This tsunami was detected by three DART buoys located along the Aleutian Trench. The real-time data were combined with the tsunami source function database to produce a tsunami source of T_{Mw} 7.8 by inversion. The offshore model scenario was used as input for the Hilo forecast model, which was the only forecast model available at that time. The forecasted maximum wave height at Hilo tide station is 0.43 m, while the observation is 0.45 m (–5% error); the error of the arrival time of the maximum wave is less than 1 min. The accuracy of the forecast is reflected by the excellent agreement between the model prediction and observation. It was the first time in history that a forecast of a tsunami time series was available to a coastal city before tsunami waves arrived. Since then, the model was updated with the newest bathymetry and topography data sources and produced accurate real-time forecasting for several past tsunamis (Wei *et al.*, 2008; Titov, 2009).

This report describes the development, testing, and application of the Hilo forecast model. The objective in developing this model is to provide NOAA's Tsunami Warning Centers the ability to assess danger posed to Hilo following tsunami generation in the Pacific Ocean Basin with a goal to provide accurate and timely forecasts to enable the community to respond appropriately. A secondary objective is to explore the potential tsunami impact to the city from earthquakes at major subduction zones in the Pacific by using the developed forecast model.

The report is organized as follows. Section 2 briefly introduces NOAA's tsunami forecast methodology. Section 3 describes the model development. Section 4 presents the results and discussion, which includes sensitivity of the forecast model to grid coupling schemes, model validation, verification, and testing for past and simulated tsunamis. A tsunami hazard assessment study utilizing the validated forecast model is also included. A summary and conclusion are provided in section 5.

2. Forecast Methodology

NOAA's real-time tsunami forecasting scheme is a two-step process: (1) construction of a tsunami source via inversion of deep-ocean DART observations with pre-computed tsunami source functions; and (2) coastal predictions by running high-resolution forecast models in real time (Titov *et al.*, 1999; 2005; Tang *et al.*, 2009). The DART-constrained tsunami source, the corresponding offshore scenario from the tsunami source function database, and high-resolution forecast models cover the entire cycle of earthquake-generated tsunamis, generation, propagation, and coastal inundation, providing a complete tsunami forecast capability.

2.1 Construction of a tsunami source based on DART observations and tsunami source functions

Several real-time data sources, including seismic data, coastal tide gauge, and deep-ocean data have been used for tsunami warning and forecast (Satake *et al.*, 2008; Whitmore, 2003; Titov, 2009). NOAA's strategy for the real-time forecasting is to use deep-ocean measurements at DART buoys as the primary data source due to several key features. (1) The buoys provide a direct measure of tsunami waves, unlike seismic data, which is an indirect measure of tsunamis. (2) The deep-ocean tsunami measurements are in general the earliest tsunami information available, since tsunamis propagate much faster in the deep ocean than in shallow coastal areas where coastal tide gauges are used for tsunami measurements. (3) Compared to coastal tide gauges, DART data with a high signal-to-noise ratio can be obtained without interference from harbor and local shelf effects. (4) The linear process of tsunamis in the deep ocean allows for the application of efficient inversion schemes.

Time series of tsunami observations in the deep ocean can be decomposed into a linear combination of a set of tsunami source functions in the time domain by a linear least squares method. We call coefficients obtained through this inversion process tsunami source coefficients. The magnitude computed from the sum of the moment of tsunami source functions multiplied by the corresponding coefficients is referred to as the *tsunami moment magnitude* (T_{Mw}), to distinguish it from the *seismic moment magnitude* M_w, which is the magnitude of the associated earthquake source. While the seismic and tsunami sources are in general not the same, this approach provides a link between the seismically derived earthquake magnitude and the tsunami observation-derived tsunami magnitude.

During a real-time tsunami forecast, seismic waves propagate much faster than tsunami waves, so the initial seismic magnitude can be estimated before the DART measurements are available. Since time is of the essence, the initial tsunami forecast is based on the seismic magnitude only. The T_{Mw} will update

the forecast when it is available via DART inversion using the tsunami source function database.

Titov *et al.* (1999; 2001) conducted sensitivity studies of far-field deep-water tsunamis to different parameters of the elastic deformation model described in Gusiakov (1978) and Okada (1985). The results showed that source magnitude and location essentially define far-field tsunami signals for a wide range of subduction zone earthquakes. Other parameters have secondary influence and can be pre-defined during forecast. Based on these results, tsunami source function databases for the Pacific, Atlantic, and Indian oceans have been built using pre-defined source parameters, length = 100 km, width = 50 km, slip = 1 m, rake = 90 and rigidity = 4.5×10^{10} N/m^2. Other parameters are location-specific; details of the databases are described in Gica *et al.* (2008). Pacific Ocean unit sources are provided in **Appendix B**. Each tsunami source function is equivalent to a tsunami from a typical Mw = 7.5 earthquake with defined source parameters. **Figure 2** shows the locations of tsunami source functions in the Pacific Ocean.

The database can provide offshore forecasts of tsunami amplitudes and all other wave parameters immediately once the inversion is complete. The tsunami source, which combines real-time tsunami measurements with tsunami source functions, provides an accurate offshore tsunami scenario without additional time-consuming model runs.

2.2 Real-time coastal predictions by high-resolution forecast models

High-resolution forecast models are designed for the final stage of the evolution of tsunami waves: coastal runup and inundation. Once the DART-constrained tsunami source is obtained (as a linear combination of tsunami source functions), the pre-computed time series of offshore wave height and depth-averaged velocity from the model propagation scenario are applied as the dynamic boundary conditions for the forecast models. This saves the simulation time of basin-wide tsunami propagation. Tsunami inundation is a highly nonlinear process, therefore a linear combination would not, in general, provide accurate solutions. A high-resolution model is also required to resolve shorter tsunami wavelengths nearshore with accurate bathymetric/topographic data. The forecast models are constructed with the Method of Splitting Tsunami (MOST) model, a finite difference tsunami inundation model based on nonlinear shallow-water wave equations (Titov and González, 1997). Each forecast model contains three telescoping computational grids with increasing resolution, covering regional, intermediate, and nearshore areas. Runup and inundation are computed at the coastline. The highest-resolution grid includes the population center and tide stations for forecast verification. The grids are derived from the best available bathymetric/topographic data at the time of development, and will be updated as new survey data become available.

The forecast models are optimized for speed and accuracy. By reducing the computational areas and grid resolutions, each model is optimized to provide 4-hr event forecasting results in minutes of computational time using a single

processor, while still providing good accuracy for forecasting. To ensure forecast accuracy at every step of the process, the model outputs are validated with historical tsunami records and compared to numerical results from a reference inundation model with higher resolutions and larger computational domains. In order to provide warning guidance for a long duration during a tsunami event, each forecast model has been tested to output up to a 24-hr simulation after the tsunami generation.

3. Model Development

3.1 Forecast area and tsunami data

The main Hawaiian Islands are the youngest and are located at the southern portion of the Hawaii Archipelago. From northeast to southwest, the islands form four natural geographic groups by shared channels and inter-island shelves, including (1) Ni'ihau, Ka'ula Rock, and Kauai (Kauai complex) (2) Oahu, (3) Molokai, Maui, Lanai, and Kaho'olawe (the Maui Complex), and (4) Hawaii.

Hilo is located on the east coast of the Big Island of Hawaii. The port of Hilo is one of the two deep draft harbors on the island. **Figure 3** shows an aerial photo of Hilo with a breakwater in Hilo Bay. The city is the second most populous of all Hawaiian Island cities and the most densely populated on the island of Hawaii itself, as shown in **Figure 4**. A National Ocean Service (NOS) tide station in Hilo Harbor was established in November 1946. The present installation was in February 1989 (`http://tidesandcurrents.noaa.gov/`). The water level sensor is located in the vicinity of Pier 2. At the sensor, the mean tidal range (MN) is 0.508 m. Mean high water level (MHW) is 1.795 m, and mean sea level (MSL) is 1.545 m. Mean high water is used as the reference level for the forecast model to provide a worst case for inundation forecast.

Hilo has a long history of being impacted by destructive tsunamis (Pararas-Carayannis, 1969; NGDC, 2009). The earliest record of a destructive tsunami at Hilo occurred on 7 November 1837, which was generated by a magnitude 8.5 earthquake in South Chile (NGDC). In Hilo, "Lowlands were submerged, houses were swept away, and 14 people were killed" (Pararas-Carayannis, 1969). The first wave of 6.1 m above high-water mark was observed in Hilo Bay. On 13 August 1868, a tsunami generated by a magnitude 8.5 earthquake in North Chile caused severe damage in Hilo. The watermark left on a coconut tree near the railway station measured 4.6 m above the ordinary low water and 1.4 m above ground. On 10 May 1877, a magnitude 8.3 earthquake in North Chile generated a tsunami that caused severe damage in Hilo. The tsunami water height was reported to be 3.7 m above the low watermark. Every house within 92 m of the beach at Waiakea was swept away. The total extent of human and property impact to the Hilo area included 5 dead, 17 badly injured, and 37 houses destroyed. Total damage was estimated at $12,000 to $14,000 (Pararas-Carayannis, 1969). On 31 January 1906, a tsunami generated by a magnitude 8.8 earthquake off the coast of Ecuador flooded the wharf and a tsunami wave of 3.6 m above normal was visually observed. The 3 February 1923 Kamchatka tsunami generated by a magnitude 8.3 earthquake was reported as having water as high as 6.1 m above mean low sea level at the mouth of Wailoa River. The bridge was destroyed, houses and wharves were badly damaged, and one man was killed.

The tsunami on 1 April 1946 was considered the most destructive tsunami that ever hit the Hawaiian Islands in terms of loss of life and property (Pararas-Carayannis, 1969). It was generated by an earthquake of magnitude 8.5 in the Aleutian Islands. The tsunami claimed the lives of 159 people in the State of Hawaii (122 from the Big Island) and caused $26 million in damage (**Figure 1a–e**). In Hilo, 488 buildings were demolished and 936 were damaged. The Hilo tide gauge was destroyed. Pier 1 was washed by the third wave, which was the highest (Pararas-Carayannis, 1969). This earthquake prompted the establishment of NOAA's first Tsunami Warning Center in Ewa Beach on the southern shore of Oahu.

On 4 November 1952, a tsunami originating in Kamchatka caused moderate property damage of about $0.4 million in Hilo. All damage at Hilo was the result of gentle flooding. A 0.45-m bore was reported in Wailoa estuary only. On 9 March 1957, an Aleutian tsunami caused an estimated $300,000 damage in Hilo and total damage of $5 million for the Hawaiian Islands. Buildings along the Hilo waterfront were badly damaged.

The 23 May 1960 Chile tsunami caused heavy damage in Hilo. Sixty-one people were killed, 282 injured, and 537 buildings were destroyed (**Figure 1f**). A total damage of $23 million was estimated. The highest wave was seen as a wall of water about 6.1-m high moving toward the city, with a roar that was heard offshore. This wave knocked out the power lines and inundated 600 acres in the harbor area. Rocks weighing as much as 22 tons were washed 182 m inland from the seawall. The period of waves after the third became shorter. The tsunami continued across the Pacific and struck Japan 7 hr later, killing 142 people.

The latest destructive tsunami was generated by the Great Alaska Earthquake of 27 March 1964, which caused $15,000 damage in Hilo. As a population center that has been repeatedly damaged by Pacific tsunamis, Hilo is in need of a forecast model to aid site-specific evacuation decisions.

Tsunami water level data are available for 14 of the 16 tsunamis (**Table 1**) in this study, while the tide station was either damaged or not functional during the 1946, 1957, and 1960 tsunamis. The recorded maximum wave height is 3.84 m during the 1964 Alaska tsunami. The maximum recorded runup heights at Hilo are 9.1, 3.9, 10.6, and 3.0 m for the 1946, 1957, 1960, and 1964 tsunamis, respectively (Pararas-Carayannis, 1969). Inundation data are available for the 1946, 1957, and 1960 tsunamis in the area (Shepard *et al.*, 1950; Fraser *et al.*, 1959).

3.2 Bathymetry and topography

Tsunami inundation modeling requires accurate bathymetry in the coastal area as well as high-resolution topography and bathymetry in the nearshore area. Digital elevation models (DEMs) were developed at a medium resolution of 6 arc sec (180 m) covering all of the major Hawaiian Islands (**Figure 5**), and a high resolution of 1/3 arc sec (10 m) covering the east Hawaii area around Hilo (**Figure 6**). Both grids include topographic and bathymetric elevations. The

Table 1: Tsunami sources for 16 historical tsunamis.

Event	Earthquake Date Time (UTC)	Lat. (°)	Lon. (°)	Subduction Zone	Seismic Moment Magnitude (Mw)	Tsunami Magnitude[1]	Model Tsunami Source
1–2010 Chile	2010-02-27 6:35:15.4	35.95S	73.15W	South America (CSSZ)	8.8 (CMT)	8.8	[3]a88 × 17.24 + a90 × 8.82 + b88 × 11.86 + b89 × 18.39 + b90 × 16.75 + z88 × 20.78 + z90 × 7.06
2–2009 Samoa	2009-09-29 17:48:26.8	15.13S	171.97W	New Zealand-Kermadec-Tonga (NTSZ)	8.1 (CMT)	8.1	[3]3.96 × a34 + 3.96 × b34
3–2007 Peru	2007-08-15 23:41:57.9	13.73S	77.04W	South America (SASZ)	[2]8.0 (CMT)	8.1	[3]4.1 × a9 + 4.32 × b9
4–2007 Kuril	2007-01-13 04:23:48.1	46.17N	154.80E	Kamchatka-Yap-Mariana-Izu-Bonin (KISZ)	[2]8.1 (CMT)	7.9	–3.64 × b13
5–2006 Kuril	2006-11-15 11:15:08.0	46.71N	154.33E	Kamchatka-Yap-Mariana-Izu-Bonin (KISZ)	[2]8.3 (CMT)	8.1	[3]4 × a12 + 0.5 × b12 + 2 × a13 + 1.5 × b13
6–2006 Tonga	2006-05-03 15:27:03.7	20.39S	173.47W	New Zealand-Kermadec-Tonga (NTSZ)	[2]8.0 (CMT)	8.0	6.6 × b29
7–2003 Rat Island	2003-11-17 06:43:31.0	51.14N	177.86E	Aleutian-Alaska-Canada (ACSZ)	[2]7.7 (CMT)	7.8	[3]2.81 × b11
8–2003 Hokkaido	2003-09-25 19:50:38.2	42.21N	143.84E	Kamchatka-Yap-Mariana-Izu-Bonin (KISZ)	[2]8.3 (CMT)	8.0	3.6m × (100 × 100 km), 109#rake, 20#dip, 230#strike, 25 m depth
9–2001 Peru	2001-06-23 20:34:23.3	17.28S	72.71W	South America (SASZ)	[2]8.4 (CMT)	8.2	5.70 × a15 + 2.90 × b16 + 1.98 × a16
10–1996 Andreanov	1996-06-10 04:04:03.4	51.10N	177.410W	Aleutian-Alaska-Canada (ACSZ)	[2]7.9 (CMT)	7.8	2.40 × a15 + 0.80 × b16
11–1994 East Kuril	1994-10-04 13:23:28.5	43.60N	147.63E	Kamchatka-Yap-Mariana-Izu-Bonin (KISZ)	[2]8.3 (CMT)	8.1	9.00 × a20
12–1964 Alaska	1964-03-28 03:36:14	61.10N	147.50W	Aleutian-Alaska-Canada (ACSZ)	9.2 (USGS)	[4]9.0	Tang *et al.* (2006)
13–1960 Chile	1960-05-22 19:11:14	39.50S	74.5W	South America (SASZ)	9.5 (Kanamori and Cipar, 1974)		
14–1957 Andreanov	1957-03-09 14:22:31.9	51.292N	175.629W	Aleutian-Alaska-Canada (ACSZ)	8.6 (USGS)	[4]8.7	31.4 × a15 + 10.6 × a16 + 12.2 × a17
15–1952 Kamchatka	1952-11-04 16:58:26.0	52.75N	159.50E	Kamchatka-Yap-Mariana-Izu-Bonin (KISZ)	9.0 (USGS)	[4]8.7	
16–1946 Unimak	1946-04-01 12:28:56	53.32N	163.19W	Aleutian-Alaska-Canada (ACSZ)	8.5 (López and Okal, 2006)	[4]8.5	7.5 × b23 + 19.7 × b24 + 3.7 × b25

[1]Equivalent tsunami source moment magnitude from model source constrained by tsunami observations.
[2]Centroid Moment Tensor
[3]The tsunami source was obtained during real time and applied to the forecast.
[4]Preliminary source

Table 2: MOST setup of the reference and forecast models for Hilo, Hawaii.

		Reference Model				Forecast Model			
Grid	**Region**	**Coverage Lat. [°N] Lon. [°E]**	**Cell Size [″]**	**nx × ny**	**Time Step [sec]**	**Coverage Lat. [°N] Lon. [°E]**	**Cell Size [″]**	**nx × ny**	**Time Step [sec]**
A	Hawaii	18–23 199–205.98	36 × 36	699 × 500	2.25	18.0317–22.9983 199–205.9667	120 × 120	210 × 150	8
B	Big Island, Maui complex	18.693–21.428 202.848–205.398	6 × 6	1531 × 1642	0.45	18.68–20.4155 203.738–205.403	18 × 18	334 × 347	2.0
C	Hilo	19.7–19.79 204.899–205.025	10 × 10	1356 × 973	0.15	19.700–19.790 204.899–204.990	4 × 2	164 × 163	1.0
Minimum offshore depth [m]				1			1		
Water depth for dry land [m]				0.1			0.1		
Friction coefficient (n^2)				0.00625			0.0009		
CPU time for a 4-hr simulation				~34 hr			<10 min		

Computations were performed on a single Intel Xeon processor at 3.6 GHz, Dell PowerEdge 1850.

source grids were compiled from several data sources. **Figures 5 and 6** show the spatial extent of each data source used.

Raw data sources were imported to ESRI ArcGIS-compatible file formats. Data values were converted, where necessary, to the WGS84 horizontal geodetic datum. In the point datasets, single sounding points that differed substantially from neighboring data were removed. Gridded datasets were checked for extreme values by examination of contour lines and, where available, by comparison between multiple data sources. All selected input datasets were converted to the mean high water (MHW) vertical datum, when necessary, using offsets on the National Ocean Service tidal benchmark datasheet for the Hilo tide station.

3.3 Grid setups

Tang *et al.* (2009) show forecast model setup for several sites in Hawaii. Each forecast model contains three levels of telescoping computational grids with increasing resolution:

1. One regional grid of 2-arc-min (~3600 m) resolution covers the main Hawaiian Islands (A grid).
2. Then the Hawaiian Islands are divided into four intermediate grids of 12 to 18 arc sec (~360–540 m) for the four natural geographic areas (B grid).
3. Each intermediate grid contains 2-arc-sec (~60 m) nearshore grids (C grid).

By sub-sampling from the DEMs described in section 3.2, two sets of computational grids were derived for Hilo, a reference model (**Figure 7**) and a forecast model (**Figure 8**). The regional grids cover the major Hawaiian Islands and the intermediate grids cover the Islands of Hawaii, Maui, Lanai, and east

Molokai. Runup and inundation simulations are computed at the coastline in the nearshore grids. Grid details at each level and input parameters are summarized in **Table 2**. The input file parameters for running the forecast and reference models are presented in **Appendix A**.

4. Results and Discussion

4.1 Sensitivity of modeled time series by the Hilo forecast model to grid coupling schemes

MOST version 1.0 employs a two-way coupling scheme. The coupling is achieved at each time step by interpolation of the low-resolution field from the coarse to the fine resolution level, and vice versa. This two-way coupling scheme has relatively rigorous requirements on bathymetric consistency as well as on time steps between adjacent grids. Time steps used for the three telescoping grids need to be carefully tested in order to provide stable model runs of long duration. To overcome these difficulties, a one-way coupling scheme was employed in MOST version 2.0, e.g., no interpolation of the fine-resolution field to the coarser resolution level, for forecast purposes. This one-way coupling scheme is robust and can handle bathymetric grids from varieties of data sources with any time steps that satisfy CFL conditions. MOST version 2.0 passed the benchmark tests and in general provided good comparisons with model results from version 1.0.

There are some exceptions for Hilo. **Figure 9** compares the modeled tsunami time series by MOST one- and two-way coupling schemes for 16 past tsunamis. So far, we have seen that one-way coupling overestimates amplitude of the 3rd trough and the 4th peak at Hilo tide station for five events, the 2010 Chile, 2007 and 2006 Kuril Islands, 2003 Rat Island, and 1996 Andreanov tsunamis (**Figures 9.1, 9.4, 9.5, 9.7, and 9.10**). The reason is still under investigation. We recommend double checking results for the Hilo forecast model by using the two-way coupling scheme. In the next section, we discuss the results computed by the forecast model using the two-way coupling scheme.

4.2 Validation, verification, and testing of the forecast model

4.2.1 Validation

Both the reference model and the forecast model for Hilo were tested with the 16 past tsunamis summarized in **Table 1**. Tide gauge data of the recent tsunamis, Nos. 1 to 11, were from the NOAA National Water Level Observation Network (NWLON) (Allen *et al.*, 2008), while others were digitized from Shepard *et al.* (1950), Zerbe (1953), Salsman (1959), Berkman and Symons (1964), and Spaeth and Berkman (1967). The observations were filtered by a low-pass Butterworth filter to remove tidal components with periods longer than a cut-off period, such as 1 or 2 hr. **Figure 10** shows observed and modeled tsunami time series at Hilo tide station.

The most recent tested event is the 27 February 2010 Chile tsunami. The Chile tsunami was generated by a Mw 8.8 earthquake NNE of Concepcion, Chile. In approximately 3 hours, the tsunami was recorded at DART station 32412. The real-time data was combined with the propagation database to produce a tsunami source. **Figure 10.1** shows the comparison of observations and model time series. The observed maximum wave height is 1.71 m, while the model shows 2.24 m with the two-way coupling scheme. The 0.53-m error in the maximum wave height is the largest error the forecast model has produced among the tested past tsunamis. The model time series were shifted 9 min late in the plot.

The 29 September 2009 Samoa tsunami was generated by a Mw 8.1 earthquake which occurred near the northern end of the Tonga Trench. Data recorded at DART stations 51425 and 51426 were inverted to produce a tsunami source in real time. **Figure 10.2** shows good agreements between the model results and observations at Hilo.

A detailed description of the real-time experimental forecast for the 15 August Peru tsunami can be found in Wei *et al.* (2008). At Hilo tide station, the observed maximum wave height is 67 cm, while the forecast is 65 cm. The forecast showed an arrival around 12 min earlier. After this 12-min time difference was adjusted in **Figure 10.3**, the forecast and observation matched well in period.

The 13 January 2007 Kuril Islands earthquake occurred as normal faulting (USGS, 2007). The T_{Mw} 7.9 source was inverted from tsunami data recorded at three DARTs, 21414, 46413, and 21413, by a linear least squares fit to negative tsunami source functions near the epicenter. The maximum wave height was overestimated (**Figure 10.4**).

The Kuril Islands tsunami of 15 November 2006 provided ample tsunami data and the first test of NOAA's new experimental tsunami forecast system. The tsunami source was inverted with tsunami data recorded at several DART buoys along the Aleutian Trench. The modeled first waves agree well with the observations (**Figure 10.5**).

The 3 May 2006 Tonga earthquake generated a tsunami that was detected about 6 hr later by two offshore DARTs located to the south of the Hawaiian Islands. These data were combined with the TSF database to produce the tsunami source by inversion (Tang *et al.*, 2008a). Excellent agreement is obtained for the first six waves over 2 hr, including the amplitudes, arrival time, and wave period (**Figure 10.6**). The forecast model reproduced the maximum waves that arrived 1.5 hr after the first arrival. Those are the 4th waves at Hilo. As shown in Tang *et al.* (2008a), the Hilo forecast model also modeled well the large amplitude later waves reflected from North America and scattered by South Pacific bottom features that reached the Hawaiian Islands 16 hr and 18.5 hr, respectively, after the earthquake.

The 17 November 2003 Rat Island tsunami provided the first real-time test of NOAA's forecast methodology, which became the proof of concept for the development of the tsunami forecast system (Titov *et al.*, 2005). This tsunami was detected by three DARTs located along the Aleutian Trench. The real-time data was combined with the TSF database to produce a tsunami source of T_{Mw} 7.8 by inversion. The offshore model scenario was then used as input to the

earlier version of the Hilo forecast model, which was the only forecast model available at that time. The model runtime is about 10 min by using a single processor on a Dell PowerEdge 2650 with 2 Intel Xeon CPUs of 2.8 GHz, each with 512 KB cache and 4 GB memory. The accuracy of the forecast is reflected by the excellent agreement between the model prediction and observation at Hilo tide station (**Figure 10.7**). This event was the first time in history that the forecast of tsunami time series was available to a coastal city before tsunami waves arrived. The offshore forecasts of the maximum tsunami amplitude and arrival time are in **Figure 2**.

The 25 September 2003 Hokkaido earthquake generated tsunami waves of very long periods recorded at the tide station. The wave amplitude decreased slowly and steadily (**Figure 10.8**).

DART station 51406, located midway between South America and Hawaii, was not deployed until 1 mon after the 23 June 2001 Peru tsunami. Therefore, the source for this event was derived based on an inversion of Kahului tide gauge records using the Kahului forecast model. It produced good comparisons of first waves at the other three stations (**Figure 10.9**).

Deep-ocean research bottom-pressure recorder data are also available for two other early tsunamis. The inversion of the 1994 Kuril Islands tsunami data was done by using five BPR recordings, while the 1996 Andreanov used one (Titov *et al.*, 2005). Model results agree quite well with observations for the first several waves (**Figures 10.10 and 10.11**). Only 6-min data are available at Hilo tide station. The 6-min resolution was unable to fully resolve the tsunami waves so the wave height at Hilo was under-recorded (**Figure 10.11**).

DART buoy records are not available for five destructive tsunamis, the 1964 Alaska, 1960 Chile, 1957 Andreanov, 1952 Kamchatka, and 1946 Unimak events. Previous studies of seismic, geodetic, and water-level data have estimated source parameters for some of the events (Kanamori and Ciper, 1974; Johnson *et al.*, 1994; 1996; Johnson and Satake, 1999; López and Okal, 2006). However, some of the sources are subject to debate and adjustment. Most of the source estimates that have been done are based on low-resolution tsunami propagation models. The forecast system provides a unique chance to reinvestigate the historical sources by inversion of the water level data with the high-resolution-quality inundation and propagation models. Preliminary results are available for the 1964, 1957, 1952, and 1946 tsunamis. The incomplete tide gauge records in Hawaii and the distance from the source to the developed forecast models in the U.S. present a substantial challenge to the reinvestigation of the 1960 Chile tsunami. So the source parameters of the tsunami are taken from Kanamori and Ciper (1974) in this study. Model results are plotted in **Figures 10.12 to 10.16**, respectively.

Figure 11a shows the error of the maximum wave height computed by the Hilo forecast model for the past tsunamis that have complete wave-height records. When the observed maximum wave height is less than 0.5 m, the maximum computed error is less than 0.3 m. At small amplitudes, noise in the observed signals and numerical error in the model are large compared to the observations. When the maximum wave height is greater than 0.5 m, the error is within ±35%; this uncertainty can be attributed primarily to uncertainties in the tsunami source, model setup, and bathymetry. Arrival time of the first wave

peak in general agrees well with the observations, with errors less than ±3% of the travel time. So far, the largest discrepancy between the modeled and observed first arrival time is the 12 min for the 2007 Peru tsunami. However, with an earthquake epicenter 460 km to the northwest of the 2007 Peru earthquake, the 2001 Peru tsunami has only a 3-min discrepancy in arrival time. This 12-min arrival discrepancy is currently under investigation.

Tsunami waves are known to produce time series with complex frequency structure that varies in space and time. To explore the tsunami frequency responses at different forecast sites, a complex Morlet wavelet transform was applied to both observations and model results. A description of the time series of wavelet-derived amplitude spectra can be found in Tang *et al.* (2008a). As an example, **Figure 12** shows the real parts of the wavelet-derived amplitude spectra for the observation and forecast at Hilo for the November 2006 Kuril Islands tsunami. The modulated spectrogram shows the first incident wave has a peak period near 20 min (**Figure 12b**). The tsunami quickly excited two major oscillations with near 15- and 32-min periods in Hilo Harbor. Those changes of frequency structure were correctly captured by the forecast time series computed by the Hilo forecast model (**Figure 12c**).

The same approach was applied to the tsunami time series in **Figure 10**. **Figure 11b** compares the observed and modeled peak wave periods. At Hilo, the observed peak wave periods fall into one of the three groups near 15-, 22-, or 32-min periods (±2 min) (**Figure 11b**). The Hilo forecast model produced the peak wave periods reasonably well, especially in the highest frequency group (15-min period).

Figure 13a shows the inundation at Hilo computed by the forecast model for the 1946 Unimak tsunami. The modeled inundation, after being converted to MLLW, correctly reproduced the inundation limit of the survey data from Shepard *et al.* (1950) (**Figure 13b**).

4.2.2 Verification

The computed maximum water elevation above MHW and maximum current of the 16 tsunamis are plotted in **Figure 14**. Both the reference and forecast models produced similar patterns and values. The 1946 Unimak tsunami caused the most severe impact on Hilo. In general, the tsunami wave amplitude increases dramatically due to shoaling when the tsunami waves enter a nearshore area shallower than 20 m and even more so because of local shelf and harbor resonances and other coastal effects. This emphasizes the importance of using high-resolution inundation models, which resolve the local coast and harbor geometries, in order to achieve accurate tsunami amplitude forecasts for coastal communities.

4.2.3 Robustness and stability tests

Recorded historical tsunamis provide only a limited number of events, from limited locations. More comprehensive test cases of destructive tsunamis with different directionalities are needed to check the stability and robustness for

SIMs. The same set of 18 simulated T_{Mw} 9.3 tsunamis as in Tang *et al.* (2008b) was selected here for further examination. Results computed by the forecast model are compared with those from the high-resolution reference model in **Figures 15 and 16**. Both models were numerically stable for all of the scenarios. Waveforms computed by the forecast model agree well with those from the reference model (**Figure 15**). Both models compute similar maximum water elevation and inundation in the study area (**Figure 16**). These results indicate the Hilo forecast model is capable of providing robust and stable predictions of long duration for Pacific-wide tsunamis.

Tsunami waves in the study area vary significantly for the 18 magnitude 9.3 scenarios. These results show the complexity and high nonlinearity of tsunami waves nearshore, which again demonstrate the value of the forecast model for providing accurate site-specific forecast details. The No. 3 scenario in the middle of the Aleutian subduction zone generates severe inundation at Hilo. The computed maximum water elevation reaches 7 m at the tide station.

4.3 Tsunami hazard assessment for Hilo from simulated magnitude 7.5, 8.2, 8.7, and 9.3 tsunamis

A tsunami hazard assessment for a model site can provide forecast guidance by determining in advance which subduction zone regions and tsunami magnitudes pose the greatest threat to the location. The validated forecast models, in combination with the forecast tsunami source function database, provide powerful tools to address this long-term forecast. Here, we apply our forecast modeling tools, including the previously described Hilo forecast model, to produce long-term forecast assessment for Hilo.

Four different magnitudes, T_{Mw} 7.5, 8.2, 8.7, and 9.3, as in Tang *et al.* (2008b; 2009), were tested. The details of the simulated tsunami sources and results are summarized in **Figure 17**. The maximum water elevation, $\eta_{\max}$, at Hilo tide station from T_{Mw} 7.5 tsunamis computed by the Hilo forecast model, is plotted in bars in **Figure 17b**. Color represents the first arrival at the station, which is the time when the water level reaches 20% of the height of the first significant peak or trough. Bars in **Figure 17a** indicate the maximum elevation at deep water offshore Hilo from the same sources, which are from the TSF database. **Figures 17c, d, and e** show at Hilo tide station from T_{Mw} 8.2, 8.7, and 9.3 tsunamis, respectively. The color represents the difference in time between the arrival of the maximum elevation, t_{max}, and first arrival, t_1. These results show an impressive local variability of tsunami amplitudes even for far-field tsunamis, which illustrate the complexity of forecasting tsunami amplitudes at coastal locations. Tang *et al.* (2009) have shown that the location of the most "effective" source for a given location also differs from site to site.

To further investigate the transformations of tsunami amplitudes from offshore to the tide gauges, we have looked at the ratios of these amplitudes. The ratio of the offshore and nearshore $\eta_{\max}$ for all computed scenarios are plotted and the linear regression analyses were performed in **Figure 18**. To better illustrate the data trends, both the logarithmic and Cartesian coordinates were plotted with the same datasets. The logarithmic scales give a full picture of the

wide range of values, while the Cartesian coordinates better illustrate the actual spread and trends of the data. In **Figure 18b**, the red dots, which represent the T_{Mw} 7.5 tsunamis, are hardly seen due to the overlapping dots representing other magnitude scenarios. The solid black lines are the best fit to the data. The dashed black lines are the prediction bounds based on a 95% confidence level. The results show:

1. The relationship between tide-gauge maximum amplitude and offshore maximum amplitude appears to be complex and nonlinear in nature.
2. Larger amplitudes offshore do not necessarily produce larger amplitudes at tide gauges, and larger tsunami magnitudes may not produce larger waves either offshore, or at tide-gauges.
3. The simple relationships obtained through regression analysis (**Figure 18a**) are insufficient to provide warning guidance during an event. The 95% confidence interval is too wide to provide any certainty for the forecast accuracy.

Tang *et al.* (2009) also show that the trends of offshore/tide gauge amplitudes are site-specific. Different sites show different regression analysis curves. These results indicate that high-resolution tsunami models are essential for providing useful accuracy for coastal amplitude forecast. If the high-resolution tsunami near-shore dynamics is not included in the forecast procedures, the accuracy and the uncertainty of the amplitude forecast appear to be too high for practical guidance.

5. Summary and Conclusions

This study describes the development, testing, and application of a site-specific tsunami inundation model for Hilo for use in NOAA's tsunami forecast and warning system. The final forecast model grid resolution was 2 arc sec (~60 m) to enable a 4-hr inundation simulation within 10-min of computational time. A higher-resolution reference inundation model of 1/3 arc sec (~10 m) was also developed in parallel to provide modeling references for the forecast model. Both models were tested for 16 past tsunamis and a set of 18 simulated magnitude 9.3 tsunamis.

The error of the maximum wave height computed by the forecast model is within 35% when the observation is greater than 0.5 m; when the observation is below 0.5 m the error is less than 0.3 m. The error of the modeled arrival time of the first peak is within 3% of the travel time. Wavelet analysis of the tsunami time series indicates that the peak wave period often coincides with one of the resonant periods of the harbor where the tide gauge is located. This peak period may partially depend on the geographic location of the tsunami source.

The developed forecast models were further applied to hazard assessment from 1435 scenarios of simulated magnitude 7.5, 8.2, 8.7, and 9.3 tsunamis based on subduction zone earthquakes in the Pacific. The results demonstrate the nonlinearity between offshore and nearshore maximum wave amplitudes. The study indicates that use of a seismic magnitude alone for a tsunami source assessment is inadequate to achieve such accuracy for tsunami amplitude forecasts. The forecast models apply local bathymetric and topographic information, and utilize dynamic boundary conditions from the tsunami source function database, to provide site- and event-specific coastal predictions.

6. Acknowledgments

The authors thank Harold Loomis and Michael Spillane for their reviews and valuable suggestions; Jean Newman for assistance; Eddie N. Bernard, Marie C. Eble, and Robert Weiss for comments and discussion; Nazila Merati and Ryan Layne Whitney for editing; Burak Uslu for providing propagation database tables and graphics. Collaborative contributions of the National Weather Service, the National Geophysical Data Center, and the National Data Buoy Center were invaluable.

Funding for this publication and all work leading to development of a tsunami forecast model for Hilo, Hawaii was provided by the National Oceanic and Atmospheric Administration. This publication was partially funded by the Joint Institute for the Study of the Atmosphere and Ocean (JISAO) under NOAA

Cooperative Agreement No. NA17RJ1232, JISAO Contribution No. 1766. This is PMEL Contribution No. 3340.

7. References

Allen, A.L., N.A. Donoho, S.A. Duncan, S.K. Gill, C.R. McGrath, R.S. Meyer, and M.R. Samant (2008): NOAA's National Ocean Service supports tsunami detection and warning through operation of coastal tide stations. In *Solutions to Coastal Disasters 2008/Tsunamis: Proceedings of Sessions of the Conference*, American Society of Civil Engineers, Turtle Bay, Oahu, Hawaii, 13–16 April.

Berkman, S.C., and J.M. Symons (1964): The tsunami of May 22, 1960 as recorded at tide stations. Coastal and Geodetic Survey, U.S. Department of Commerce, 79 pp.

Bernard, E.N., H.O. Mofjeld, V.V. Titov, C.E. Synolakis, and F.I. González (2006): Tsunami: Scientific frontiers, mitigation, forecasting, and policy implications. *Proc. Roy. Soc. Lond. A*, *364*(1845), 1989–2007, doi: 10.1098/rsta.2006.1809.

Bernard, E.N., and V.V. Titov (2007): Improving tsunami forecast skill using deep ocean observations. *Mar. Technol. Soc. J.*, *40*(4), 23–26.

Dudley, W.C., and S.C. Stone (2000): *The tsunami of 1946 and 1960 and the devastation of Hilo Town*. Donning Company Publisher, Virginia Beach, VA, 64 pp.

Fraser, G.D., P.J. Eaton, and C.K. Wentworth (1959): The tsunami of March 9, 1957, on the Island of Hawaii. *Bull. Seismol. Soc. Am.*, *49*(1), 79–90.

Gica, E., M.C. Spillane, V.V. Titov, C.D. Chamberlin, and J.C. Newman (2008): Development of the forecast propagation database for NOAA's Short-term Inundation Forecast for Tsunamis (SIFT). NOAA Tech. Memo. OAR PMEL-139, NTIS: PB2008-109391, NOAA/Pacific Marine Environmental Laboratory, Seattle, WA, 89 pp.

González, F.I., E.N. Bernard, C. Meinig, M. Eble, H.O. Mofjeld, and S. Stalin (2005): The NTHMP tsunameter network. *Nat. Hazards*, *35*(1), 25–39, Special Issue, U.S. National Tsunami Hazard Mitigation Program.

Gusiakov, V.K. (1978): Static displacement on the surface of an elastic space. Ill-posed problems of mathematical physics and interpretation of geophysical data. *VC SOAN SSSR*, 23–51, Novosibirsk (in Russian).

Johnson, J.M., and K. Satake (1999): Asperity distribution of the 1952 Great Kamchatka earthquake and its relation to future earthquake potential in Kamchatka. *Pure Appl. Geophys.*, *154*(3–4), 541–553.

Johnson, J.M., K. Satake, S.R. Holdahl, and J. Sauber (1996): The 1964 Prince William earthqake: Joint inversion of tsunami and geodetic data. *J. Geophys. Res.*, *101*(B1), 523–532.

Johnson, J.M., Y. Tanioka, L.J. Ruff, K. Satake, H. Kanamori, and L.R. Sykes (1994): The 1957 Great Aleutian Earthquake. *Pure Appl. Geophys.*, *142*(1), 3–28.

Kanamori, H., and J.J. Ciper (1974): Focal process of the great Chilean earthquake, May 22, 1960. *Phys. Earth Planet. In.*, *9*, 128–136.

López, A.M., and E.A. Okal (2006): A seismological reassessment of the source of the 1946 Aleutian "tsunami" earthquake. *Geophys. J. Int.*, *165*(3), 835–849, doi: 10.1111/j.1365-246x.2006.02899.x.

NGDC (2009): Global Tsunami Database (2000 BC to present). National Geophysical Data Center, `http://www.ngdc.noaa.gov/seg/hazard/tsu_db.shtml`.

Okada, Y. (1985): Surface deformation due to shear and tensile faults in a half-space. *Bull. Seismol. Soc. Am.*, *75*, 1135–1154.

Pararas-Carayannis, G. (1969): Catalog of Tsunamis in The Hawaii Islands. World Data Center A Tsunami, ESSA Coast and Geodetic Survey, 94 pp.

Salsman, G.G. (1959): The tsunami of March 9, 1957, as recorded at tide stations. U.S. Coast and Geodetic Survey, 18 pp.

Satake, K., Y. Hasegawa, Y. Nishimae, and Y. Igarashi (2008): Recent tsunamis that affected the Japanese coasts and evaluation of JMA's tsunami warnings. OS42B-03, AGU Fall Meeting, San Francisco.

Shepard, F.P., G.A. Macdonald, and D.C. Cox (1950): The tsunami of April 1, 1946. *Bull. Scripps Inst. Oceanogr. Univ. Calif.*, *5*, 391–528.

Spaeth, M.G., and S.C. Berkman (1967): The tsunami of March 28, 1964, as recorded at tide stations. ESSA Technical Report Coast and Geodetic Survey Technical Bulletin No. 33, U.S. Dept. of Commerce, Coast and Geodetic Survey, Rockville, MD, 86 pp.

Synolakis, C.E., E.N. Bernard, V.V. Titov, U. Kânoğlu, and F.I. González (2008): Validation and verification of tsunami numerical models. *Pure Appl. Geophys.*, *165*(11–12), 2197–2228.

Tang, L., C.D. Chamberlin, and V.V. Titov (2008a): Developing tsunami forecast inundation models for Hawaii: Procedures and testing. NOAA Tech. Memo. OAR PMEL-141, NTIS: PB2009-100620, NOAA/Pacific Marine Environmental Laboratory, Seattle, WA, 46 pp.

Tang, L., V.V. Titov, and C.D. Chamberlin (2009): Development, testing, and applications of site-specific tsunami inundation models for real-time forecasting. *J. Geophys. Res.*, 6, doi: 10.1029/2009JC005476, in press.

Tang, L., V.V. Titov, Y. Wei, H.O. Mofjeld, M. Spillane, D. Arcas, E.N. Bernard, C. Chamberlin, E. Gica, and J. Newman (2008b): Tsunami forecast analysis for the May 2006 Tonga tsunami. *J. Geophys. Res.*, *113*, C12015, doi: 10.1029/2008JC004922.

Titov, V.V. (2009): Tsunami forecasting. In *The Sea*, Vol. 15, Chapter 12, Harvard University Press, Cambridge, MA, and London, England, 371–400.

Titov, V.V., and F.I. González (1997): Implementation and testing of the Method of Splitting Tsunami (MOST) model. NOAA Tech. Memo. ERL PMEL-112 (PB98-122773), NOAA/Pacific Marine Environmental Laboratory, Seattle, WA, 11 pp.

Titov, V.V., F.I. González, E.N. Bernard, M.C. Eble, H.O. Mofjeld, J.C. Newman, and A.J. Venturato (2005): Real-time tsunami forecasting: Challenges and solutions. *Nat. Hazards*, *35*(1), Special Issue, U.S. National Tsunami Hazard Mitigation Program, 41–58.

Titov, V.V., H.O. Mofjeld, F.I. González, and J.C. Newman (1999): Offshore forecasting of Alaska-Aleutian Subduction Zone tsunamis in Hawaii. NOAA Tech. Memo. ERL PMEL-114, NTIS PB2002-101567, NOAA/Pacific Marine Environmental Laboratory, Seattle, WA, 22 pp.

Titov, V.V., H.O. Mofjeld, F.I. González, and J.C. Newman (2001): Offshore forecasting of Alaska tsunamis in Hawaii. In *Tsunami Research at the End of a Critical Decade*, G.T. Hebenstreit (ed.), Kluwer Academic Publishers, 75–90.

Titov, V.V., and C.E. Synolakis (1998): Numerical modeling of tidal wave runup. *J. Waterw. Port Coast. Ocean Eng.*, *124*(4), 157–171.

USGS (2007): M 8.1 Kuril Islands earthquake of 13 January 2007. Earthquake Summary Map XXX, U.S. Geological Survey.

Wei, Y., E. Bernard, L. Tang, R. Weiss, V. Titov, C. Moore, M. Spillane, M. Hopkins, and U. Kânoğlu (2008): Real-time experimental forecast of the Peruvian tsunami of August 2007 for U.S. coastlines. *Geophys. Res. Lett.*, *35*, L04609, doi: 10.1029/2007GL032250.

Whitmore, P.M. (2003): Tsunami amplitude prediction during events: A test based on previous tsunamis. *Sci. Tsunami Haz.*, *21*, 135–143.

Zerbe, W.B. (1953): The tsunami of November 4, 1952, as recorded at tide stations. C&GS Special Publication #300, U.S. Dept. of Commerce, C&GS, 62 pp.

FIGURES

Figure 1: Photos showing damage at Hilo caused by the (a–e) 1946 and (f) 1960 tsunamis (images courtesy of Pacific Tsunami Museum). (a) Tsunami wave washing over and destroying the Hilo Harbor Pier (Immel Collection). (b) The badly damaged Pier 2 on the Hilo Waterfront (Smith Collection). (c) A person about to be overcome by tsunami waves (Enskine Collection). (d) The Hilo Bay Waterfront (Nakagawa Collection). (e) Devastation to downtown Hilo (Smith Collection). (f) Damage to property at Waiakea (Polhemus Collection).

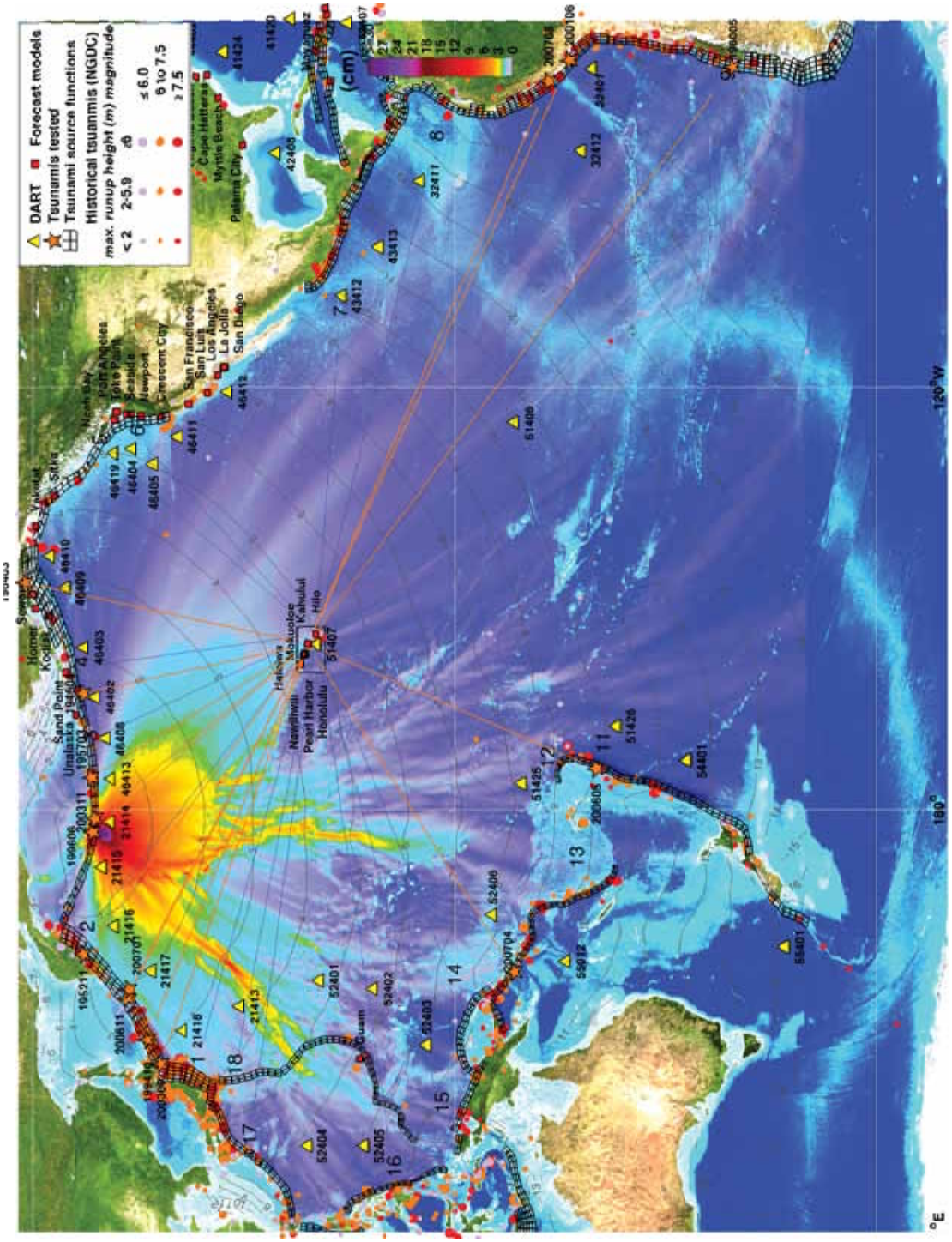

Figure 2: Overview of the Tsunami Forecast System. Filled colors show the offshore forecast of the maximum computed tsunami amplitude in cm for the 17 November 2003 Rat Islands tsunami in the Pacific. Contours indicate the first arrival time in hours. ——, Fourteen past tsunamis and —— eighteen simulated tsunamis tested in this study.

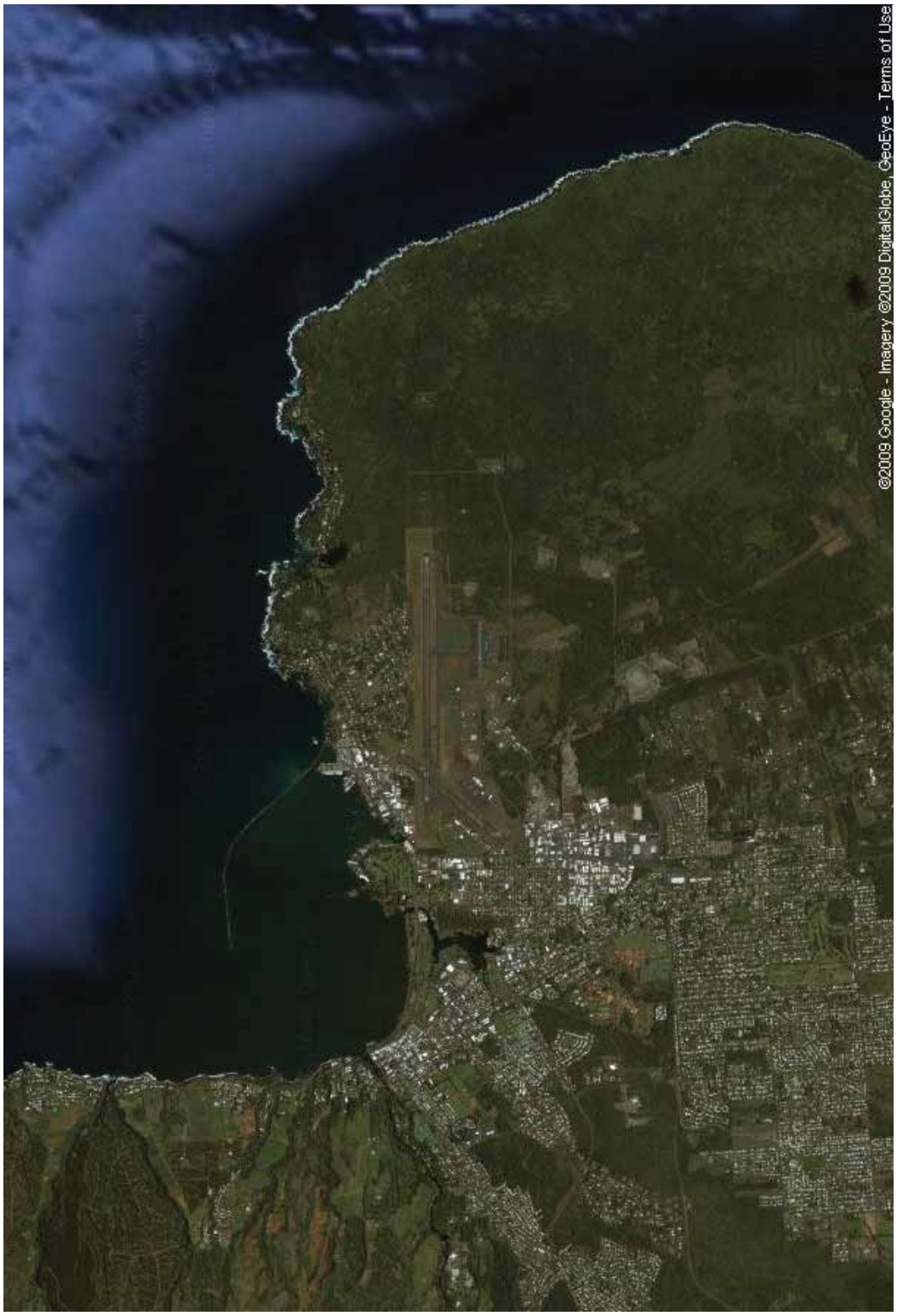

Figure 3: An aerial photo of Hilo (image from Google Earth).

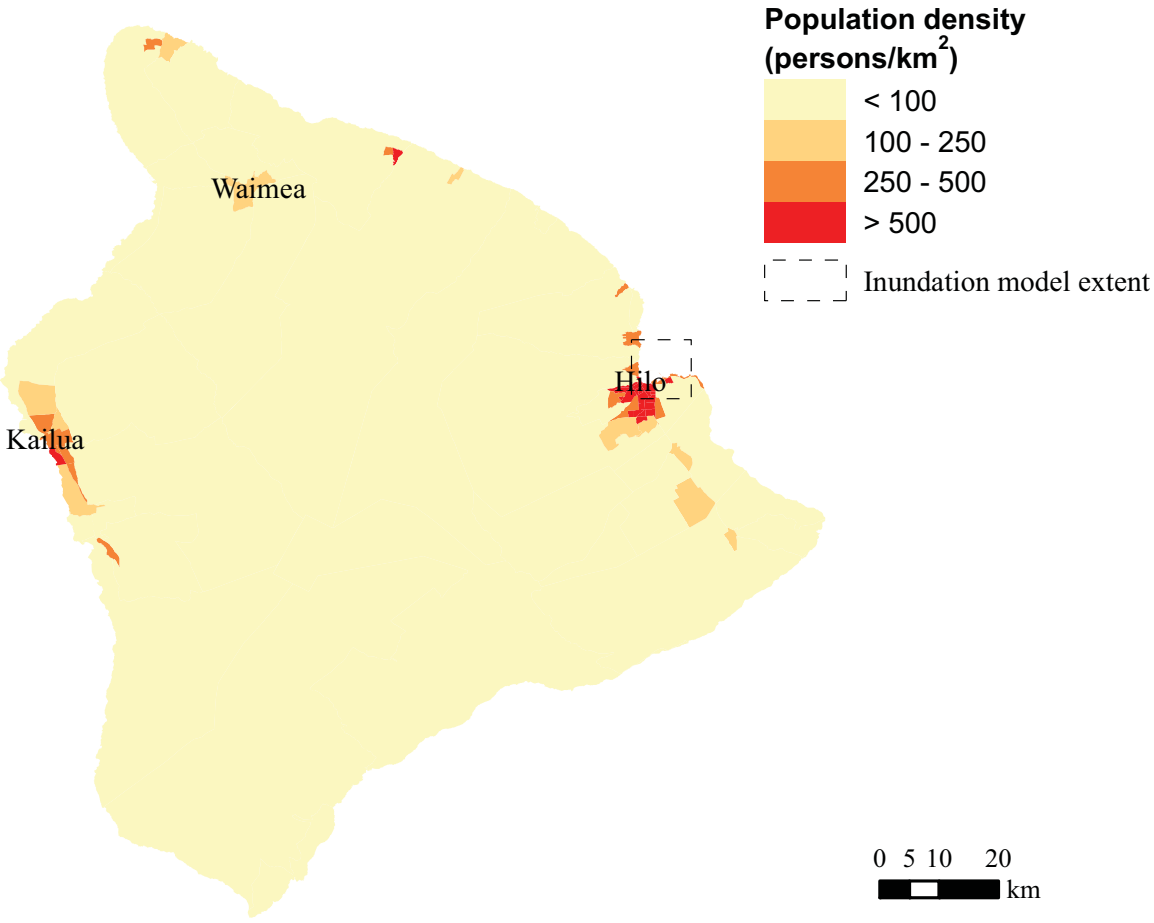

Figure 4: Population density, Hawaii (source: 2000 Census).

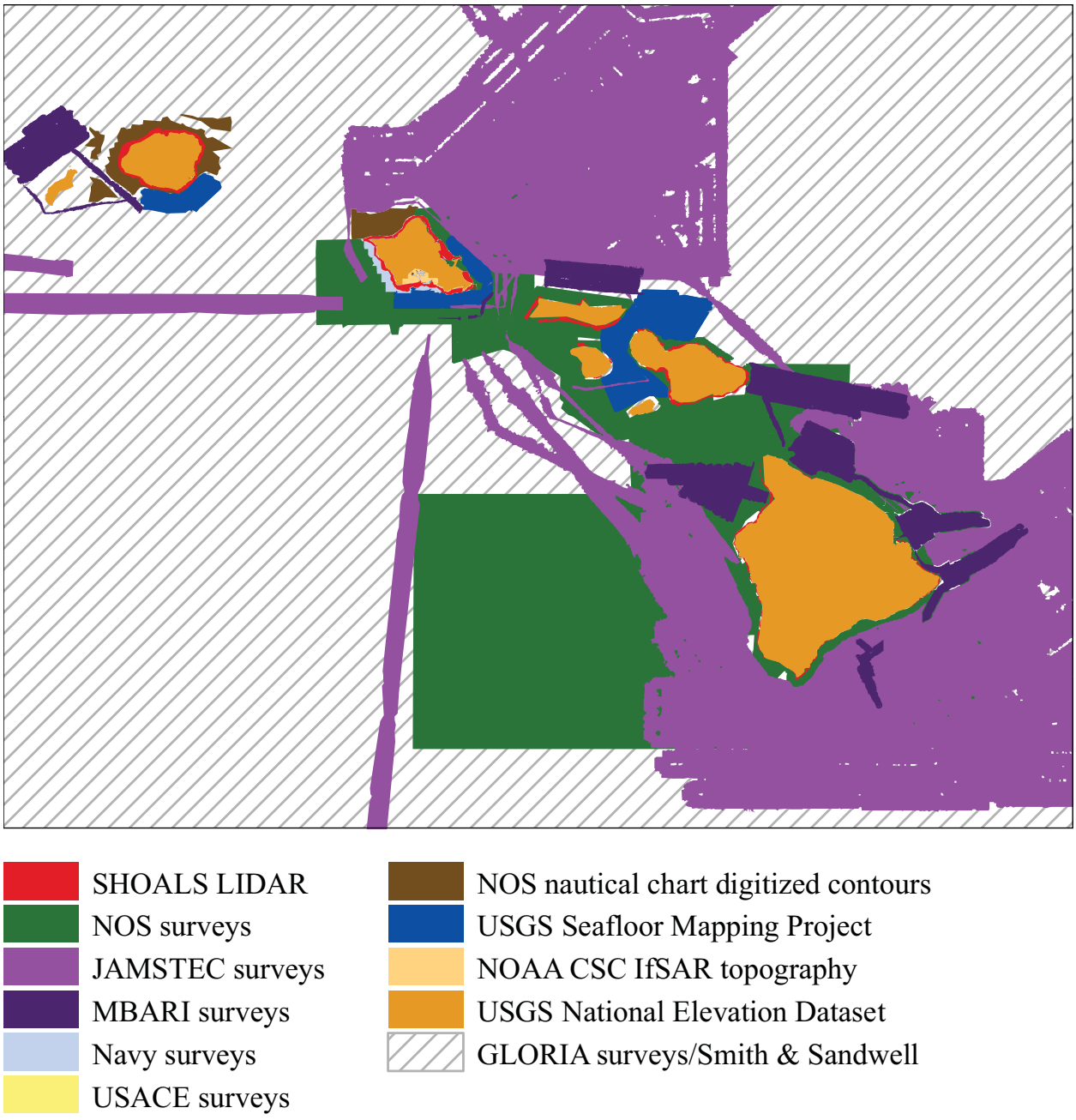

Figure 5: Bathymetric and topographic data source overview for the Hawaiian Islands with 6-arc-sec (~180 m) resolution.

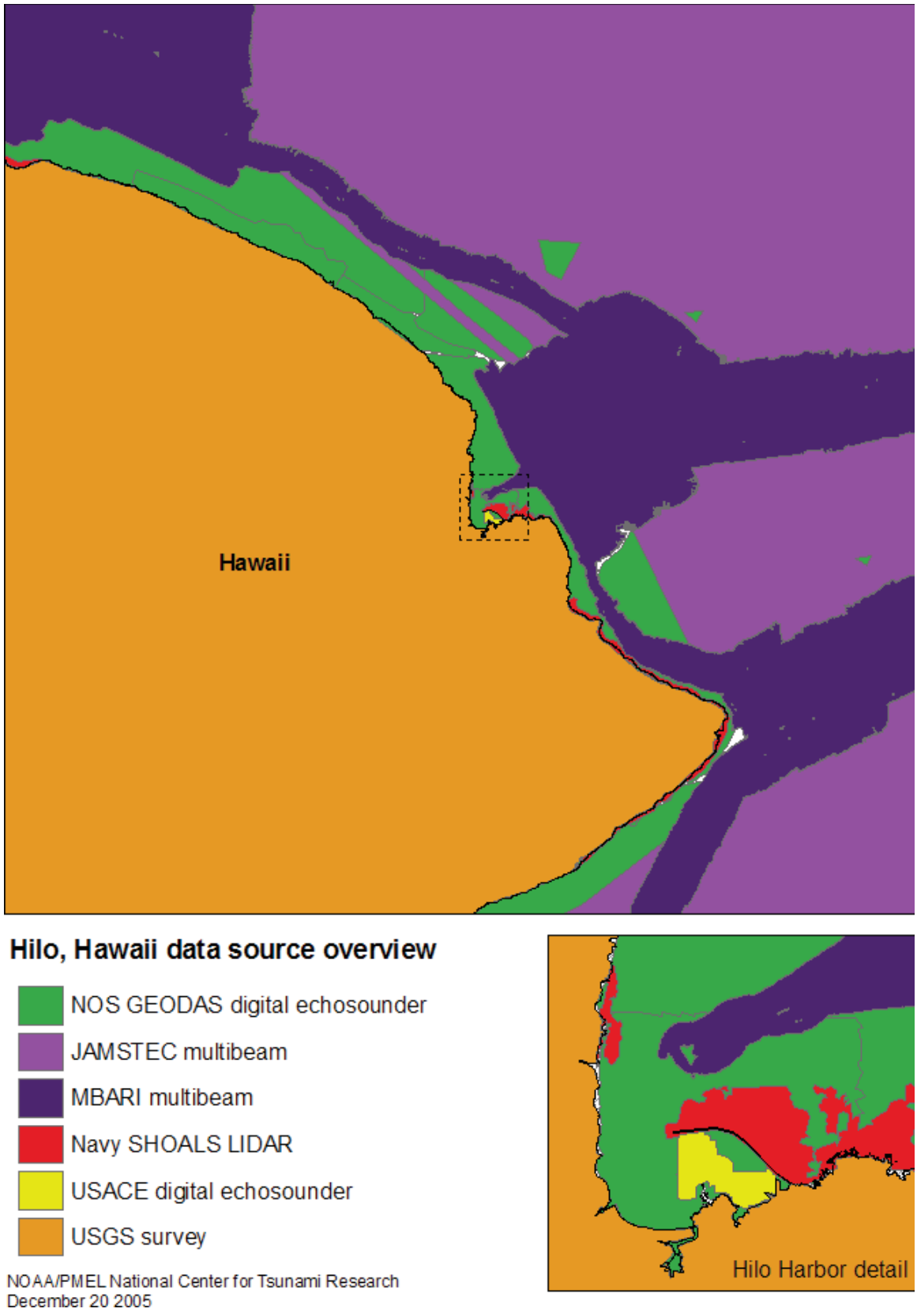

Figure 6: Bathymetric and topographic data source overview for Hilo with 1/3-arc-sec (~10 m) resolution.

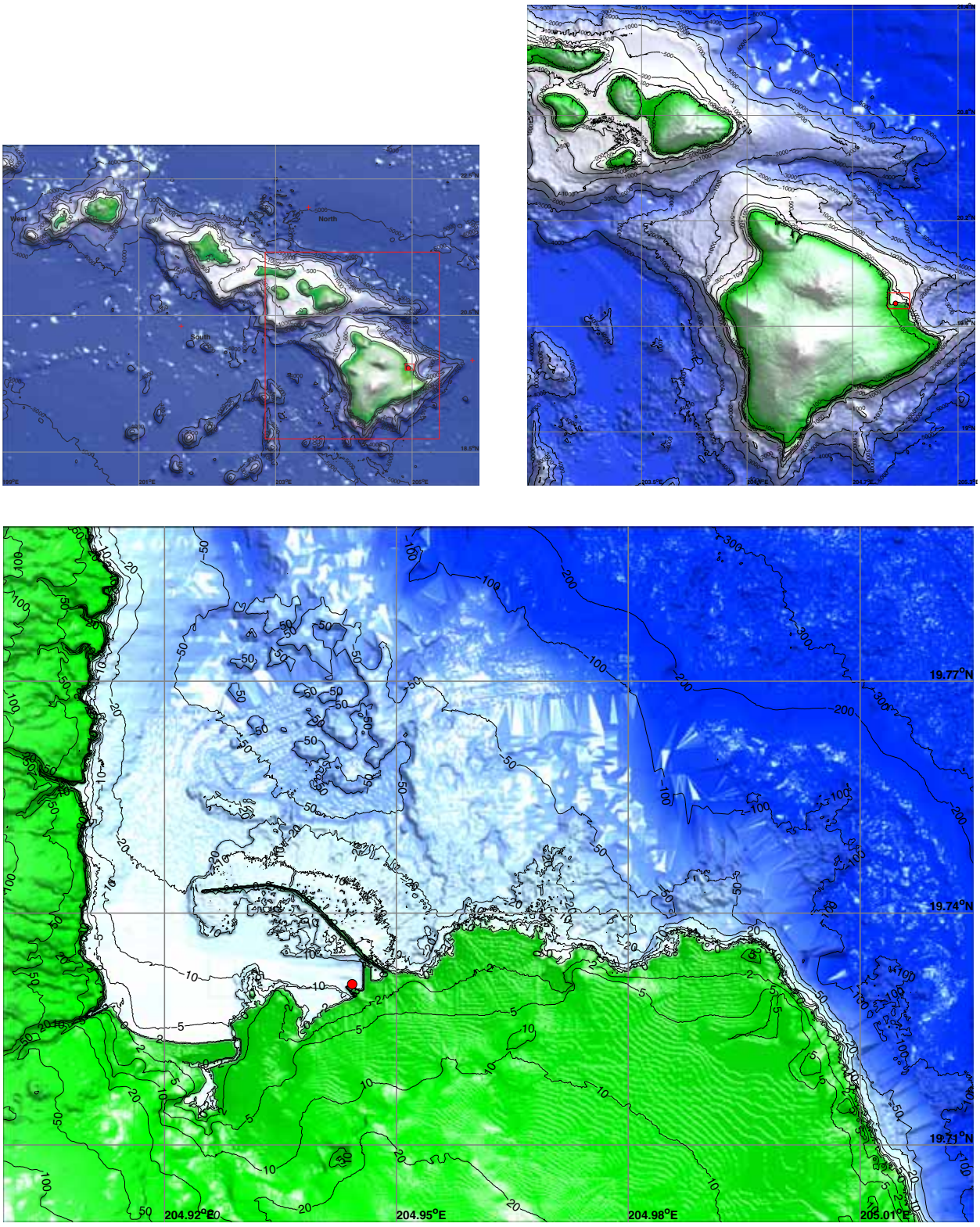

Figure 7: Grid setup for the Hilo reference model with resolution of (a) 36″ (1080 m), (b) 6″ (180 m) and (c) 1/3″ (10 m). □, nested grid boundary; ●, Hilo tide station.

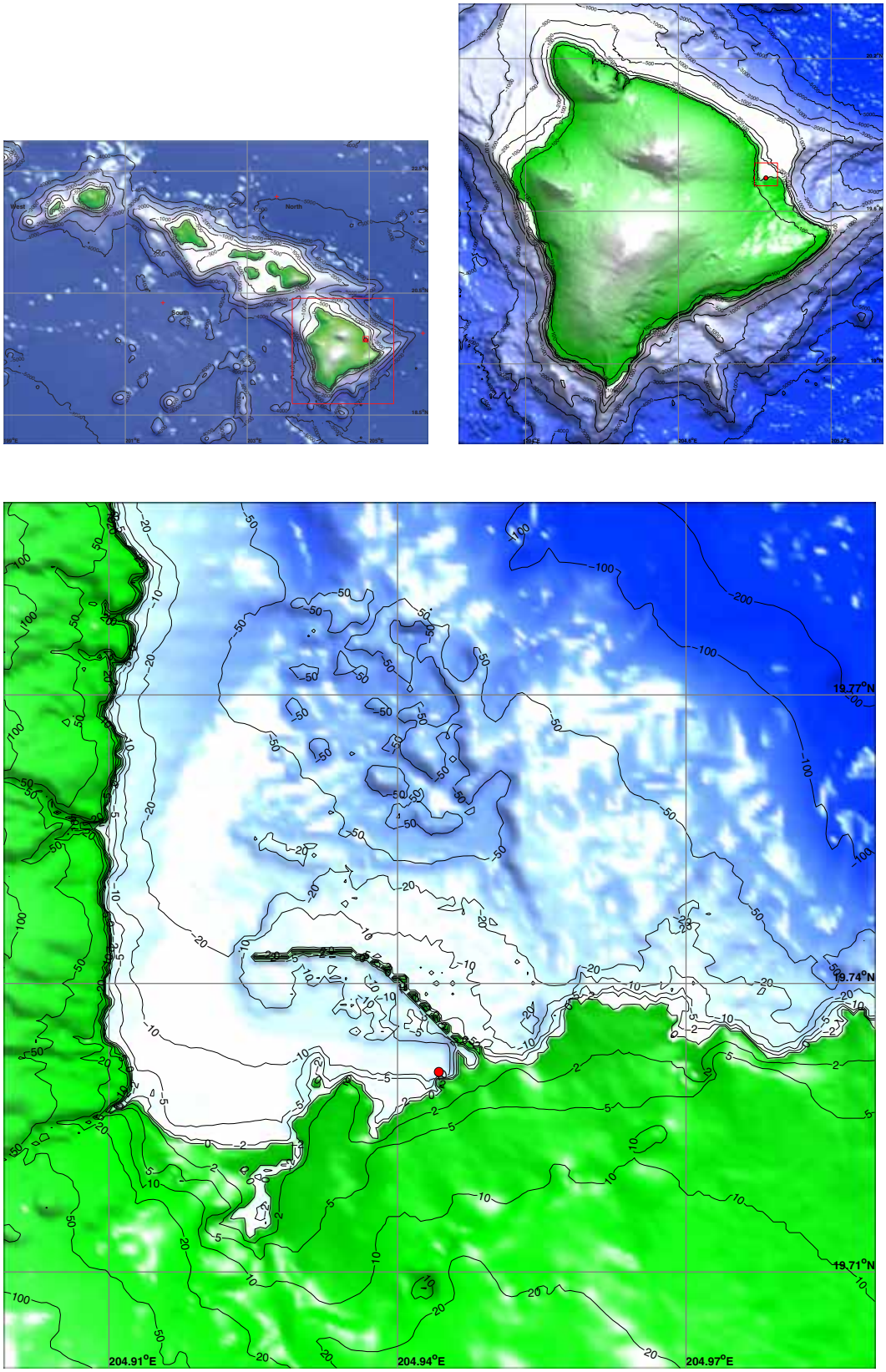

Figure 8: Grid setup for the Hilo forecast model with resolutions of (a) 120″ (3600 m), (b) 18″ (540 m) and (c) 2″ (60 m). □, nested grid boundary; ●, Hilo tide station.

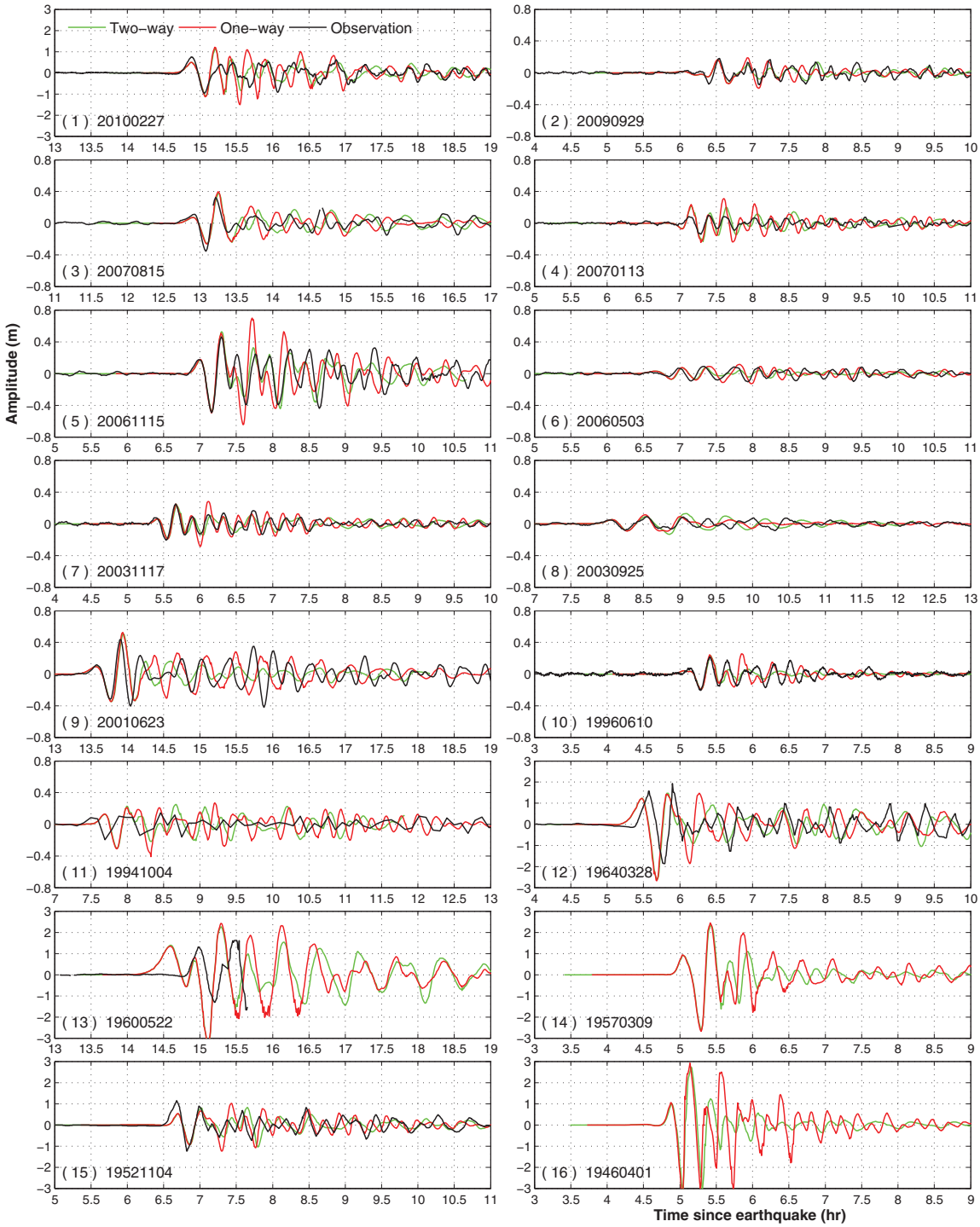

Figure 9: Tsunami time series at Hilo tide station computed by the MOST with one- and two-way coupling schemes from the Hilo forecast for 16 past tsunamis.

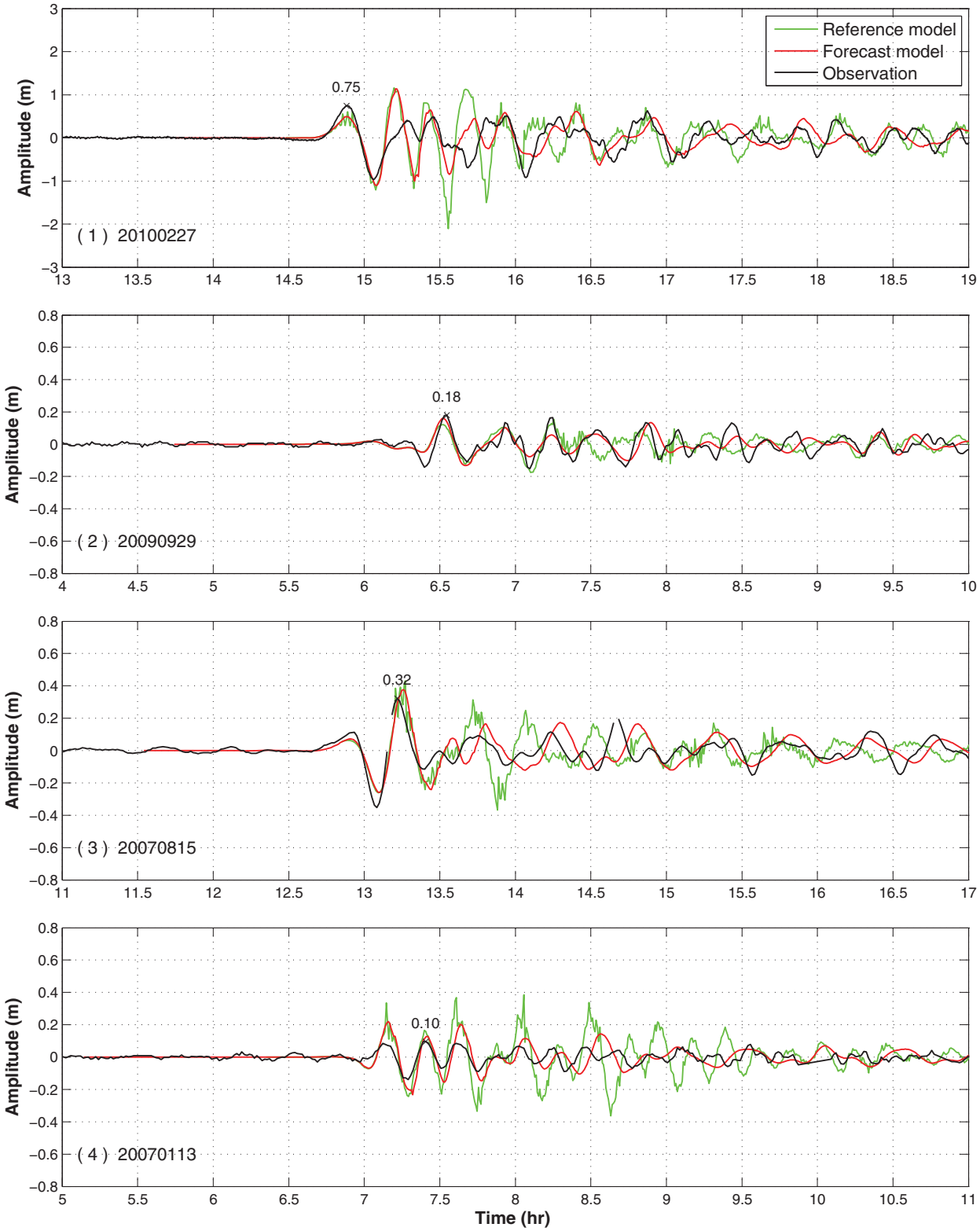

Figure 10: Tsunami time series of observed and modeled amplitudes by the Hilo reference inundation model and the forecast model for the 16 past tsunamis.

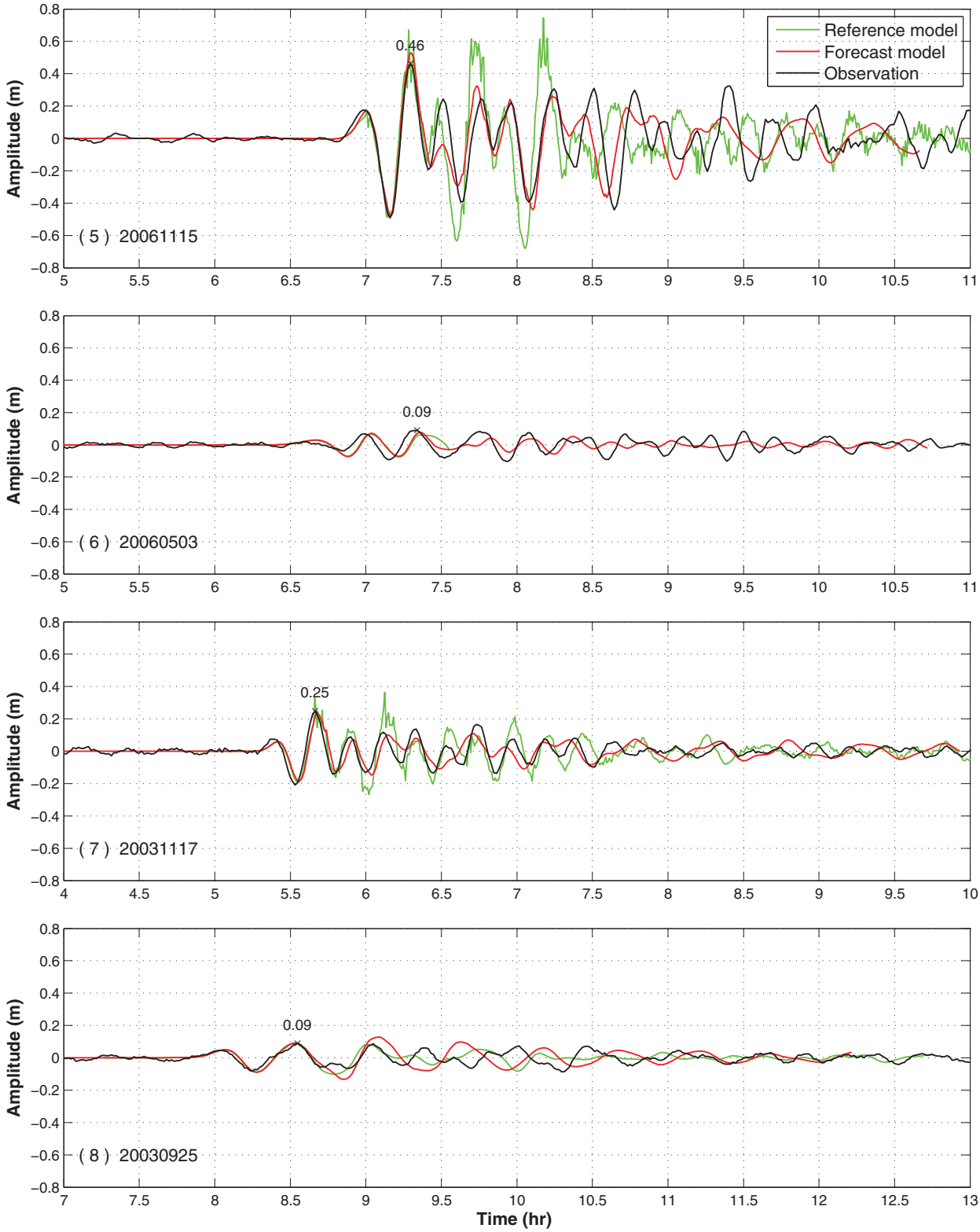

Figure 10: (continued).

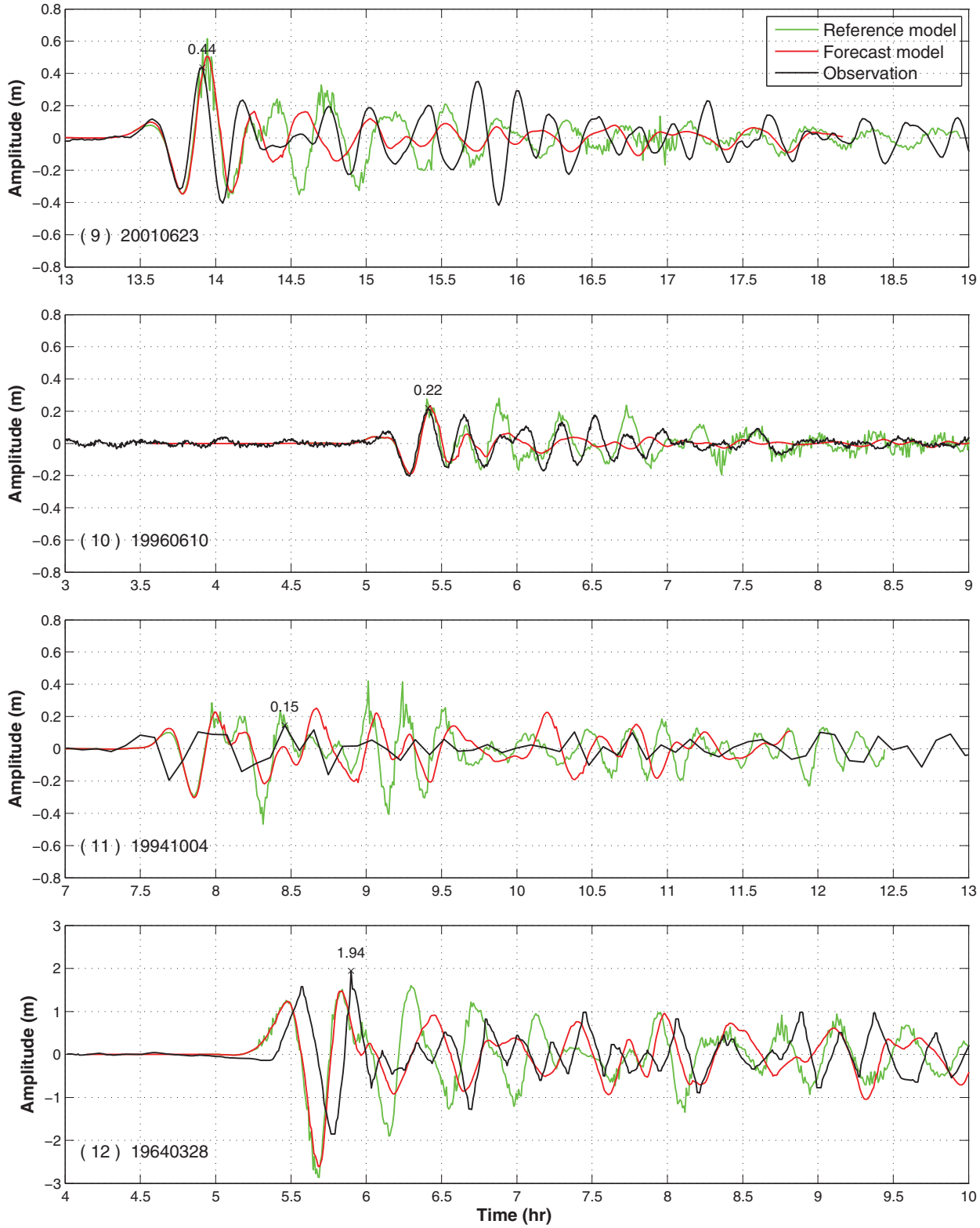

Figure 10: (continued).

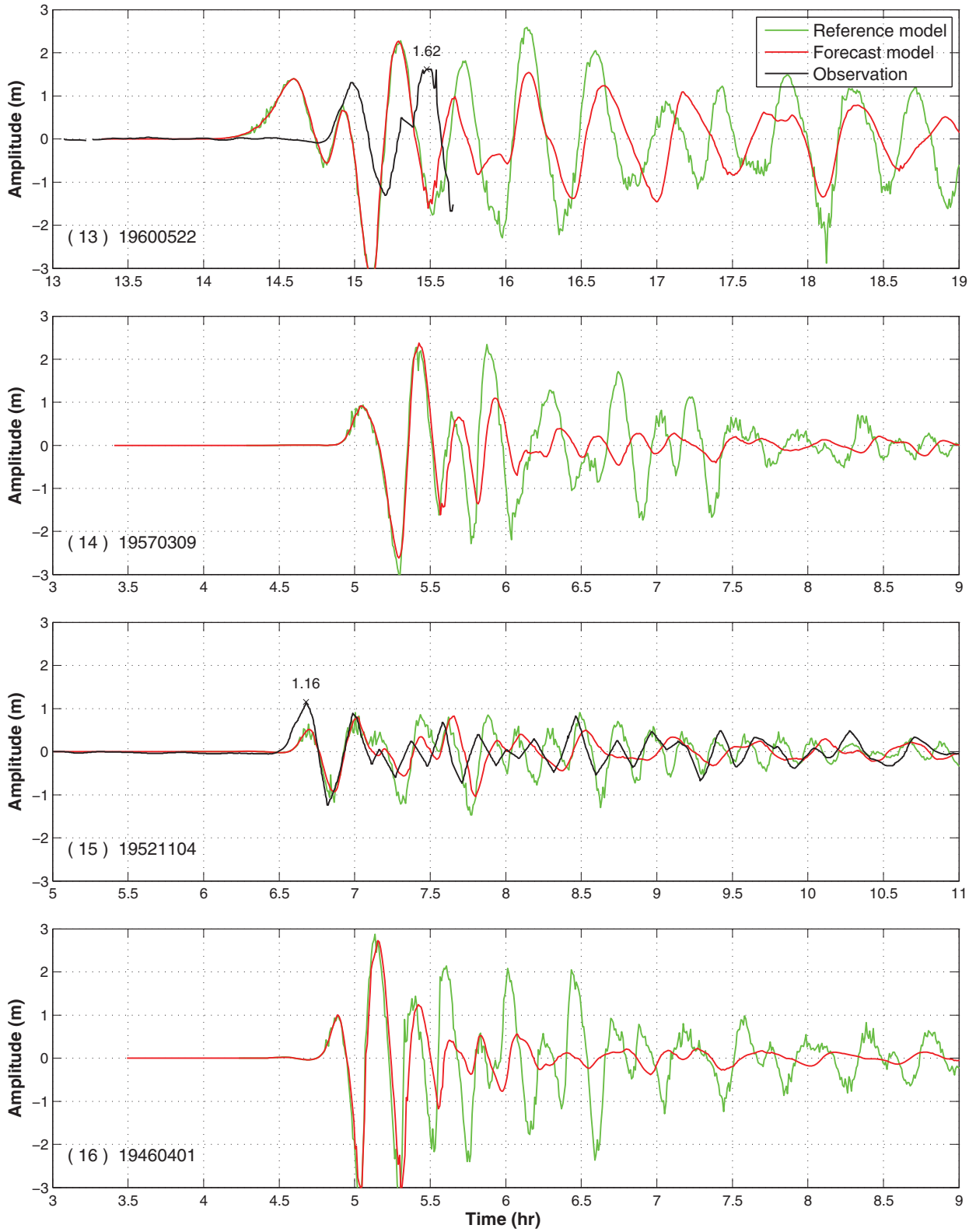

Figure 10: (continued).

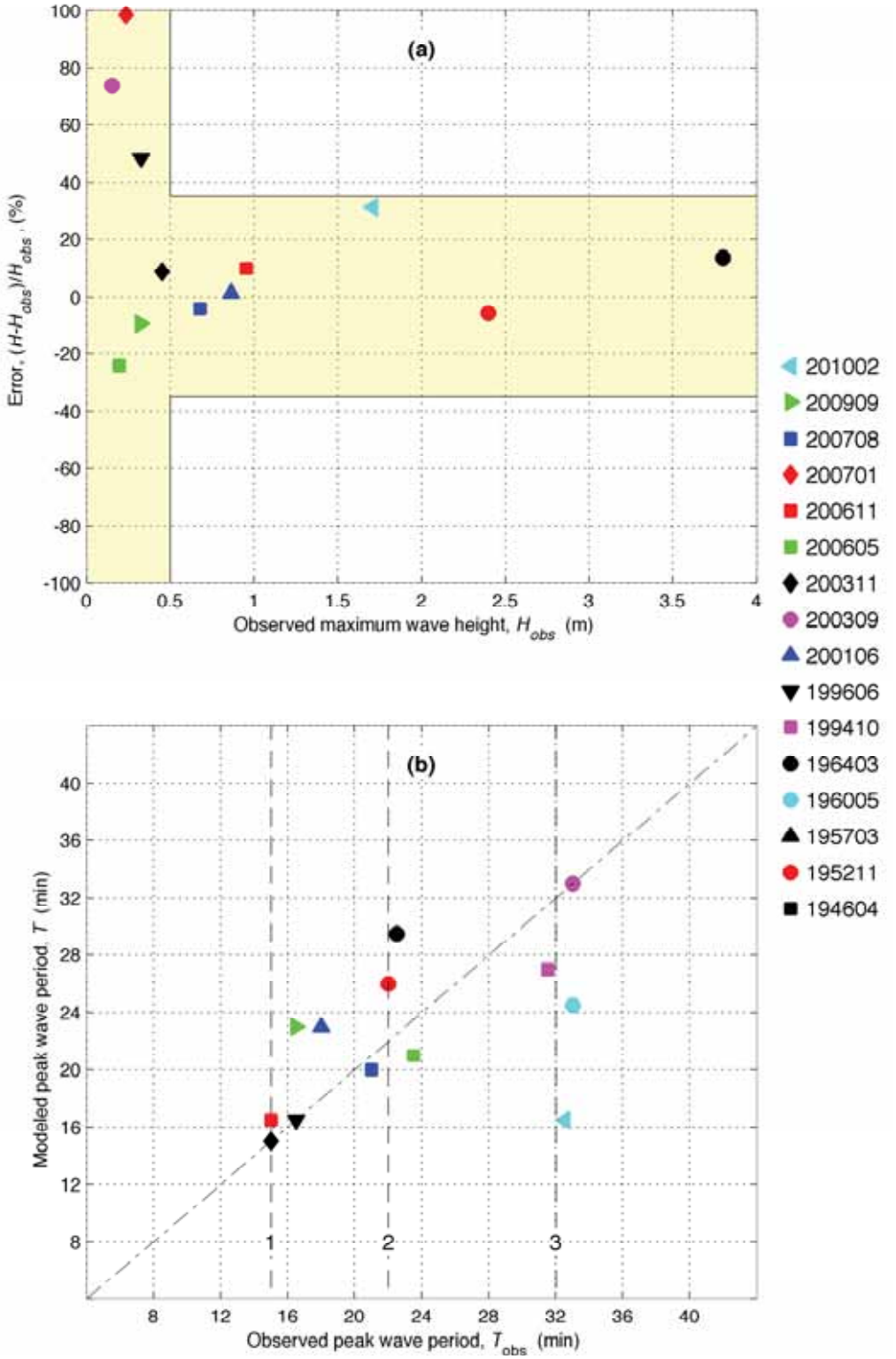

Figure 11: (a) Error of the maximum wave height, and (b) peak wave period from observations and results computed by the Hilo forecast model. Error = $(H–H_{obs})/H_{obs}$, where H is the modeled maximum wave height and H_{obs} is the observation. Colors represent subduction zones of the earthquakes. Red, central Kuril and Kamchatka; magenta, Hokkaido and west Kuril; black, Aleutian and Alaska; green, Tonga; blue, Peru; cyan, Chile.

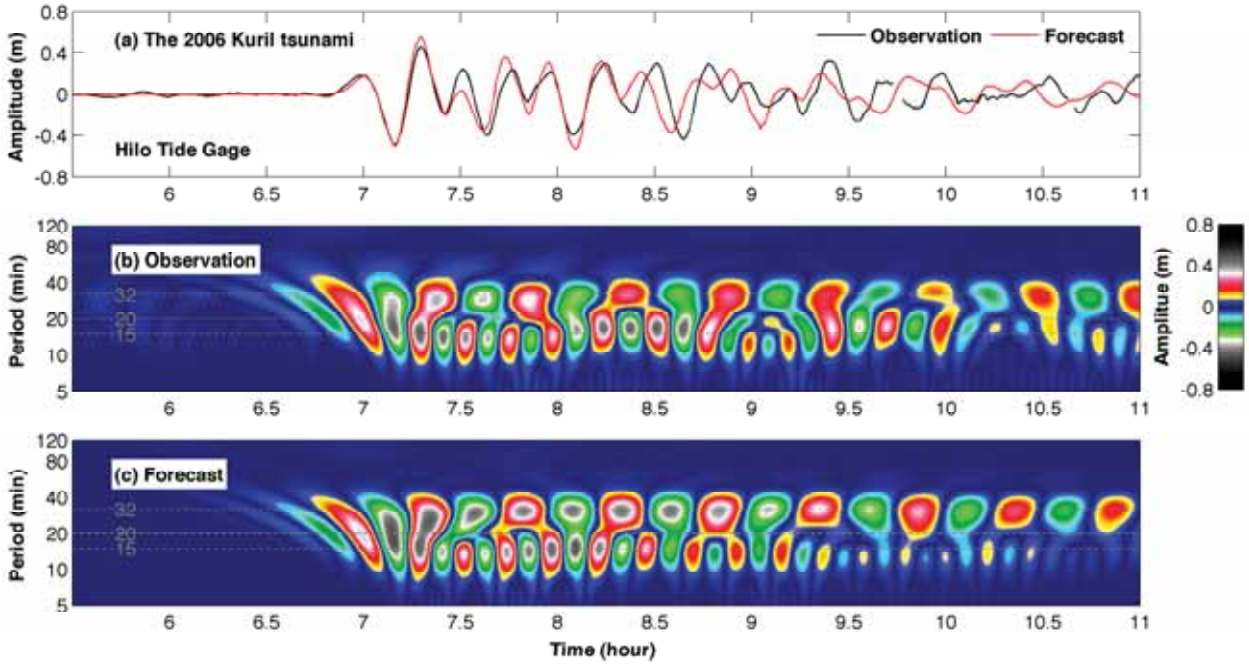

Figure 12: (a) Time series of observed and forecast wave amplitudes at Hilo tide gauge computed by the Hilo forecast model in real time during the November 2006 Kuril Islands tsunami. Real parts of the wavelet-derived amplitude spectra of the observed and modeled tsunami waves are plotted in (b) and (c), respectively.

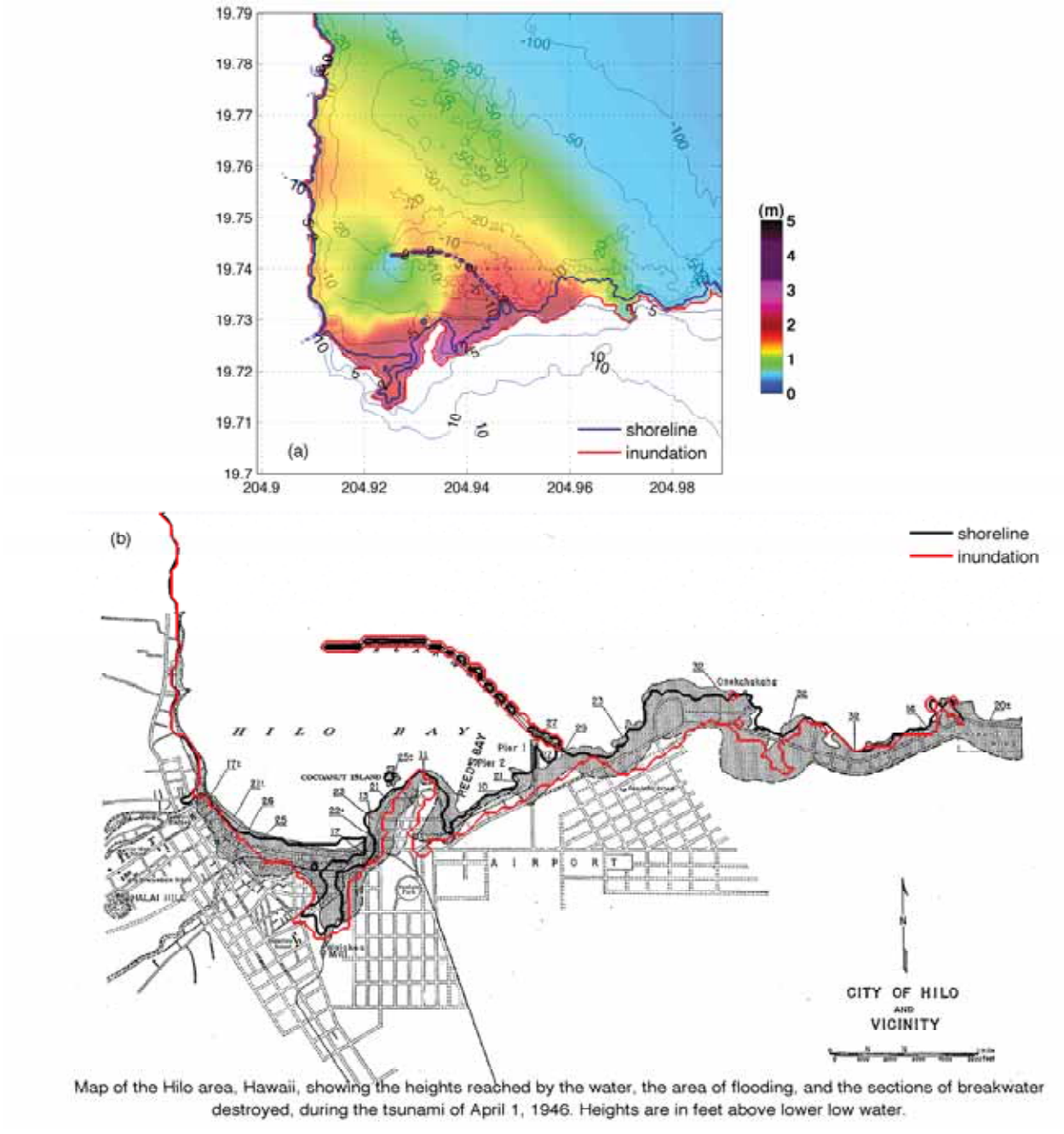

Figure 13: (a) Maximum water elevations at Hilo computed by the forecast model for the 1946 Unimak tsunami. (b) Comparison between computed inundation in (a) and survey data from Shepard *et al.* (1950).

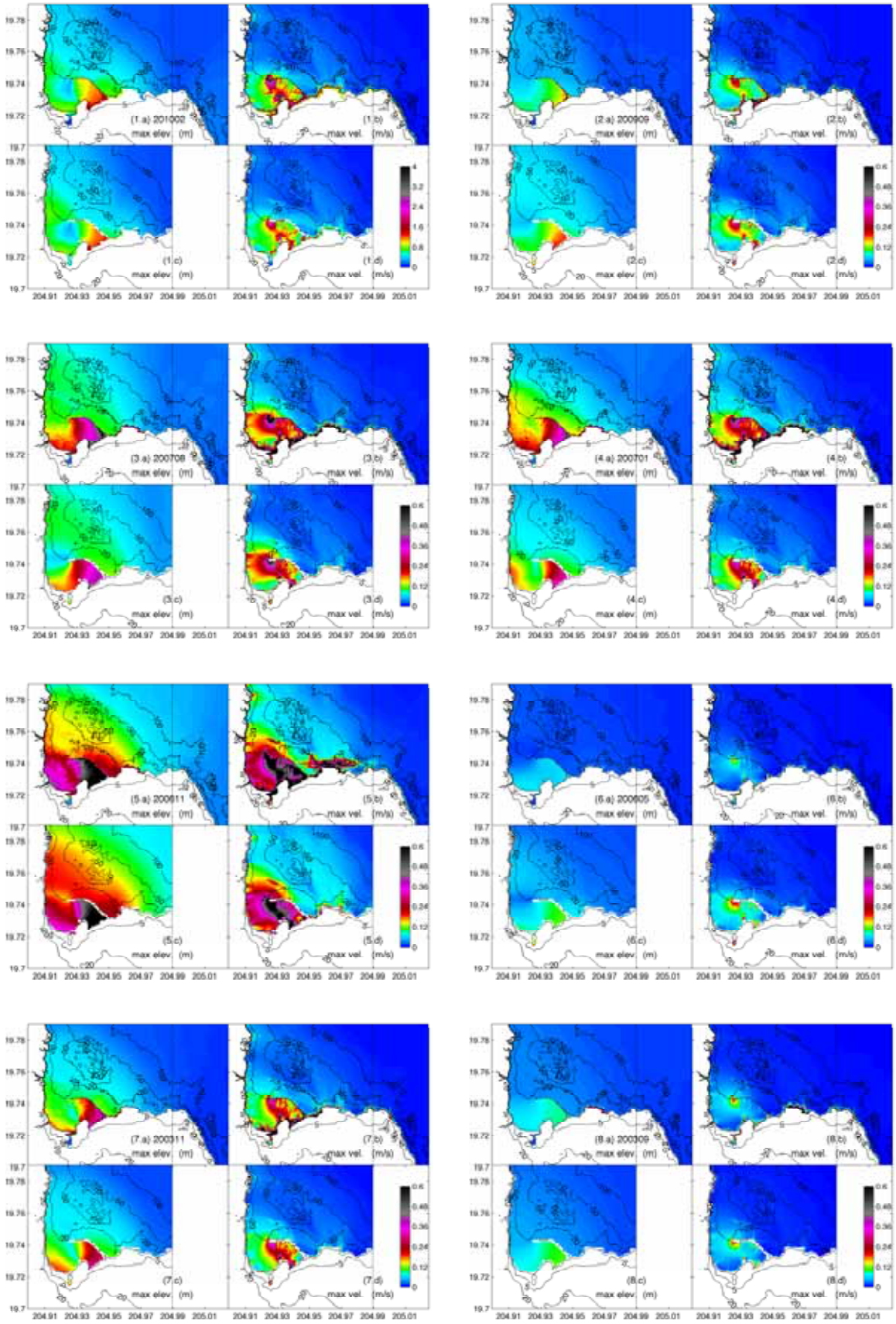

Figure 14: Computed maximum amplitude and velocity by the (a and b) Hilo reference model and (c and d) forecast model for the 16 past tsunamis.

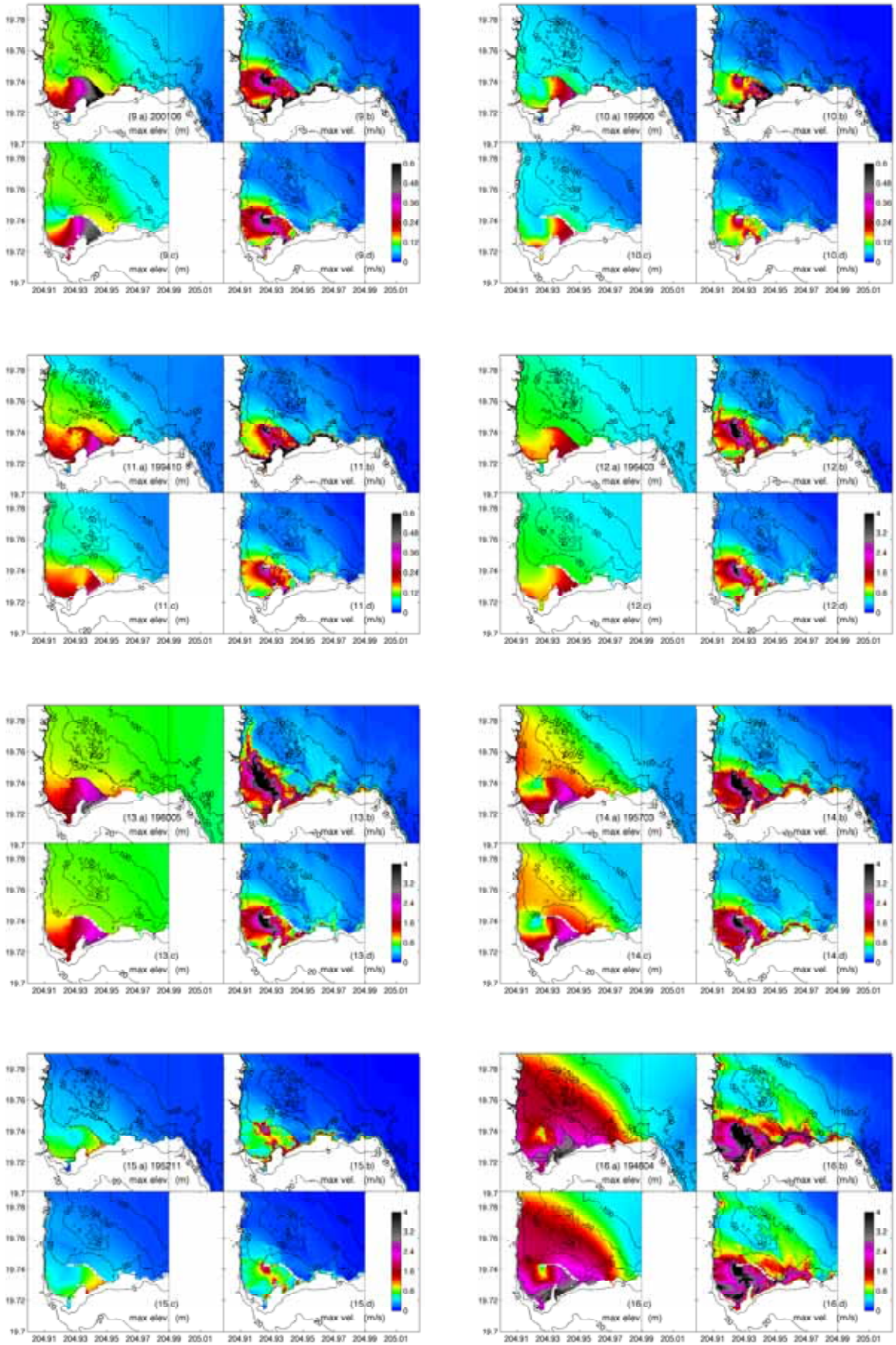

Figure 14: (continued).

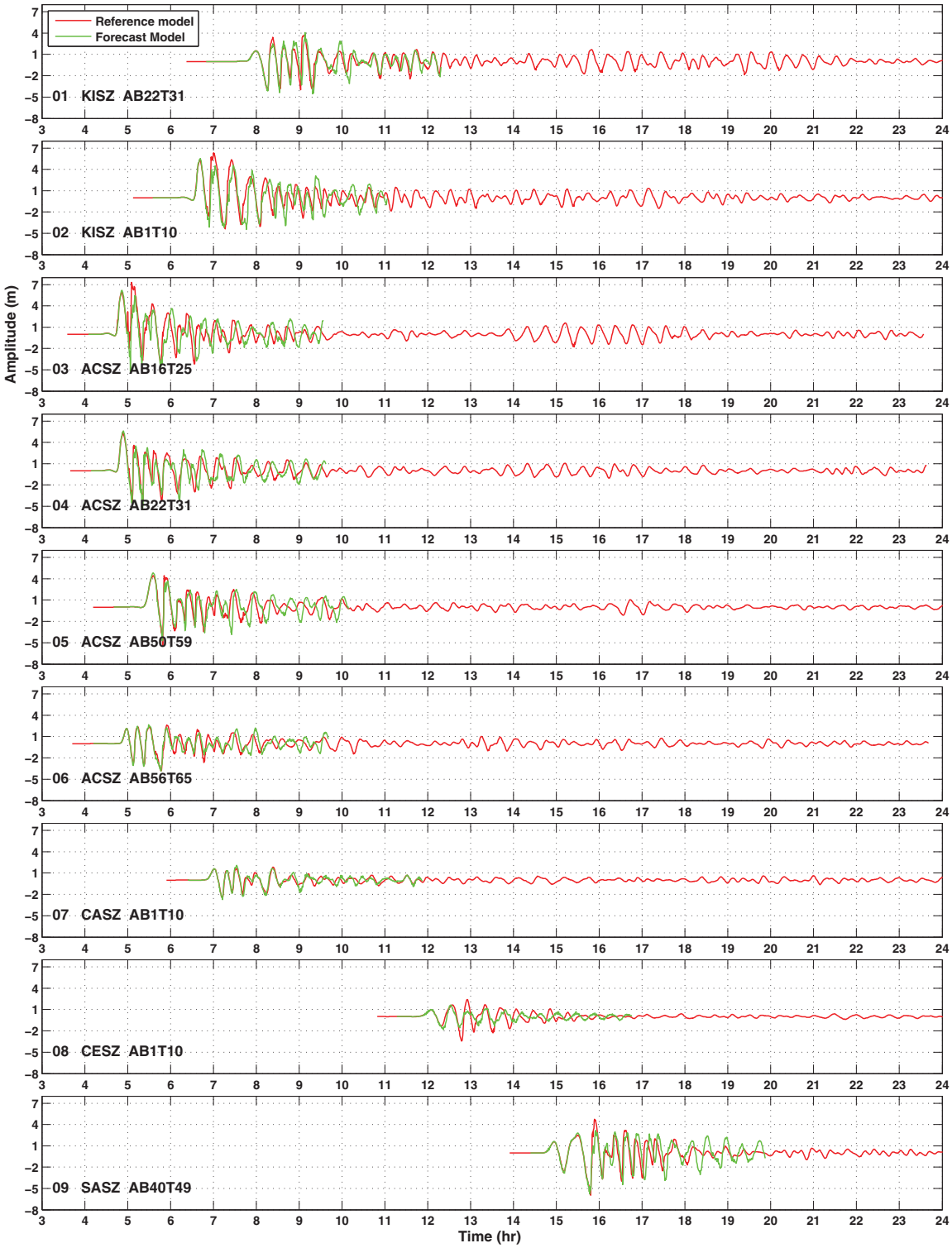

Figure 15: Modeled tsunami time series by the Hilo reference model and forecast model for 18 simulated magnitude 9.3 tsunamis. Locations of the tsunamis can be found in **Figure 1.**

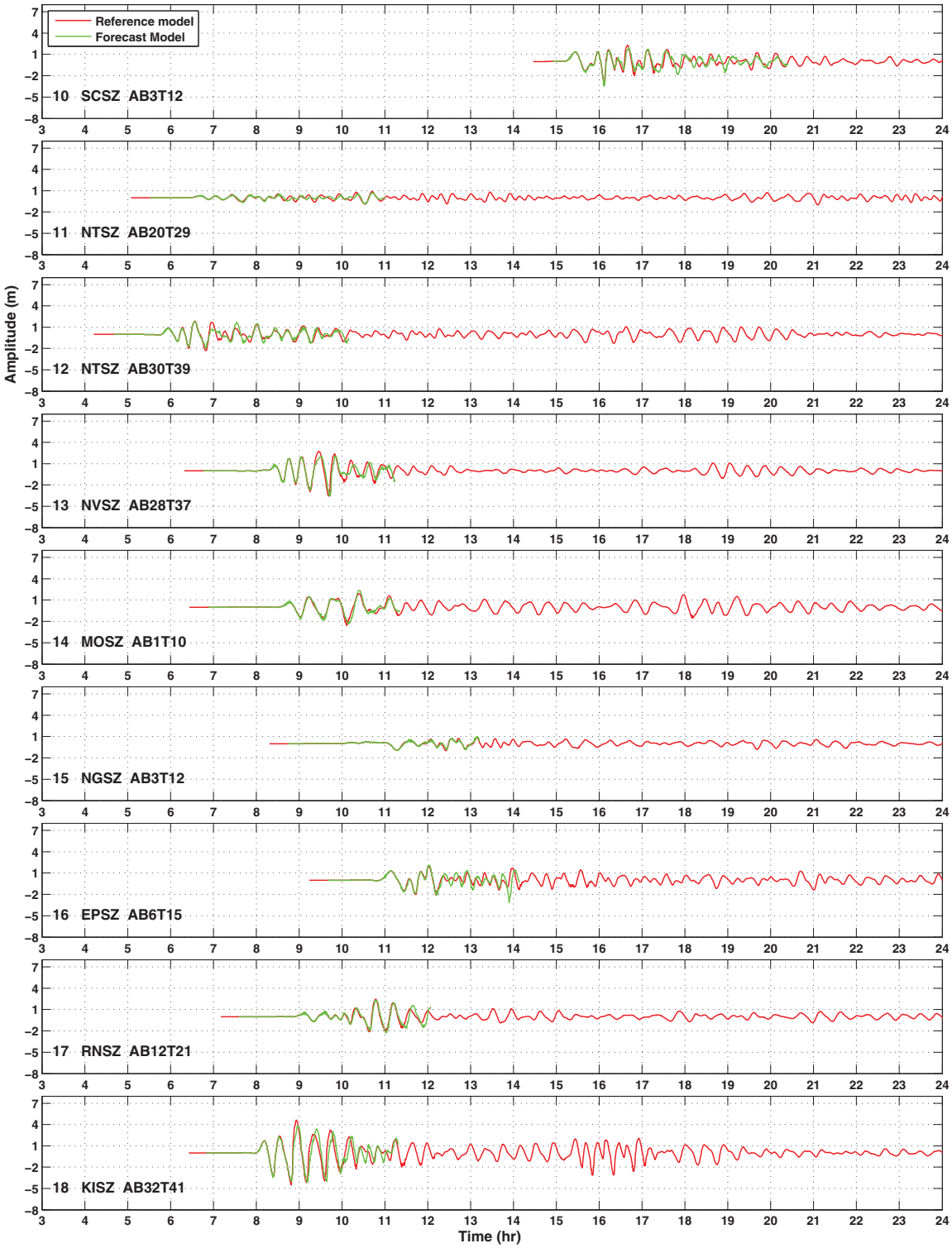

Figure 15: (continued).

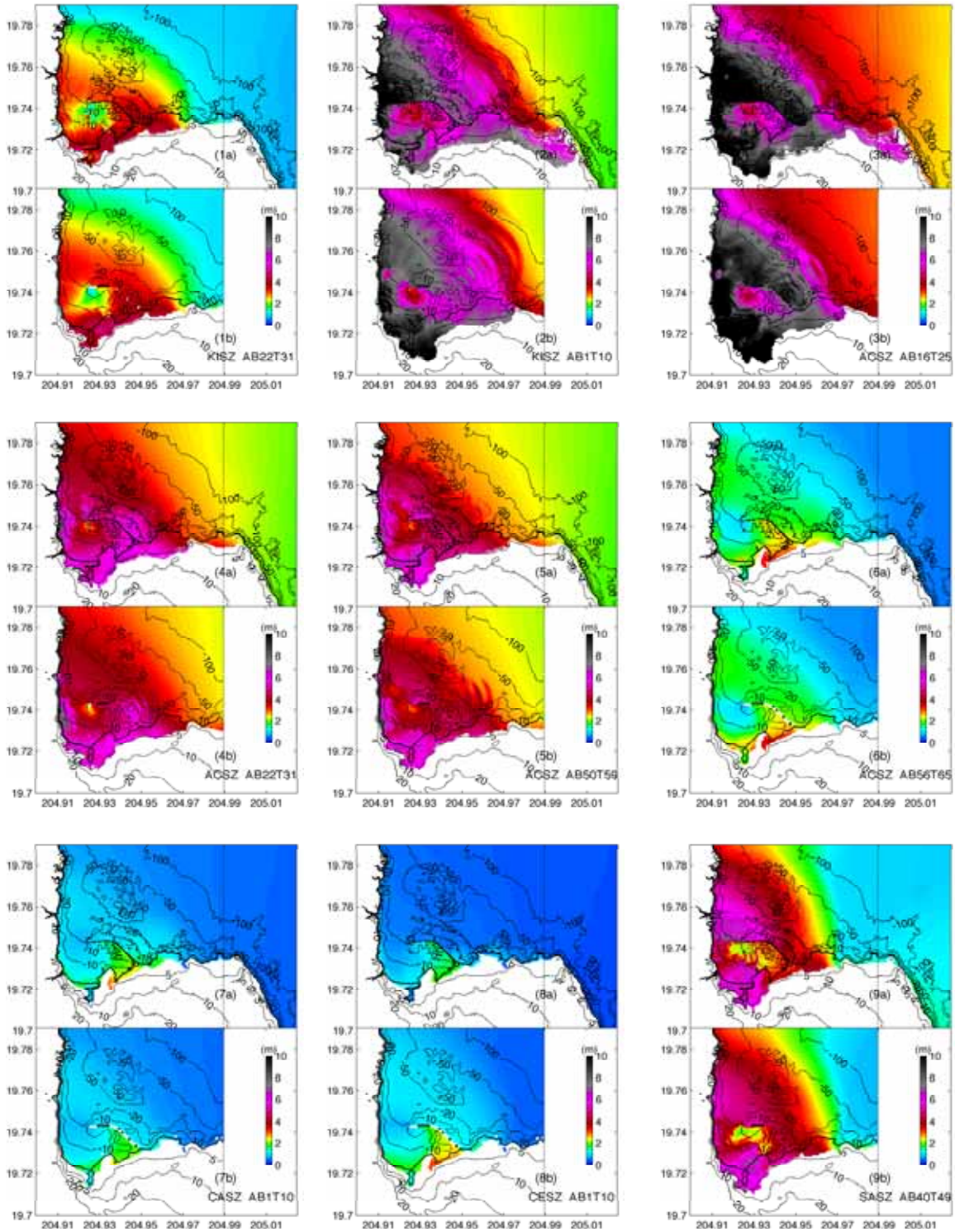

Figure 16: Maximum water elevation computed by the (a) Hilo reference model and (b) forecast model for the 18 simulated magnitude 9.3 tsunamis. Locations of the tsunamis can be found in **Figure 1**.

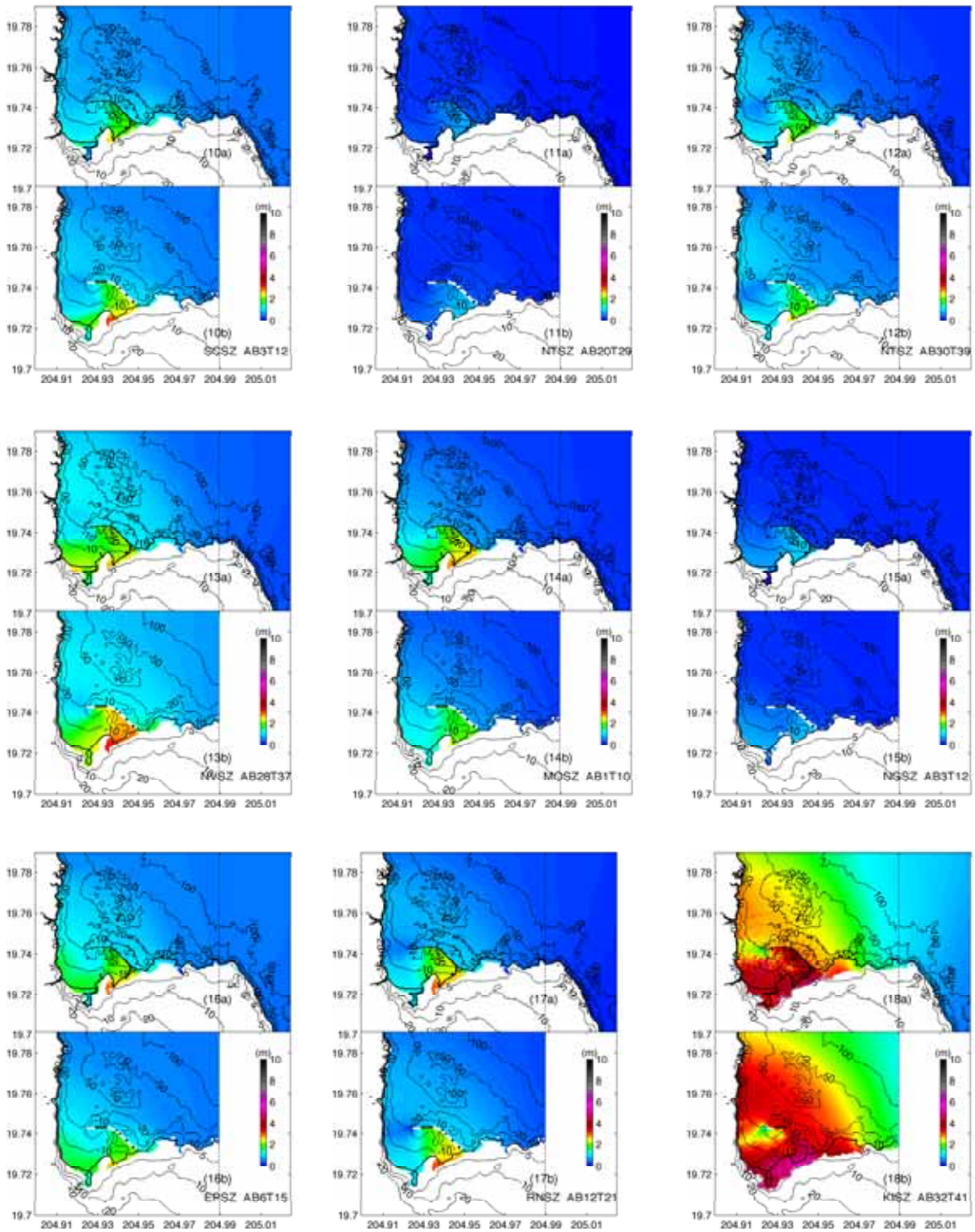

Figure 16: (continued).

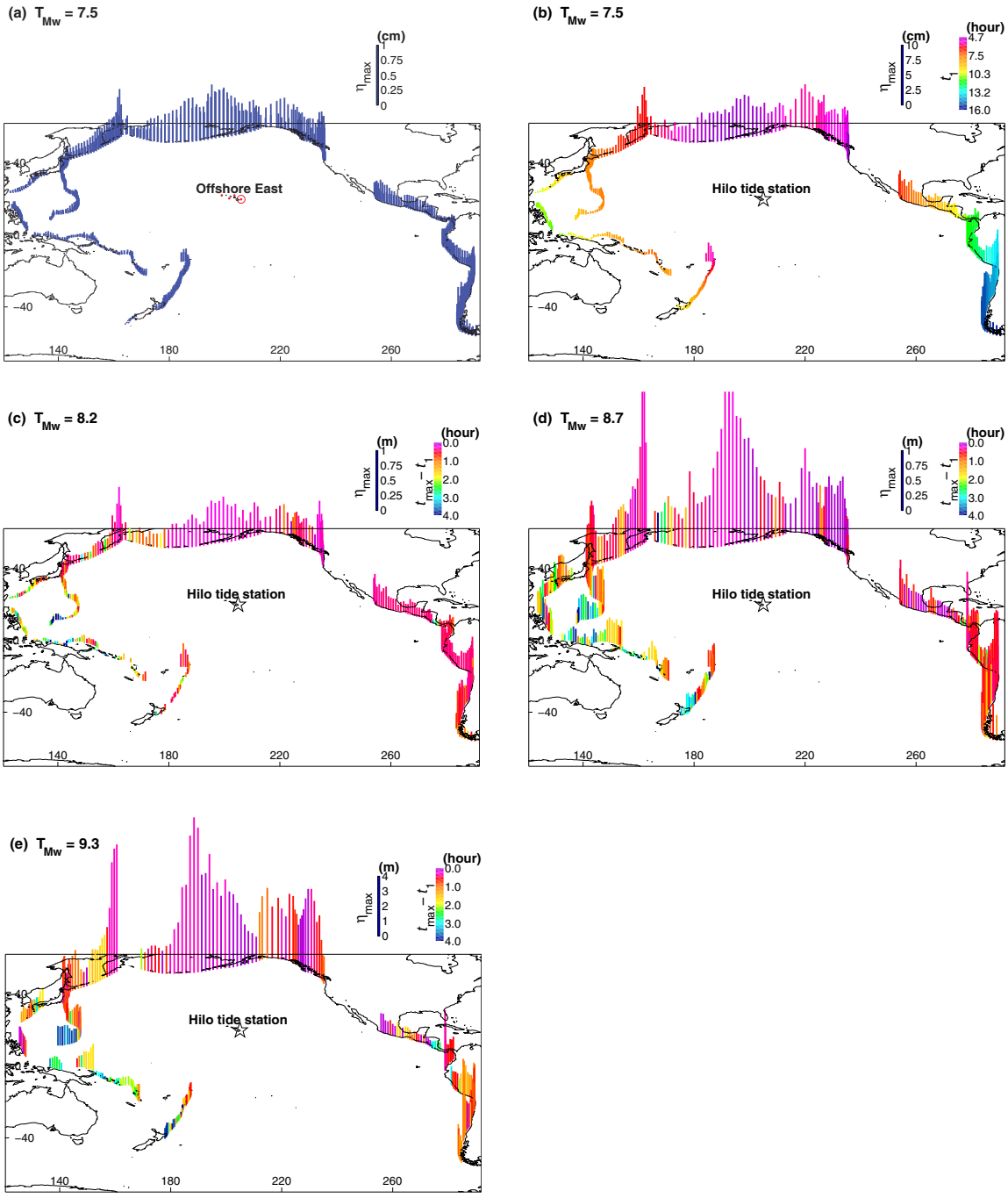

Figure 17: Maximum water elevation at (a) Hilo offshore from the propagation database and (b, c, d, and e) at Hilo tide station computed by the forecast model for simulated magnitude 7.5, 8.2, 8.7, and 9.3 tsunamis. Colors in (b) represent the first arrival at the station. Colors in (c), (d), and (e) represent the difference in time between the arrival of the maximum elevation and the first arrival.

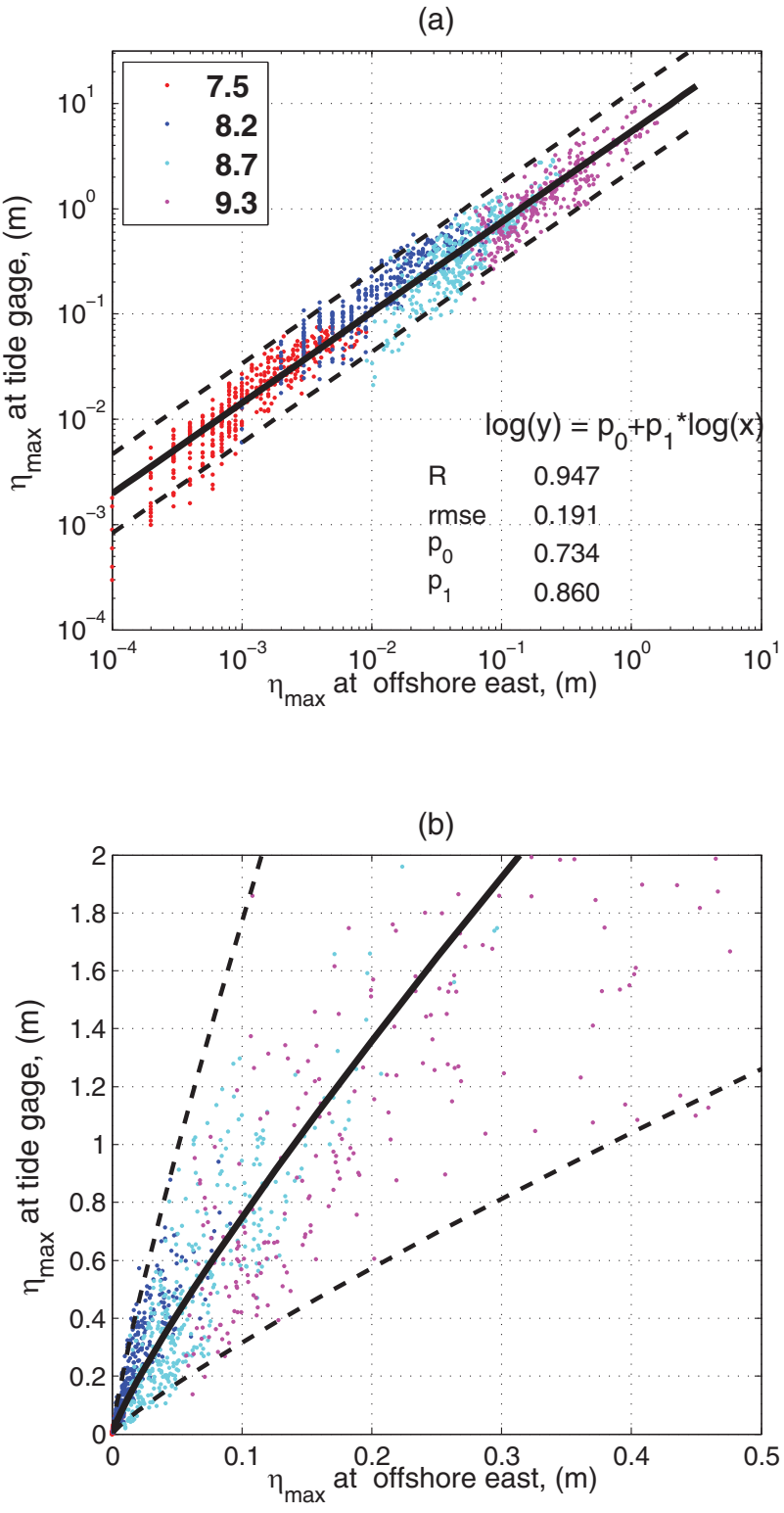

Figure 18: Maximum computed water elevation at offshore deep water and coastal tide stations in (a) logarithmic and (b) Cartesian coordinates. Colors represent tsunami moment magnitudes. Solid lines are the fits by regression analysis in logarithmic scale. Dashed lines are the prediction bounds based on 95% confident level. R, square of the correlation; rmse: root mean squared error; p_0 and p_1, parameters.

Appendix A.

Since the initial development of the Hilo, Hawaii, forecast model (SIM), the parameters for the input file for running the forecast model and reference model (RIM) in MOST have been changed to reflect changes to the MOST model code. The following appendix lists the new input files for Hilo.

A1. Reference model *.in file for Hilo, Hawaii—updated for 2009

```
0.001    Minimum amplitude of input offshore wave (m):
1        Input minimum depth for offshore (m)
0.1      Input "dry land" depth for inundation (m)
0.000625 Input friction coefficient (n**2)
1        runup flag for grids A and B (1=yes,0=no)
300.0    blowup limit
0.15     Input time step (sec)
96000    Input amount of steps
15       Compute "A" arrays every n-th time step, n=
3        Compute "B" arrays every n-th time step, n=
195      Input number of steps between snapshots
1        ...Starting from
1        ...Saving grid every n-th node, n=
```

A2. Forecast model *.in file for Hilo, Hawaii—updated for 2009

```
0.0001   Minimum amplitude of input offshore wave (m):
1        Input minimum depth for offshore (m)
0.1      Input "dry land" depth for inundation (m)
0.000625 Input friction coefficient (n**2)
1        runup flag for grids A and B (1 = yes, 0 = no)
300.0    blowup limit
1.0      Input time step (sec)
36000    Input amount of steps
8        Compute "A" arrays every n-th time step, n=
2        Compute "B" arrays every n-th time step, n=
32       Input number of steps between snapshots
1        ...Starting from
1        ...Saving grid every n-th node, n=
```

Appendix B. Propagation Database: Pacific Ocean Unit Sources

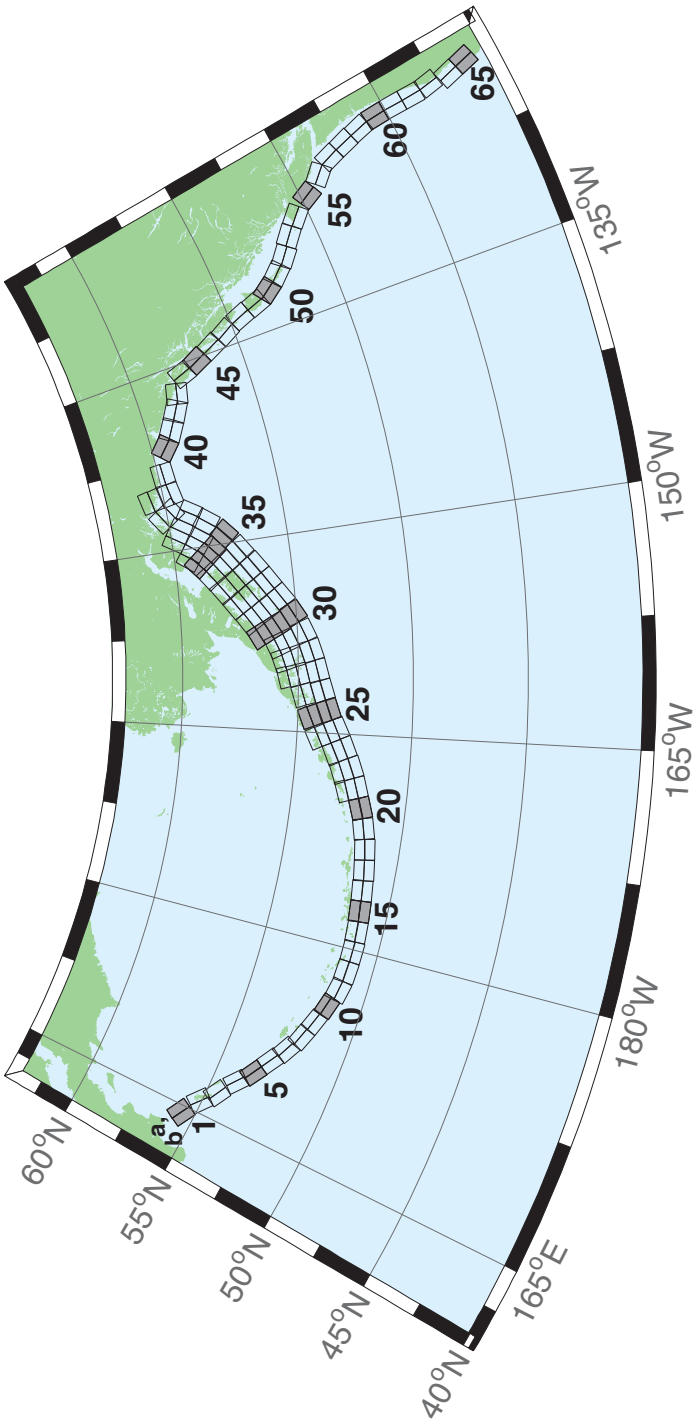

Figure B1: Aleutian–Alaska–Cascadia Subduction Zone unit sources.

Table B1: Earthquake parameters for Aleutian–Alaska–Cascadia Subduction Zone unit sources.

Segment	Description	Longitude (°E)	Latitude (°N)	Strike (°)	Dip (°)	Depth (km)
acsz–1a	Aleutian–Alaska–Cascadia	164.7994	55.9606	299	17	19.61
acsz–1b	Aleutian–Alaska–Cascadia	164.4310	55.5849	299	17	5
acsz–2a	Aleutian–Alaska–Cascadia	166.3418	55.4016	310.2	17	19.61
acsz–2b	Aleutian–Alaska–Cascadia	165.8578	55.0734	310.2	17	5
acsz–3a	Aleutian–Alaska–Cascadia	167.2939	54.8919	300.2	23.36	24.82
acsz–3b	Aleutian–Alaska–Cascadia	166.9362	54.5356	300.2	23.36	5
acsz–4a	Aleutian–Alaska–Cascadia	168.7131	54.2852	310.2	38.51	25.33
acsz–4b	Aleutian–Alaska–Cascadia	168.3269	54.0168	310.2	24	5
acsz–5a	Aleutian–Alaska–Cascadia	169.7447	53.7808	302.8	37.02	23.54
acsz–5b	Aleutian–Alaska–Cascadia	169.4185	53.4793	302.8	21.77	5
acsz–6a	Aleutian–Alaska–Cascadia	171.0144	53.3054	303.2	35.31	22.92
acsz–6b	Aleutian–Alaska–Cascadia	170.6813	52.9986	303.2	21	5
acsz–7a	Aleutian–Alaska–Cascadia	172.1500	52.8528	298.2	35.56	20.16
acsz–7b	Aleutian–Alaska–Cascadia	171.8665	52.5307	298.2	17.65	5
acsz–8a	Aleutian–Alaska–Cascadia	173.2726	52.4579	290.8	37.92	20.35
acsz–8b	Aleutian–Alaska–Cascadia	173.0681	52.1266	290.8	17.88	5
acsz–9a	Aleutian–Alaska–Cascadia	174.5866	52.1434	289	39.09	21.05
acsz–9b	Aleutian–Alaska–Cascadia	174.4027	51.8138	289	18.73	5
acsz–10a	Aleutian–Alaska–Cascadia	175.8784	51.8526	286.1	40.51	20.87
acsz–10b	Aleutian–Alaska–Cascadia	175.7265	51.5245	286.1	18.51	5
acsz–11a	Aleutian–Alaska–Cascadia	177.1140	51.6488	280	15	17.94
acsz–11b	Aleutian–Alaska–Cascadia	176.9937	51.2215	280	15	5
acsz–12a	Aleutian–Alaska–Cascadia	178.4500	51.5690	273	15	17.94
acsz–12b	Aleutian–Alaska–Cascadia	178.4130	51.1200	273	15	5
acsz–13a	Aleutian–Alaska–Cascadia	179.8550	51.5340	271	15	17.94
acsz–13b	Aleutian–Alaska–Cascadia	179.8420	51.0850	271	15	5
acsz–14a	Aleutian–Alaska–Cascadia	181.2340	51.5780	267	15	17.94
acsz–14b	Aleutian–Alaska–Cascadia	181.2720	51.1290	267	15	5
acsz–15a	Aleutian–Alaska–Cascadia	182.6380	51.6470	265	15	17.94
acsz–15b	Aleutian–Alaska–Cascadia	182.7000	51.2000	265	15	5
acsz–16a	Aleutian–Alaska–Cascadia	184.0550	51.7250	264	15	17.94
acsz–16b	Aleutian–Alaska–Cascadia	184.1280	51.2780	264	15	5
acsz–17a	Aleutian–Alaska–Cascadia	185.4560	51.8170	262	15	17.94
acsz–17b	Aleutian–Alaska–Cascadia	185.5560	51.3720	262	15	5
acsz–18a	Aleutian–Alaska–Cascadia	186.8680	51.9410	261	15	17.94
acsz–18b	Aleutian–Alaska–Cascadia	186.9810	51.4970	261	15	5
acsz–19a	Aleutian–Alaska–Cascadia	188.2430	52.1280	257	15	17.94
acsz–19b	Aleutian–Alaska–Cascadia	188.4060	51.6900	257	15	5
acsz–20a	Aleutian–Alaska–Cascadia	189.5810	52.3550	251	15	17.94
acsz–20b	Aleutian–Alaska–Cascadia	189.8180	51.9300	251	15	5
acsz–21a	Aleutian–Alaska–Cascadia	190.9570	52.6470	251	15	17.94
acsz–21b	Aleutian–Alaska–Cascadia	191.1960	52.2220	251	15	5
acsz–21z	Aleutian–Alaska–Cascadia	190.7399	53.0443	250.8	15	30.88
acsz–22a	Aleutian–Alaska–Cascadia	192.2940	52.9430	247	15	17.94
acsz–22b	Aleutian–Alaska–Cascadia	192.5820	52.5300	247	15	5
acsz–22z	Aleutian–Alaska–Cascadia	192.0074	53.3347	247.8	15	30.88
acsz–23a	Aleutian–Alaska–Cascadia	193.6270	53.3070	245	15	17.94
acsz–23b	Aleutian–Alaska–Cascadia	193.9410	52.9000	245	15	5
acsz–23z	Aleutian–Alaska–Cascadia	193.2991	53.6768	244.6	15	30.88
acsz–24a	Aleutian–Alaska–Cascadia	194.9740	53.6870	245	15	17.94
acsz–24b	Aleutian–Alaska–Cascadia	195.2910	53.2800	245	15	5
acsz–24y	Aleutian–Alaska–Cascadia	194.3645	54.4604	244.4	15	43.82
acsz–24z	Aleutian–Alaska–Cascadia	194.6793	54.0674	244.6	15	30.88
acsz–25a	Aleutian–Alaska–Cascadia	196.4340	54.0760	250	15	17.94
acsz–25b	Aleutian–Alaska–Cascadia	196.6930	53.6543	250	15	5

(continued on next page)

Table B1: (continued)

Segment	Description	Longitude (°E)	Latitude (°N)	Strike (°)	Dip (°)	Depth (km)
acsz–25y	Aleutian–Alaska–Cascadia	195.9009	54.8572	247.9	15	43.82
acsz–25z	Aleutian–Alaska–Cascadia	196.1761	54.4536	248.1	15	30.88
acsz–26a	Aleutian–Alaska–Cascadia	197.8970	54.3600	253	15	17.94
acsz–26b	Aleutian–Alaska–Cascadia	198.1200	53.9300	253	15	5
acsz–26y	Aleutian–Alaska–Cascadia	197.5498	55.1934	253.1	15	43.82
acsz–26z	Aleutian–Alaska–Cascadia	197.7620	54.7770	253.3	15	30.88
acsz–27a	Aleutian–Alaska–Cascadia	199.4340	54.5960	256	15	17.94
acsz–27b	Aleutian–Alaska–Cascadia	199.6200	54.1600	256	15	5
acsz–27x	Aleutian–Alaska–Cascadia	198.9736	55.8631	256.5	15	56.24
acsz–27y	Aleutian–Alaska–Cascadia	199.1454	55.4401	256.6	15	43.82
acsz–27z	Aleutian–Alaska–Cascadia	199.3135	55.0170	256.8	15	30.88
acsz–28a	Aleutian–Alaska–Cascadia	200.8820	54.8300	253	15	17.94
acsz–28b	Aleutian–Alaska–Cascadia	201.1080	54.4000	253	15	5
acsz–28x	Aleutian–Alaska–Cascadia	200.1929	56.0559	252.5	15	56.24
acsz–28y	Aleutian–Alaska–Cascadia	200.4167	55.6406	252.7	15	43.82
acsz–28z	Aleutian–Alaska–Cascadia	200.6360	55.2249	252.9	15	30.88
acsz–29a	Aleutian–Alaska–Cascadia	202.2610	55.1330	247	15	17.94
acsz–29b	Aleutian–Alaska–Cascadia	202.5650	54.7200	247	15	5
acsz–29x	Aleutian–Alaska–Cascadia	201.2606	56.2861	245.7	15	56.24
acsz–29y	Aleutian–Alaska–Cascadia	201.5733	55.8888	246	15	43.82
acsz–29z	Aleutian–Alaska–Cascadia	201.8797	55.4908	246.2	15	30.88
acsz–30a	Aleutian–Alaska–Cascadia	203.6040	55.5090	240	15	17.94
acsz–30b	Aleutian–Alaska–Cascadia	203.9970	55.1200	240	15	5
acsz–30w	Aleutian–Alaska–Cascadia	201.9901	56.9855	239.5	15	69.12
acsz–30x	Aleutian–Alaska–Cascadia	202.3851	56.6094	239.8	15	56.24
acsz–30y	Aleutian–Alaska–Cascadia	202.7724	56.2320	240.2	15	43.82
acsz–30z	Aleutian–Alaska–Cascadia	203.1521	55.8534	240.5	15	30.88
acsz–31a	Aleutian–Alaska–Cascadia	204.8950	55.9700	236	15	17.94
acsz–31b	Aleutian–Alaska–Cascadia	205.3400	55.5980	236	15	5
acsz–31w	Aleutian–Alaska–Cascadia	203.0825	57.3740	234.5	15	69.12
acsz–31x	Aleutian–Alaska–Cascadia	203.5408	57.0182	234.9	15	56.24
acsz–31y	Aleutian–Alaska–Cascadia	203.9904	56.6607	235.3	15	43.82
acsz–31z	Aleutian–Alaska–Cascadia	204.4315	56.3016	235.7	15	30.88
acsz–32a	Aleutian–Alaska–Cascadia	206.2080	56.4730	236	15	17.94
acsz–32b	Aleutian–Alaska–Cascadia	206.6580	56.1000	236	15	5
acsz–32w	Aleutian–Alaska–Cascadia	204.4129	57.8908	234.3	15	69.12
acsz–32x	Aleutian–Alaska–Cascadia	204.8802	57.5358	234.7	15	56.24
acsz–32y	Aleutian–Alaska–Cascadia	205.3385	57.1792	235.1	15	43.82
acsz–32z	Aleutian–Alaska–Cascadia	205.7880	56.8210	235.5	15	30.88
acsz–33a	Aleutian–Alaska–Cascadia	207.5370	56.9750	236	15	17.94
acsz–33b	Aleutian–Alaska–Cascadia	207.9930	56.6030	236	15	5
acsz–33w	Aleutian–Alaska–Cascadia	205.7126	58.3917	234.2	15	69.12
acsz–33x	Aleutian–Alaska–Cascadia	206.1873	58.0371	234.6	15	56.24
acsz–33y	Aleutian–Alaska–Cascadia	206.6527	57.6808	235	15	43.82
acsz–33z	Aleutian–Alaska–Cascadia	207.1091	57.3227	235.4	15	30.88
acsz–34a	Aleutian–Alaska–Cascadia	208.9371	57.5124	236	15	17.94
acsz–34b	Aleutian–Alaska–Cascadia	209.4000	57.1400	236	15	5
acsz–34w	Aleutian–Alaska–Cascadia	206.9772	58.8804	233.5	15	69.12
acsz–34x	Aleutian–Alaska–Cascadia	207.4677	58.5291	233.9	15	56.24
acsz–34y	Aleutian–Alaska–Cascadia	207.9485	58.1760	234.3	15	43.82
acsz–34z	Aleutian–Alaska–Cascadia	208.4198	57.8213	234.7	15	30.88
acsz–35a	Aleutian–Alaska–Cascadia	210.2597	58.0441	230	15	17.94
acsz–35b	Aleutian–Alaska–Cascadia	210.8000	57.7000	230	15	5
acsz–35w	Aleutian–Alaska–Cascadia	208.0204	59.3199	228.8	15	69.12
acsz–35x	Aleutian–Alaska–Cascadia	208.5715	58.9906	229.3	15	56.24

(continued on next page)

Table B1: (continued)

Segment	Description	Longitude (°E)	Latitude (°N)	Strike (°)	Dip (°)	Depth (km)
acsz–35y	Aleutian–Alaska–Cascadia	209.1122	58.6590	229.7	15	43.82
acsz–35z	Aleutian–Alaska–Cascadia	209.6425	58.3252	230.2	15	30.88
acsz–36a	Aleutian–Alaska–Cascadia	211.3249	58.6565	218	15	17.94
acsz–36b	Aleutian–Alaska–Cascadia	212.0000	58.3800	218	15	5
acsz–36w	Aleutian–Alaska–Cascadia	208.5003	59.5894	215.6	15	69.12
acsz–36x	Aleutian–Alaska–Cascadia	209.1909	59.3342	216.2	15	56.24
acsz–36y	Aleutian–Alaska–Cascadia	209.8711	59.0753	216.8	15	43.82
acsz–36z	Aleutian–Alaska–Cascadia	210.5412	58.8129	217.3	15	30.88
acsz–37a	Aleutian–Alaska–Cascadia	212.2505	59.2720	213.7	15	17.94
acsz–37b	Aleutian–Alaska–Cascadia	212.9519	59.0312	213.7	15	5
acsz–37x	Aleutian–Alaska–Cascadia	210.1726	60.0644	213	15	56.24
acsz–37y	Aleutian–Alaska–Cascadia	210.8955	59.8251	213.7	15	43.82
acsz–37z	Aleutian–Alaska–Cascadia	211.6079	59.5820	214.3	15	30.88
acsz–38a	Aleutian–Alaska–Cascadia	214.6555	60.1351	260.1	0	15
acsz–38b	Aleutian–Alaska–Cascadia	214.8088	59.6927	260.1	0	15
acsz–38y	Aleutian–Alaska–Cascadia	214.3737	60.9838	259	0	15
acsz–38z	Aleutian–Alaska–Cascadia	214.5362	60.5429	259	0	15
acsz–39a	Aleutian–Alaska–Cascadia	216.5607	60.2480	267	0	15
acsz–39b	Aleutian–Alaska–Cascadia	216.6068	59.7994	267	0	15
acsz–40a	Aleutian–Alaska–Cascadia	219.3069	59.7574	310.9	0	15
acsz–40b	Aleutian–Alaska–Cascadia	218.7288	59.4180	310.9	0	15
acsz–41a	Aleutian–Alaska–Cascadia	220.4832	59.3390	300.7	0	15
acsz–41b	Aleutian–Alaska–Cascadia	220.0382	58.9529	300.7	0	15
acsz–42a	Aleutian–Alaska–Cascadia	221.8835	58.9310	298.9	0	15
acsz–42b	Aleutian–Alaska–Cascadia	221.4671	58.5379	298.9	0	15
acsz–43a	Aleutian–Alaska–Cascadia	222.9711	58.6934	282.3	0	15
acsz–43b	Aleutian–Alaska–Cascadia	222.7887	58.2546	282.3	0	15
acsz–44a	Aleutian–Alaska–Cascadia	224.9379	57.9054	340.9	12	11.09
acsz–44b	Aleutian–Alaska–Cascadia	224.1596	57.7617	340.9	7	5
acsz–45a	Aleutian–Alaska–Cascadia	225.4994	57.1634	334.1	12	11.09
acsz–45b	Aleutian–Alaska–Cascadia	224.7740	56.9718	334.1	7	5
acsz–46a	Aleutian–Alaska–Cascadia	226.1459	56.3552	334.1	12	11.09
acsz–46b	Aleutian–Alaska–Cascadia	225.4358	56.1636	334.1	7	5
acsz–47a	Aleutian–Alaska–Cascadia	226.7731	55.5830	332.3	12	11.09
acsz–47b	Aleutian–Alaska–Cascadia	226.0887	55.3785	332.3	7	5
acsz–48a	Aleutian–Alaska–Cascadia	227.4799	54.6763	339.4	12	11.09
acsz–48b	Aleutian–Alaska–Cascadia	226.7713	54.5217	339.4	7	5
acsz–49a	Aleutian–Alaska–Cascadia	227.9482	53.8155	341.2	12	11.09
acsz–49b	Aleutian–Alaska–Cascadia	227.2462	53.6737	341.2	7	5
acsz–50a	Aleutian–Alaska–Cascadia	228.3970	53.2509	324.5	12	11.09
acsz–50b	Aleutian–Alaska–Cascadia	227.8027	52.9958	324.5	7	5
acsz–51a	Aleutian–Alaska–Cascadia	229.1844	52.6297	318.4	12	11.09
acsz–51b	Aleutian–Alaska–Cascadia	228.6470	52.3378	318.4	7	5
acsz–52a	Aleutian–Alaska–Cascadia	230.0306	52.0768	310.9	12	11.09
acsz–52b	Aleutian–Alaska–Cascadia	229.5665	51.7445	310.9	7	5
acsz–53a	Aleutian–Alaska–Cascadia	231.1735	51.5258	310.9	12	11.09
acsz–53b	Aleutian–Alaska–Cascadia	230.7150	51.1935	310.9	7	5
acsz–54a	Aleutian–Alaska–Cascadia	232.2453	50.8809	314.1	12	11.09
acsz–54b	Aleutian–Alaska–Cascadia	231.7639	50.5655	314.1	7	5
acsz–55a	Aleutian–Alaska–Cascadia	233.3066	49.9032	333.7	12	11.09
acsz–55b	Aleutian–Alaska–Cascadia	232.6975	49.7086	333.7	7	5
acsz–56a	Aleutian–Alaska–Cascadia	234.0588	49.1702	315	11	12.82
acsz–56b	Aleutian–Alaska–Cascadia	233.5849	48.8584	315	9	5
acsz–57a	Aleutian–Alaska–Cascadia	234.9041	48.2596	341	11	12.82
acsz–57b	Aleutian–Alaska–Cascadia	234.2797	48.1161	341	9	5

(continued on next page)

Table B1: (continued)

Segment	Description	Longitude (°E)	Latitude (°N)	Strike (°)	Dip (°)	Depth (km)
acsz–58a	Aleutian–Alaska–Cascadia	235.3021	47.3812	344	11	12.82
acsz–58b	Aleutian–Alaska–Cascadia	234.6776	47.2597	344	9	5
acsz–59a	Aleutian–Alaska–Cascadia	235.6432	46.5082	345	11	12.82
acsz–59b	Aleutian–Alaska–Cascadia	235.0257	46.3941	345	9	5
acsz–60a	Aleutian–Alaska–Cascadia	235.8640	45.5429	356	11	12.82
acsz–60b	Aleutian–Alaska–Cascadia	235.2363	45.5121	356	9	5
acsz–61a	Aleutian–Alaska–Cascadia	235.9106	44.6227	359	11	12.82
acsz–61b	Aleutian–Alaska–Cascadia	235.2913	44.6150	359	9	5
acsz–62a	Aleutian–Alaska–Cascadia	235.9229	43.7245	359	11	12.82
acsz–62b	Aleutian–Alaska–Cascadia	235.3130	43.7168	359	9	5
acsz–63a	Aleutian–Alaska–Cascadia	236.0220	42.9020	350	11	12.82
acsz–63b	Aleutian–Alaska–Cascadia	235.4300	42.8254	350	9	5
acsz–64a	Aleutian–Alaska–Cascadia	235.9638	41.9818	345	11	12.82
acsz–64b	Aleutian–Alaska–Cascadia	235.3919	41.8677	345	9	5
acsz–65a	Aleutian–Alaska–Cascadia	236.2643	41.1141	345	11	12.82
acsz–65b	Aleutian–Alaska–Cascadia	235.7000	41.0000	345	9	5
acsz–238a	Aleutian–Alaska–Cascadia	213.2878	59.8406	236.8	15	17.94
acsz–238y	Aleutian–Alaska–Cascadia	212.3424	60.5664	236.8	15	43.82
acsz–238z	Aleutian–Alaska–Cascadia	212.8119	60.2035	236.8	15	30.88

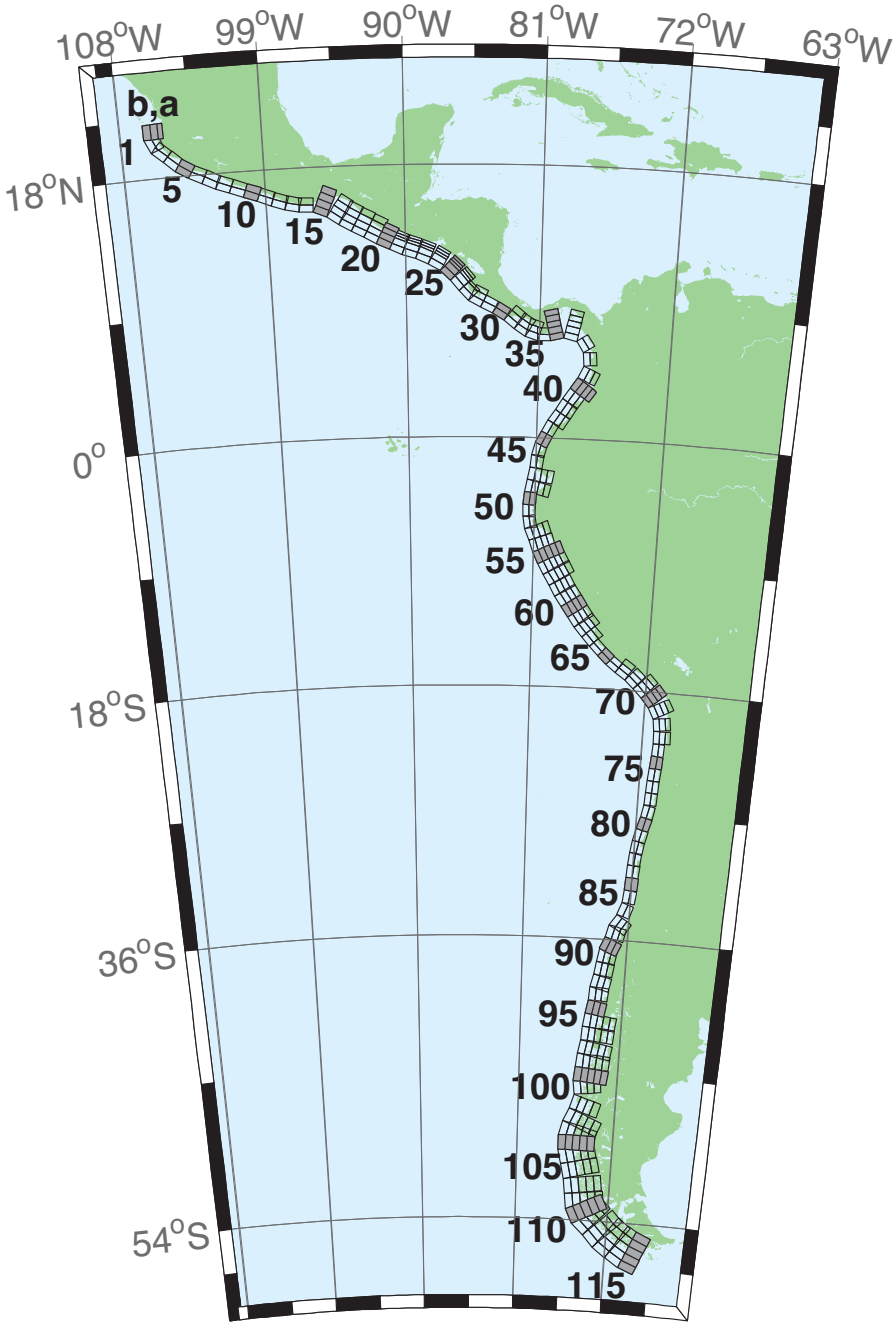

Figure B2: Central and South America Subduction Zone unit sources.

Table B2: Earthquake parameters for Central and South America Subduction Zone unit sources.

Segment	Description	Longitude (°E)	Latitude (°N)	Strike (°)	Dip (°)	Depth (km)
cssz–1a	Central and South America	254.4573	20.8170	359	19	15.4
cssz–1b	Central and South America	254.0035	20.8094	359	12	5
cssz–1z	Central and South America	254.7664	20.8222	359	50	31.67
cssz–2a	Central and South America	254.5765	20.2806	336.8	19	15.4
cssz–2b	Central and South America	254.1607	20.1130	336.8	12	5
cssz–3a	Central and South America	254.8789	19.8923	310.6	18.31	15.27
cssz–3b	Central and South America	254.5841	19.5685	310.6	11.85	5
cssz–4a	Central and South America	255.6167	19.2649	313.4	17.62	15.12
cssz–4b	Central and South America	255.3056	18.9537	313.4	11.68	5
cssz–5a	Central and South America	256.2240	18.8148	302.7	16.92	15
cssz–5b	Central and South America	255.9790	18.4532	302.7	11.54	5
cssz–6a	Central and South America	256.9425	18.4383	295.1	16.23	14.87
cssz–6b	Central and South America	256.7495	18.0479	295.1	11.38	5
cssz–7a	Central and South America	257.8137	18.0339	296.9	15.54	14.74
cssz–7b	Central and South America	257.6079	17.6480	296.9	11.23	5
cssz–8a	Central and South America	258.5779	17.7151	290.4	14.85	14.61
cssz–8b	Central and South America	258.4191	17.3082	290.4	11.08	5
cssz–9a	Central and South America	259.4578	17.4024	290.5	14.15	14.47
cssz–9b	Central and South America	259.2983	16.9944	290.5	10.92	5
cssz–10a	Central and South America	260.3385	17.0861	290.8	13.46	14.34
cssz–10b	Central and South America	260.1768	16.6776	290.8	10.77	5
cssz–11a	Central and South America	261.2255	16.7554	291.8	12.77	14.21
cssz–11b	Central and South America	261.0556	16.3487	291.8	10.62	5
cssz–12a	Central and South America	262.0561	16.4603	288.9	12.08	14.08
cssz–12b	Central and South America	261.9082	16.0447	288.9	10.46	5
cssz–13a	Central and South America	262.8638	16.2381	283.2	11.38	13.95
cssz–13b	Central and South America	262.7593	15.8094	283.2	10.31	5
cssz–14a	Central and South America	263.6066	16.1435	272.1	10.69	13.81
cssz–14b	Central and South America	263.5901	15.7024	272.1	10.15	5
cssz–15a	Central and South America	264.8259	15.8829	293	10	13.68
cssz–15b	Central and South America	264.6462	15.4758	293	10	5
cssz–15y	Central and South America	265.1865	16.6971	293	10	31.05
cssz–15z	Central and South America	265.0060	16.2900	293	10	22.36
cssz–16a	Central and South America	265.7928	15.3507	304.9	15	15.82
cssz–16b	Central and South America	265.5353	14.9951	304.9	12.5	5
cssz–16y	Central and South America	266.3092	16.0619	304.9	15	41.7
cssz–16z	Central and South America	266.0508	15.7063	304.9	15	28.76
cssz–17a	Central and South America	266.4947	14.9019	299.5	20	17.94
cssz–17b	Central and South America	266.2797	14.5346	299.5	15	5
cssz–17y	Central and South America	266.9259	15.6365	299.5	20	52.14
cssz–17z	Central and South America	266.7101	15.2692	299.5	20	35.04
cssz–18a	Central and South America	267.2827	14.4768	298	21.5	17.94
cssz–18b	Central and South America	267.0802	14.1078	298	15	5
cssz–18y	Central and South America	267.6888	15.2148	298	21.5	54.59
cssz–18z	Central and South America	267.4856	14.8458	298	21.5	36.27
cssz–19a	Central and South America	268.0919	14.0560	297.6	23	17.94
cssz–19b	Central and South America	267.8943	13.6897	297.6	15	5
cssz–19y	Central and South America	268.4880	14.7886	297.6	23	57.01
cssz–19z	Central and South America	268.2898	14.4223	297.6	23	37.48
cssz–20a	Central and South America	268.8929	13.6558	296.2	24	17.94
cssz–20b	Central and South America	268.7064	13.2877	296.2	15	5
cssz–20y	Central and South America	269.1796	14.2206	296.2	45.5	73.94
cssz–20z	Central and South America	269.0362	13.9382	296.2	45.5	38.28
cssz–21a	Central and South America	269.6797	13.3031	292.6	25	17.94
cssz–21b	Central and South America	269.5187	12.9274	292.6	15	5

(continued on next page)

Table B2: (continued)

Segment	Description	Longitude (°E)	Latitude (°N)	Strike (°)	Dip (°)	Depth (km)
cssz–21x	Central and South America	269.8797	13.7690	292.6	68	131.8
cssz–21y	Central and South America	269.8130	13.6137	292.6	68	85.43
cssz–21z	Central and South America	269.7463	13.4584	292.6	68	39.07
cssz–22a	Central and South America	270.4823	13.0079	288.6	25	17.94
cssz–22b	Central and South America	270.3492	12.6221	288.6	15	5
cssz–22x	Central and South America	270.6476	13.4864	288.6	68	131.8
cssz–22y	Central and South America	270.5925	13.3269	288.6	68	85.43
cssz–22z	Central and South America	270.5374	13.1674	288.6	68	39.07
cssz–23a	Central and South America	271.3961	12.6734	292.4	25	17.94
cssz–23b	Central and South America	271.2369	12.2972	292.4	15	5
cssz–23x	Central and South America	271.5938	13.1399	292.4	68	131.8
cssz–23y	Central and South America	271.5279	12.9844	292.4	68	85.43
cssz–23z	Central and South America	271.4620	12.8289	292.4	68	39.07
cssz–24a	Central and South America	272.3203	12.2251	300.2	25	17.94
cssz–24b	Central and South America	272.1107	11.8734	300.2	15	5
cssz–24x	Central and South America	272.5917	12.6799	300.2	67	131.1
cssz–24y	Central and South America	272.5012	12.5283	300.2	67	85.1
cssz–24z	Central and South America	272.4107	12.3767	300.2	67	39.07
cssz–25a	Central and South America	273.2075	11.5684	313.8	25	17.94
cssz–25b	Central and South America	272.9200	11.2746	313.8	15	5
cssz–25x	Central and South America	273.5950	11.9641	313.8	66	130.4
cssz–25y	Central and South America	273.4658	11.8322	313.8	66	84.75
cssz–25z	Central and South America	273.3366	11.7003	313.8	66	39.07
cssz–26a	Central and South America	273.8943	10.8402	320.4	25	17.94
cssz–26b	Central and South America	273.5750	10.5808	320.4	15	5
cssz–26x	Central and South America	274.3246	11.1894	320.4	66	130.4
cssz–26y	Central and South America	274.1811	11.0730	320.4	66	84.75
cssz–26z	Central and South America	274.0377	10.9566	320.4	66	39.07
cssz–27a	Central and South America	274.4569	10.2177	316.1	25	17.94
cssz–27b	Central and South America	274.1590	9.9354	316.1	15	5
cssz–27z	Central and South America	274.5907	10.3444	316.1	66	39.07
cssz–28a	Central and South America	274.9586	9.8695	297.1	22	14.54
cssz–28b	Central and South America	274.7661	9.4988	297.1	11	5
cssz–28z	Central and South America	275.1118	10.1643	297.1	42.5	33.27
cssz–29a	Central and South America	275.7686	9.4789	296.6	19	11.09
cssz–29b	Central and South America	275.5759	9.0992	296.6	7	5
cssz–30a	Central and South America	276.6346	8.9973	302.2	19	9.36
cssz–30b	Central and South America	276.4053	8.6381	302.2	5	5
cssz–31a	Central and South America	277.4554	8.4152	309.1	19	7.62
cssz–31b	Central and South America	277.1851	8.0854	309.1	3	5
cssz–31z	Central and South America	277.7260	8.7450	309.1	19	23.9
cssz–32a	Central and South America	278.1112	7.9425	303	18.67	8.49
cssz–32b	Central and South America	277.8775	7.5855	303	4	5
cssz–32z	Central and South America	278.3407	8.2927	303	21.67	24.49
cssz–33a	Central and South America	278.7082	7.6620	287.6	18.33	10.23
cssz–33b	Central and South America	278.5785	7.2555	287.6	6	5
cssz–33z	Central and South America	278.8328	8.0522	287.6	24.33	25.95
cssz–34a	Central and South America	279.3184	7.5592	269.5	18	17.94
cssz–34b	Central and South America	279.3223	7.1320	269.5	15	5
cssz–35a	Central and South America	280.0039	7.6543	255.9	17.67	14.54
cssz–35b	Central and South America	280.1090	7.2392	255.9	11	5
cssz–35x	Central and South America	279.7156	8.7898	255.9	29.67	79.22
cssz–35y	Central and South America	279.8118	8.4113	255.9	29.67	54.47
cssz–35z	Central and South America	279.9079	8.0328	255.9	29.67	29.72
cssz–36a	Central and South America	281.2882	7.6778	282.5	17.33	11.09

(continued on next page)

Table B2: (continued)

Segment	Description	Longitude (°E)	Latitude (°N)	Strike (°)	Dip (°)	Depth (km)
cssz–36b	Central and South America	281.1948	7.2592	282.5	7	5
cssz–36x	Central and South America	281.5368	8.7896	282.5	32.33	79.47
cssz–36y	Central and South America	281.4539	8.4190	282.5	32.33	52.73
cssz–36z	Central and South America	281.3710	8.0484	282.5	32.33	25.99
cssz–37a	Central and South America	282.5252	6.8289	326.9	17	10.23
cssz–37b	Central and South America	282.1629	6.5944	326.9	6	5
cssz–38a	Central and South America	282.9469	5.5973	355.4	17	10.23
cssz–38b	Central and South America	282.5167	5.5626	355.4	6	5
cssz–39a	Central and South America	282.7236	4.3108	24.13	17	10.23
cssz–39b	Central and South America	282.3305	4.4864	24.13	6	5
cssz–39z	Central and South America	283.0603	4.1604	24.13	35	24.85
cssz–40a	Central and South America	282.1940	3.3863	35.28	17	10.23
cssz–40b	Central and South America	281.8427	3.6344	35.28	6	5
cssz–40y	Central and South America	282.7956	2.9613	35.28	35	53.52
cssz–40z	Central and South America	282.4948	3.1738	35.28	35	24.85
cssz–41a	Central and South America	281.6890	2.6611	34.27	17	10.23
cssz–41b	Central and South America	281.3336	2.9030	34.27	6	5
cssz–41z	Central and South America	281.9933	2.4539	34.27	35	24.85
cssz–42a	Central and South America	281.2266	1.9444	31.29	17	10.23
cssz–42b	Central and South America	280.8593	2.1675	31.29	6	5
cssz–42z	Central and South America	281.5411	1.7533	31.29	35	24.85
cssz–43a	Central and South America	280.7297	1.1593	33.3	17	10.23
cssz–43b	Central and South America	280.3706	1.3951	33.3	6	5
cssz–43z	Central and South America	281.0373	0.9573	33.3	35	24.85
cssz–44a	Central and South America	280.3018	0.4491	28.8	17	10.23
cssz–44b	Central and South America	279.9254	0.6560	28.8	6	5
cssz–45a	Central and South America	279.9083	–0.3259	26.91	10	8.49
cssz–45b	Central and South America	279.5139	–0.1257	26.91	4	5
cssz–46a	Central and South America	279.6461	–0.9975	15.76	10	8.49
cssz–46b	Central and South America	279.2203	–0.8774	15.76	4	5
cssz–47a	Central and South America	279.4972	–1.7407	6.9	10	8.49
cssz–47b	Central and South America	279.0579	–1.6876	6.9	4	5
cssz–48a	Central and South America	279.3695	–2.6622	8.96	10	8.49
cssz–48b	Central and South America	278.9321	–2.5933	8.96	4	5
cssz–48y	Central and South America	280.2444	–2.8000	8.96	10	25.85
cssz–48z	Central and South America	279.8070	–2.7311	8.96	10	17.17
cssz–49a	Central and South America	279.1852	–3.6070	13.15	10	8.49
cssz–49b	Central and South America	278.7536	–3.5064	13.15	4	5
cssz–49y	Central and South America	280.0486	–3.8082	13.15	10	25.85
cssz–49z	Central and South America	279.6169	–3.7076	13.15	10	17.17
cssz–50a	Central and South America	279.0652	–4.3635	4.78	10.33	9.64
cssz–50b	Central and South America	278.6235	–4.3267	4.78	5.33	5
cssz–51a	Central and South America	279.0349	–5.1773	359.4	10.67	10.81
cssz–51b	Central and South America	278.5915	–5.1817	359.4	6.67	5
cssz–52a	Central and South America	279.1047	–5.9196	349.8	11	11.96
cssz–52b	Central and South America	278.6685	–5.9981	349.8	8	5
cssz–53a	Central and South America	279.3044	–6.6242	339.2	10.25	11.74
cssz–53b	Central and South America	278.8884	–6.7811	339.2	7.75	5
cssz–53y	Central and South America	280.1024	–6.3232	339.2	19.25	37.12
cssz–53z	Central and South America	279.7035	–6.4737	339.2	19.25	20.64
cssz–54a	Central and South America	279.6256	–7.4907	340.8	9.5	11.53
cssz–54b	Central and South America	279.2036	–7.6365	340.8	7.5	5
cssz–54y	Central and South America	280.4267	–7.2137	340.8	20.5	37.29
cssz–54z	Central and South America	280.0262	–7.3522	340.8	20.5	19.78
cssz–55a	Central and South America	279.9348	–8.2452	335.4	8.75	11.74

(continued on next page)

Table B2: (continued)

Segment	Description	Longitude (°E)	Latitude (°N)	Strike (°)	Dip (°)	Depth (km)
cssz–55b	Central and South America	279.5269	–8.4301	335.4	7.75	5
cssz–55x	Central and South America	281.0837	–7.7238	335.4	21.75	56.4
cssz–55y	Central and South America	280.7009	–7.8976	335.4	21.75	37.88
cssz–55z	Central and South America	280.3180	–8.0714	335.4	21.75	19.35
cssz–56a	Central and South America	280.3172	–8.9958	331.6	8	11.09
cssz–56b	Central and South America	279.9209	–9.2072	331.6	7	5
cssz–56x	Central and South America	281.4212	–8.4063	331.6	23	57.13
cssz–56y	Central and South America	281.0534	–8.6028	331.6	23	37.59
cssz–56z	Central and South America	280.6854	–8.7993	331.6	23	18.05
cssz–57a	Central and South America	280.7492	–9.7356	328.7	8.6	10.75
cssz–57b	Central and South America	280.3640	–9.9663	328.7	6.6	5
cssz–57x	Central and South America	281.8205	–9.0933	328.7	23.4	57.94
cssz–57y	Central and South America	281.4636	–9.3074	328.7	23.4	38.08
cssz–57z	Central and South America	281.1065	–9.5215	328.7	23.4	18.22
cssz–58a	Central and South America	281.2275	–10.5350	330.5	9.2	10.4
cssz–58b	Central and South America	280.8348	–10.7532	330.5	6.2	5
cssz–58y	Central and South America	281.9548	–10.1306	330.5	23.8	38.57
cssz–58z	Central and South America	281.5913	–10.3328	330.5	23.8	18.39
cssz–59a	Central and South America	281.6735	–11.2430	326.2	9.8	10.05
cssz–59b	Central and South America	281.2982	–11.4890	326.2	5.8	5
cssz–59y	Central and South America	282.3675	–10.7876	326.2	24.2	39.06
cssz–59z	Central and South America	282.0206	–11.0153	326.2	24.2	18.56
cssz–60a	Central and South America	282.1864	–11.9946	326.5	10.4	9.71
cssz–60b	Central and South America	281.8096	–12.2384	326.5	5.4	5
cssz–60y	Central and South America	282.8821	–11.5438	326.5	24.6	39.55
cssz–60z	Central and South America	282.5344	–11.7692	326.5	24.6	18.73
cssz–61a	Central and South America	282.6944	–12.7263	325.5	11	9.36
cssz–61b	Central and South America	282.3218	–12.9762	325.5	5	5
cssz–61y	Central and South America	283.3814	–12.2649	325.5	25	40.03
cssz–61z	Central and South America	283.0381	–12.4956	325.5	25	18.9
cssz–62a	Central and South America	283.1980	–13.3556	319	11	9.79
cssz–62b	Central and South America	282.8560	–13.6451	319	5.5	5
cssz–62y	Central and South America	283.8178	–12.8300	319	27	42.03
cssz–62z	Central and South America	283.5081	–13.0928	319	27	19.33
cssz–63a	Central and South America	283.8032	–14.0147	317.9	11	10.23
cssz–63b	Central and South America	283.4661	–14.3106	317.9	6	5
cssz–63z	Central and South America	284.1032	–13.7511	317.9	29	19.77
cssz–64a	Central and South America	284.4144	–14.6482	315.7	13	11.96
cssz–64b	Central and South America	284.0905	–14.9540	315.7	8	5
cssz–65a	Central and South America	285.0493	–15.2554	313.2	15	13.68
cssz–65b	Central and South America	284.7411	–15.5715	313.2	10	5
cssz–66a	Central and South America	285.6954	–15.7816	307.7	14.5	13.68
cssz–66b	Central and South America	285.4190	–16.1258	307.7	10	5
cssz–67a	Central and South America	286.4127	–16.2781	304.3	14	13.68
cssz–67b	Central and South America	286.1566	–16.6381	304.3	10	5
cssz–67z	Central and South America	286.6552	–15.9365	304.3	23	25.78
cssz–68a	Central and South America	287.2481	–16.9016	311.8	14	13.68
cssz–68b	Central and South America	286.9442	–17.2264	311.8	10	5
cssz–68z	Central and South America	287.5291	–16.6007	311.8	26	25.78
cssz–69a	Central and South America	287.9724	–17.5502	314.9	14	13.68
cssz–69b	Central and South America	287.6496	–17.8590	314.9	10	5
cssz–69y	Central and South America	288.5530	–16.9934	314.9	29	50.02
cssz–69z	Central and South America	288.2629	–17.2718	314.9	29	25.78
cssz–70a	Central and South America	288.6731	–18.2747	320.4	14	13.25
cssz–70b	Central and South America	288.3193	–18.5527	320.4	9.5	5

(continued on next page)

Table B2: (continued)

Segment	Description	Longitude (°E)	Latitude (°N)	Strike (°)	Dip (°)	Depth (km)
cssz–70y	Central and South America	289.3032	–17.7785	320.4	30	50.35
cssz–70z	Central and South America	288.9884	–18.0266	320.4	30	25.35
cssz–71a	Central and South America	289.3089	–19.1854	333.2	14	12.82
cssz–71b	Central and South America	288.8968	–19.3820	333.2	9	5
cssz–71y	Central and South America	290.0357	–18.8382	333.2	31	50.67
cssz–71z	Central and South America	289.6725	–19.0118	333.2	31	24.92
cssz–72a	Central and South America	289.6857	–20.3117	352.4	14	12.54
cssz–72b	Central and South America	289.2250	–20.3694	352.4	8.67	5
cssz–72z	Central and South America	290.0882	–20.2613	352.4	32	24.63
cssz–73a	Central and South America	289.7731	–21.3061	358.9	14	12.24
cssz–73b	Central and South America	289.3053	–21.3142	358.9	8.33	5
cssz–73z	Central and South America	290.1768	–21.2991	358.9	33	24.34
cssz–74a	Central and South America	289.7610	–22.2671	3.06	14	11.96
cssz–74b	Central and South America	289.2909	–22.2438	3.06	8	5
cssz–75a	Central and South America	289.6982	–23.1903	4.83	14.09	11.96
cssz–75b	Central and South America	289.2261	–23.1536	4.83	8	5
cssz–76a	Central and South America	289.6237	–24.0831	4.67	14.18	11.96
cssz–76b	Central and South America	289.1484	–24.0476	4.67	8	5
cssz–77a	Central and South America	289.5538	–24.9729	4.3	14.27	11.96
cssz–77b	Central and South America	289.0750	–24.9403	4.3	8	5
cssz–78a	Central and South America	289.4904	–25.8621	3.86	14.36	11.96
cssz–78b	Central and South America	289.0081	–25.8328	3.86	8	5
cssz–79a	Central and South America	289.3491	–26.8644	11.34	14.45	11.96
cssz–79b	Central and South America	288.8712	–26.7789	11.34	8	5
cssz–80a	Central and South America	289.1231	–27.7826	14.16	14.54	11.96
cssz–80b	Central and South America	288.6469	–27.6762	14.16	8	5
cssz–81a	Central and South America	288.8943	–28.6409	13.19	14.63	11.96
cssz–81b	Central and South America	288.4124	–28.5417	13.19	8	5
cssz–82a	Central and South America	288.7113	–29.4680	9.68	14.72	11.96
cssz–82b	Central and South America	288.2196	–29.3950	9.68	8	5
cssz–83a	Central and South America	288.5944	–30.2923	5.36	14.81	11.96
cssz–83b	Central and South America	288.0938	–30.2517	5.36	8	5
cssz–84a	Central and South America	288.5223	–31.1639	3.8	14.9	11.96
cssz–84b	Central and South America	288.0163	–31.1351	3.8	8	5
cssz–85a	Central and South America	288.4748	–32.0416	2.55	15	11.96
cssz–85b	Central and South America	287.9635	–32.0223	2.55	8	5
cssz–86a	Central and South America	288.3901	–33.0041	7.01	15	11.96
cssz–86b	Central and South America	287.8768	–32.9512	7.01	8	5
cssz–87a	Central and South America	288.1050	–34.0583	19.4	15	11.96
cssz–87b	Central and South America	287.6115	–33.9142	19.4	8	5
cssz–88a	Central and South America	287.5309	–35.0437	32.81	15	11.96
cssz–88b	Central and South America	287.0862	–34.8086	32.81	8	5
cssz–88z	Central and South America	287.9308	–35.2545	32.81	30	24.9
cssz–89a	Central and South America	287.2380	–35.5993	14.52	16.67	11.96
cssz–89b	Central and South America	286.7261	–35.4914	14.52	8	5
cssz–89z	Central and South America	287.7014	–35.6968	14.52	30	26.3
cssz–90a	Central and South America	286.8442	–36.5645	22.64	18.33	11.96
cssz–90b	Central and South America	286.3548	–36.4004	22.64	8	5
cssz–90z	Central and South America	287.2916	–36.7142	22.64	30	27.68
cssz–91a	Central and South America	286.5925	–37.2488	10.9	20	11.96
cssz–91b	Central and South America	286.0721	–37.1690	10.9	8	5
cssz–91z	Central and South America	287.0726	–37.3224	10.9	30	29.06
cssz–92a	Central and South America	286.4254	–38.0945	8.23	20	11.96
cssz–92b	Central and South America	285.8948	–38.0341	8.23	8	5
cssz–92z	Central and South America	286.9303	–38.1520	8.23	26.67	29.06

(continued on next page)

Table B2: (continued)

Segment	Description	Longitude (°E)	Latitude (°N)	Strike (°)	Dip (°)	Depth (km)
cssz–93a	Central and South America	286.2047	–39.0535	13.46	20	11.96
cssz–93b	Central and South America	285.6765	–38.9553	13.46	8	5
cssz–93z	Central and South America	286.7216	–39.1495	13.46	23.33	29.06
cssz–94a	Central and South America	286.0772	–39.7883	3.4	20	11.96
cssz–94b	Central and South America	285.5290	–39.7633	3.4	8	5
cssz–94z	Central and South America	286.6255	–39.8133	3.4	20	29.06
cssz–95a	Central and South America	285.9426	–40.7760	9.84	20	11.96
cssz–95b	Central and South America	285.3937	–40.7039	9.84	8	5
cssz–95z	Central and South America	286.4921	–40.8481	9.84	20	29.06
cssz–96a	Central and South America	285.7839	–41.6303	7.6	20	11.96
cssz–96b	Central and South America	285.2245	–41.5745	7.6	8	5
cssz–96x	Central and South America	287.4652	–41.7977	7.6	20	63.26
cssz–96y	Central and South America	286.9043	–41.7419	7.6	20	46.16
cssz–96z	Central and South America	286.3439	–41.6861	7.6	20	29.06
cssz–97a	Central and South America	285.6695	–42.4882	5.3	20	11.96
cssz–97b	Central and South America	285.0998	–42.4492	5.3	8	5
cssz–97x	Central and South America	287.3809	–42.6052	5.3	20	63.26
cssz–97y	Central and South America	286.8101	–42.5662	5.3	20	46.16
cssz–97z	Central and South America	286.2396	–42.5272	5.3	20	29.06
cssz–98a	Central and South America	285.5035	–43.4553	10.53	20	11.96
cssz–98b	Central and South America	284.9322	–43.3782	10.53	8	5
cssz–98x	Central and South America	287.2218	–43.6866	10.53	20	63.26
cssz–98y	Central and South America	286.6483	–43.6095	10.53	20	46.16
cssz–98z	Central and South America	286.0755	–43.5324	10.53	20	29.06
cssz–99a	Central and South America	285.3700	–44.2595	4.86	20	11.96
cssz–99b	Central and South America	284.7830	–44.2237	4.86	8	5
cssz–99x	Central and South America	287.1332	–44.3669	4.86	20	63.26
cssz–99y	Central and South America	286.5451	–44.3311	4.86	20	46.16
cssz–99z	Central and South America	285.9574	–44.2953	4.86	20	29.06
cssz–100a	Central and South America	285.2713	–45.1664	5.68	20	11.96
cssz–100b	Central and South America	284.6758	–45.1246	5.68	8	5
cssz–100x	Central and South America	287.0603	–45.2918	5.68	20	63.26
cssz–100y	Central and South America	286.4635	–45.2500	5.68	20	46.16
cssz–100z	Central and South America	285.8672	–45.2082	5.68	20	29.06
cssz–101a	Central and South America	285.3080	–45.8607	352.6	20	9.36
cssz–101b	Central and South America	284.7067	–45.9152	352.6	5	5
cssz–101y	Central and South America	286.5089	–45.7517	352.6	20	43.56
cssz–101z	Central and South America	285.9088	–45.8062	352.6	20	26.46
cssz–102a	Central and South America	285.2028	–47.1185	17.72	5	9.36
cssz–102b	Central and South America	284.5772	–46.9823	17.72	5	5
cssz–102y	Central and South America	286.4588	–47.3909	17.72	5	18.07
cssz–102z	Central and South America	285.8300	–47.2547	17.72	5	13.72
cssz–103a	Central and South America	284.7075	–48.0396	23.37	7.5	11.53
cssz–103b	Central and South America	284.0972	–47.8630	23.37	7.5	5
cssz–103x	Central and South America	286.5511	–48.5694	23.37	7.5	31.11
cssz–103y	Central and South America	285.9344	–48.3928	23.37	7.5	24.58
cssz–103z	Central and South America	285.3199	–48.2162	23.37	7.5	18.05
cssz–104a	Central and South America	284.3440	–48.7597	14.87	10	13.68
cssz–104b	Central and South America	283.6962	–48.6462	14.87	10	5
cssz–104x	Central and South America	286.2962	–49.1002	14.87	10	39.73
cssz–104y	Central and South America	285.6440	–48.9867	14.87	10	31.05
cssz–104z	Central and South America	284.9933	–48.8732	14.87	10	22.36
cssz–105a	Central and South America	284.2312	–49.4198	0.25	9.67	13.4
cssz–105b	Central and South America	283.5518	–49.4179	0.25	9.67	5
cssz–105x	Central and South America	286.2718	–49.4255	0.25	9.67	38.59

(continued on next page)

Table B2: (continued)

Segment	Description	Longitude (°E)	Latitude (°N)	Strike (°)	Dip (°)	Depth (km)
cssz–105y	Central and South America	285.5908	–49.4236	0.25	9.67	30.2
cssz–105z	Central and South America	284.9114	–49.4217	0.25	9.67	21.8
cssz–106a	Central and South America	284.3730	–50.1117	347.5	9.25	13.04
cssz–106b	Central and South America	283.6974	–50.2077	347.5	9.25	5
cssz–106x	Central and South America	286.3916	–49.8238	347.5	9.25	37.15
cssz–106y	Central and South America	285.7201	–49.9198	347.5	9.25	29.11
cssz–106z	Central and South America	285.0472	–50.0157	347.5	9.25	21.07
cssz–107a	Central and South America	284.7130	–50.9714	346.5	9	12.82
cssz–107b	Central and South America	284.0273	–51.0751	346.5	9	5
cssz–107x	Central and South America	286.7611	–50.6603	346.5	9	36.29
cssz–107y	Central and South America	286.0799	–50.7640	346.5	9	28.47
cssz–107z	Central and South America	285.3972	–50.8677	346.5	9	20.64
cssz–108a	Central and South America	285.0378	–51.9370	352	8.67	12.54
cssz–108b	Central and South America	284.3241	–51.9987	352	8.67	5
cssz–108x	Central and South America	287.1729	–51.7519	352	8.67	35.15
cssz–108y	Central and South America	286.4622	–51.8136	352	8.67	27.61
cssz–108z	Central and South America	285.7505	–51.8753	352	8.67	20.07
cssz–109a	Central and South America	285.2635	–52.8439	353.1	8.33	12.24
cssz–109b	Central and South America	284.5326	–52.8974	353.1	8.33	5
cssz–109x	Central and South America	287.4508	–52.6834	353.1	8.33	33.97
cssz–109y	Central and South America	286.7226	–52.7369	353.1	8.33	26.73
cssz–109z	Central and South America	285.9935	–52.7904	353.1	8.33	19.49
cssz–110a	Central and South America	285.5705	–53.4139	334.2	8	11.96
cssz–110b	Central and South America	284.8972	–53.6076	334.2	8	5
cssz–110x	Central and South America	287.5724	–52.8328	334.2	8	32.83
cssz–110y	Central and South America	286.9081	–53.0265	334.2	8	25.88
cssz–110z	Central and South America	286.2408	–53.2202	334.2	8	18.92
cssz–111a	Central and South America	286.1627	–53.8749	313.8	8	11.96
cssz–111b	Central and South America	285.6382	–54.1958	313.8	8	5
cssz–111x	Central and South America	287.7124	–52.9122	313.8	8	32.83
cssz–111y	Central and South America	287.1997	–53.2331	313.8	8	25.88
cssz–111z	Central and South America	286.6832	–53.5540	313.8	8	18.92
cssz–112a	Central and South America	287.3287	–54.5394	316.4	8	11.96
cssz–112b	Central and South America	286.7715	–54.8462	316.4	8	5
cssz–112x	Central and South America	288.9756	–53.6190	316.4	8	32.83
cssz–112y	Central and South America	288.4307	–53.9258	316.4	8	25.88
cssz–112z	Central and South America	287.8817	–54.2326	316.4	8	18.92
cssz–113a	Central and South America	288.3409	–55.0480	307.6	8	11.96
cssz–113b	Central and South America	287.8647	–55.4002	307.6	8	5
cssz–113x	Central and South America	289.7450	–53.9914	307.6	8	32.83
cssz–113y	Central and South America	289.2810	–54.3436	307.6	8	25.88
cssz–113z	Central and South America	288.8130	–54.6958	307.6	8	18.92
cssz–114a	Central and South America	289.5342	–55.5026	301.5	8	11.96
cssz–114b	Central and South America	289.1221	–55.8819	301.5	8	5
cssz–114x	Central and South America	290.7472	–54.3647	301.5	8	32.83
cssz–114y	Central and South America	290.3467	–54.7440	301.5	8	25.88
cssz–114z	Central and South America	289.9424	–55.1233	301.5	8	18.92
cssz–115a	Central and South America	290.7682	–55.8485	292.7	8	11.96
cssz–115b	Central and South America	290.4608	–56.2588	292.7	8	5
cssz–115x	Central and South America	291.6714	–54.6176	292.7	8	32.83
cssz–115y	Central and South America	291.3734	–55.0279	292.7	8	25.88
cssz–115z	Central and South America	291.0724	–55.4382	292.7	8	18.92

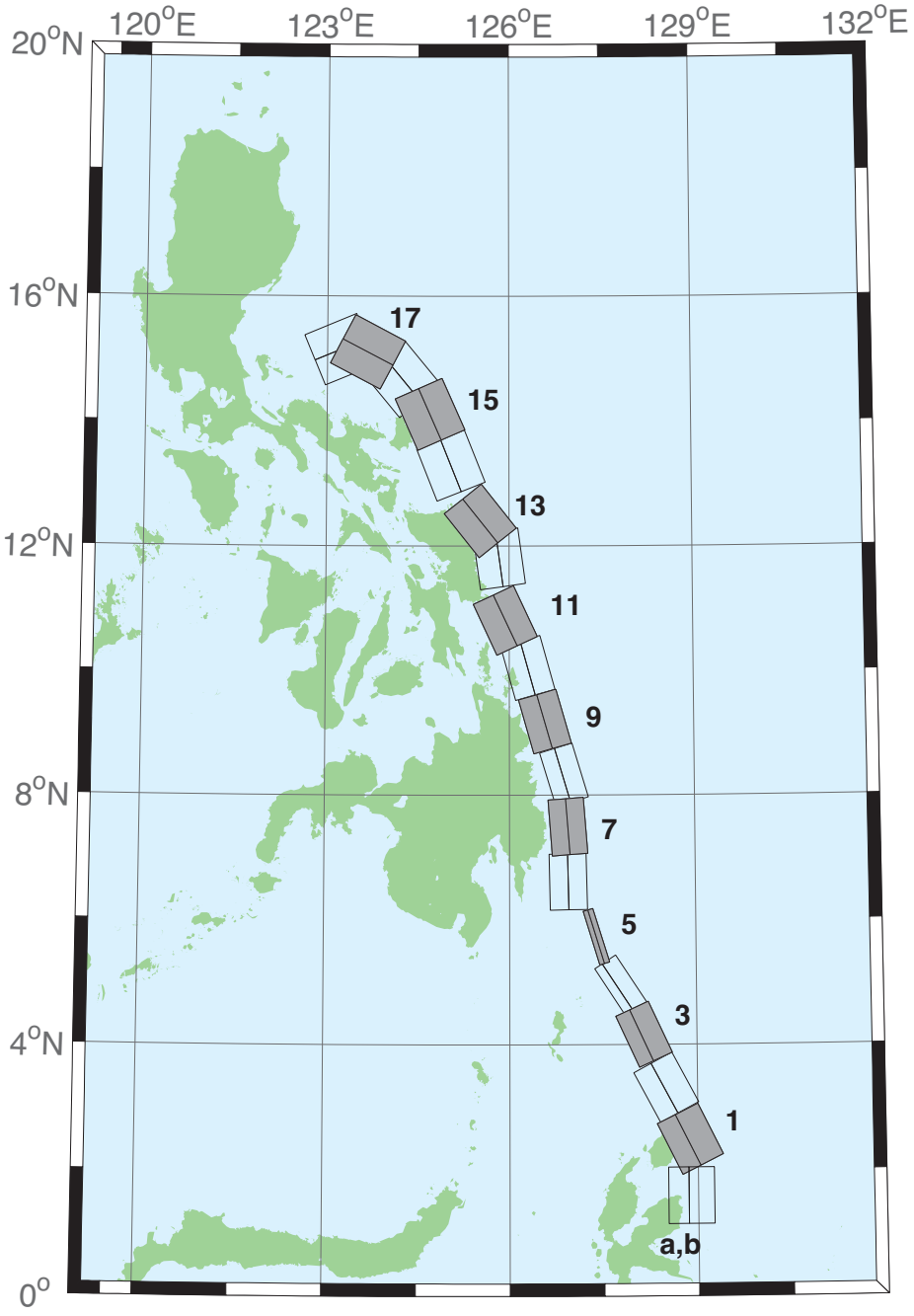

Figure B3: Eastern Philippines Subduction Zone unit sources.

Table B3: Earthquake parameters for Eastern Philippines Subduction Zone unit sources.

Segment	Description	Longitude (°E)	Latitude (°N)	Strike (°)	Dip (°)	Depth (km)
epsz–0a	Eastern Philippines	128.5264	1.5930	180	44	26.92
epsz–0b	Eastern Philippines	128.8496	1.5930	180	26	5
epsz–1a	Eastern Philippines	128.5521	2.3289	153.6	44.2	27.62
epsz–1b	Eastern Philippines	128.8408	2.4720	153.6	26.9	5
epsz–2a	Eastern Philippines	128.1943	3.1508	151.9	45.9	32.44
epsz–2b	Eastern Philippines	128.4706	3.2979	151.9	32.8	5.35
epsz–3a	Eastern Philippines	127.8899	4.0428	155.2	57.3	40.22
epsz–3b	Eastern Philippines	128.1108	4.1445	155.2	42.7	6.31
epsz–4a	Eastern Philippines	127.6120	4.8371	146.8	71.4	48.25
epsz–4b	Eastern Philippines	127.7324	4.9155	146.8	54.8	7.39
epsz–5a	Eastern Philippines	127.3173	5.7040	162.9	79.9	57.4
epsz–5b	Eastern Philippines	127.3930	5.7272	162.9	79.4	8.25
epsz–6a	Eastern Philippines	126.6488	6.6027	178.9	48.6	45.09
epsz–6b	Eastern Philippines	126.9478	6.6085	178.9	48.6	7.58
epsz–7a	Eastern Philippines	126.6578	7.4711	175.8	50.7	45.52
epsz–7b	Eastern Philippines	126.9439	7.4921	175.8	50.7	6.83
epsz–8a	Eastern Philippines	126.6227	8.2456	163.3	56.7	45.6
epsz–8b	Eastern Philippines	126.8614	8.3164	163.3	48.9	7.92
epsz–9a	Eastern Philippines	126.2751	9.0961	164.1	47	43.59
epsz–9b	Eastern Philippines	126.5735	9.1801	164.1	44.9	8.3
epsz–10a	Eastern Philippines	125.9798	9.9559	164.5	43.1	42.25
epsz–10b	Eastern Philippines	126.3007	10.0438	164.5	43.1	8.09
epsz–11a	Eastern Philippines	125.6079	10.6557	155	37.8	38.29
epsz–11b	Eastern Philippines	125.9353	10.8059	155	37.8	7.64
epsz–12a	Eastern Philippines	125.4697	11.7452	172.1	36	37.01
epsz–12b	Eastern Philippines	125.8374	11.7949	172.1	36	7.62
epsz–13a	Eastern Philippines	125.2238	12.1670	141.5	32.4	33.87
epsz–13b	Eastern Philippines	125.5278	12.4029	141.5	32.4	7.08
epsz–14a	Eastern Philippines	124.6476	13.1365	158.2	23	25.92
epsz–14b	Eastern Philippines	125.0421	13.2898	158.2	23	6.38
epsz–15a	Eastern Philippines	124.3107	13.9453	156.1	24.1	26.51
epsz–15b	Eastern Philippines	124.6973	14.1113	156.1	24.1	6.09
epsz–16a	Eastern Philippines	123.8998	14.4025	140.3	19.5	21.69
epsz–16b	Eastern Philippines	124.2366	14.6728	140.3	19.5	5
epsz–17a	Eastern Philippines	123.4604	14.7222	117.6	15.3	18.19
epsz–17b	Eastern Philippines	123.6682	15.1062	117.6	15.3	5
epsz–18a	Eastern Philippines	123.3946	14.7462	67.4	15	17.94
epsz–18b	Eastern Philippines	123.2219	15.1467	67.4	15	5

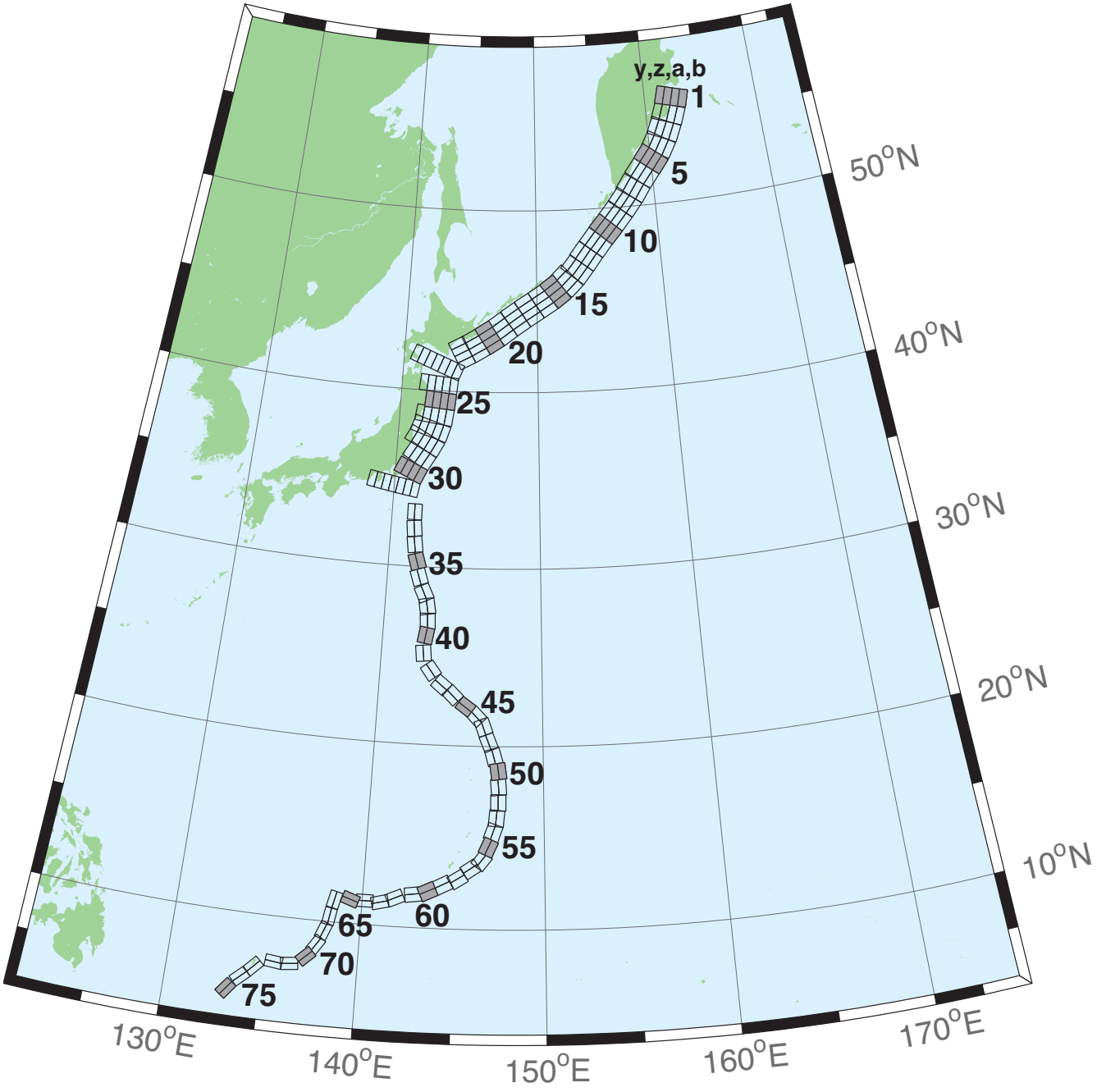

Figure B4: Kamchatka-Kuril-Japan-Izu-Mariana-Yap Subduction Zone unit sources.

Table B4: Earthquake parameters for Kamchatka-Kuril-Japan-Izu-Mariana-Yap Subduction Zone unit sources.

Segment	Description	Longitude (°E)	Latitude (°N)	Strike (°)	Dip (°)	Depth (km)
kisz–1a	Kamchatka-Kuril-Japan-Izu-Mariana-Yap	162.4318	55.5017	195	29	26.13
kisz–1b	Kamchatka-Kuril-Japan-Izu-Mariana-Yap	163.1000	55.4000	195	25	5
kisz–1y	Kamchatka-Kuril-Japan-Izu-Mariana-Yap	161.0884	55.7050	195	29	74.61
kisz–1z	Kamchatka-Kuril-Japan-Izu-Mariana-Yap	161.7610	55.6033	195	29	50.37
kisz–2a	Kamchatka-Kuril-Japan-Izu-Mariana-Yap	161.9883	54.6784	200	29	26.13
kisz–2b	Kamchatka-Kuril-Japan-Izu-Mariana-Yap	162.6247	54.5440	200	25	5
kisz–2y	Kamchatka-Kuril-Japan-Izu-Mariana-Yap	160.7072	54.9471	200	29	74.61
kisz–2z	Kamchatka-Kuril-Japan-Izu-Mariana-Yap	161.3488	54.8127	200	29	50.37
kisz–3a	Kamchatka-Kuril-Japan-Izu-Mariana-Yap	161.4385	53.8714	204	29	26.13
kisz–3b	Kamchatka-Kuril-Japan-Izu-Mariana-Yap	162.0449	53.7116	204	25	5
kisz–3y	Kamchatka-Kuril-Japan-Izu-Mariana-Yap	160.2164	54.1910	204	29	74.61
kisz–3z	Kamchatka-Kuril-Japan-Izu-Mariana-Yap	160.8286	54.0312	204	29	50.37
kisz–4a	Kamchatka-Kuril-Japan-Izu-Mariana-Yap	160.7926	53.1087	210	29	26.13
kisz–4b	Kamchatka-Kuril-Japan-Izu-Mariana-Yap	161.3568	52.9123	210	25	5
kisz–4y	Kamchatka-Kuril-Japan-Izu-Mariana-Yap	159.6539	53.5015	210	29	74.61
kisz–4z	Kamchatka-Kuril-Japan-Izu-Mariana-Yap	160.2246	53.3051	210	29	50.37
kisz–5a	Kamchatka-Kuril-Japan-Izu-Mariana-Yap	160.0211	52.4113	218	29	26.13
kisz–5b	Kamchatka-Kuril-Japan-Izu-Mariana-Yap	160.5258	52.1694	218	25	5
kisz–5y	Kamchatka-Kuril-Japan-Izu-Mariana-Yap	159.0005	52.8950	218	29	74.61
kisz–5z	Kamchatka-Kuril-Japan-Izu-Mariana-Yap	159.5122	52.6531	218	29	50.37
kisz–6a	Kamchatka-Kuril-Japan-Izu-Mariana-Yap	159.1272	51.7034	218	29	26.13
kisz–6b	Kamchatka-Kuril-Japan-Izu-Mariana-Yap	159.6241	51.4615	218	25	5
kisz–6y	Kamchatka-Kuril-Japan-Izu-Mariana-Yap	158.1228	52.1871	218	29	74.61
kisz–6z	Kamchatka-Kuril-Japan-Izu-Mariana-Yap	158.6263	51.9452	218	29	50.37
kisz–7a	Kamchatka-Kuril-Japan-Izu-Mariana-Yap	158.2625	50.9549	214	29	26.13
kisz–7b	Kamchatka-Kuril-Japan-Izu-Mariana-Yap	158.7771	50.7352	214	25	5
kisz–7y	Kamchatka-Kuril-Japan-Izu-Mariana-Yap	157.2236	51.3942	214	29	74.61
kisz–7z	Kamchatka-Kuril-Japan-Izu-Mariana-Yap	157.7443	51.1745	214	29	50.37
kisz–8a	Kamchatka-Kuril-Japan-Izu-Mariana-Yap	157.4712	50.2459	218	31	27.7
kisz–8b	Kamchatka-Kuril-Japan-Izu-Mariana-Yap	157.9433	50.0089	218	27	5
kisz–8y	Kamchatka-Kuril-Japan-Izu-Mariana-Yap	156.5176	50.7199	218	31	79.2
kisz–8z	Kamchatka-Kuril-Japan-Izu-Mariana-Yap	156.9956	50.4829	218	31	53.45
kisz–9a	Kamchatka-Kuril-Japan-Izu-Mariana-Yap	156.6114	49.5583	220	31	27.7
kisz–9b	Kamchatka-Kuril-Japan-Izu-Mariana-Yap	157.0638	49.3109	220	27	5
kisz–9y	Kamchatka-Kuril-Japan-Izu-Mariana-Yap	155.6974	50.0533	220	31	79.2
kisz–9z	Kamchatka-Kuril-Japan-Izu-Mariana-Yap	156.1556	49.8058	220	31	53.45
kisz–10a	Kamchatka-Kuril-Japan-Izu-Mariana-Yap	155.7294	48.8804	221	31	27.7
kisz–10b	Kamchatka-Kuril-Japan-Izu-Mariana-Yap	156.1690	48.6278	221	27	5
kisz–10y	Kamchatka-Kuril-Japan-Izu-Mariana-Yap	154.8413	49.3856	221	31	79.2
kisz–10z	Kamchatka-Kuril-Japan-Izu-Mariana-Yap	155.2865	49.1330	221	31	53.45
kisz–11a	Kamchatka-Kuril-Japan-Izu-Mariana-Yap	154.8489	48.1821	219	31	27.7
kisz–11b	Kamchatka-Kuril-Japan-Izu-Mariana-Yap	155.2955	47.9398	219	27	5
kisz–11y	Kamchatka-Kuril-Japan-Izu-Mariana-Yap	153.9472	48.6667	219	31	79.2
kisz–11z	Kamchatka-Kuril-Japan-Izu-Mariana-Yap	154.3991	48.4244	219	31	53.45
kisz–12a	Kamchatka-Kuril-Japan-Izu-Mariana-Yap	153.9994	47.4729	217	31	27.7
kisz–12b	Kamchatka-Kuril-Japan-Izu-Mariana-Yap	154.4701	47.2320	217	27	5
kisz–12y	Kamchatka-Kuril-Japan-Izu-Mariana-Yap	153.0856	47.9363	217	31	79.2
kisz–12z	Kamchatka-Kuril-Japan-Izu-Mariana-Yap	153.5435	47.7046	217	31	53.45
kisz–13a	Kamchatka-Kuril-Japan-Izu-Mariana-Yap	153.2239	46.7564	218	31	27.7
kisz–13b	Kamchatka-Kuril-Japan-Izu-Mariana-Yap	153.6648	46.5194	218	27	5
kisz–13y	Kamchatka-Kuril-Japan-Izu-Mariana-Yap	152.3343	47.2304	218	31	79.2
kisz–13z	Kamchatka-Kuril-Japan-Izu-Mariana-Yap	152.7801	46.9934	218	31	53.45
kisz–14a	Kamchatka-Kuril-Japan-Izu-Mariana-Yap	152.3657	46.1514	225	23	24.54
kisz–14b	Kamchatka-Kuril-Japan-Izu-Mariana-Yap	152.7855	45.8591	225	23	5

(continued on next page)

Table B4: (continued)

Segment	Description	Longitude (°E)	Latitude (°N)	Strike (°)	Dip (°)	Depth (km)
kisz–14y	Kamchatka-Kuril-Japan-Izu-Mariana-Yap	151.5172	46.7362	225	23	63.62
kisz–14z	Kamchatka-Kuril-Japan-Izu-Mariana-Yap	151.9426	46.4438	225	23	44.08
kisz–15a	Kamchatka-Kuril-Japan-Izu-Mariana-Yap	151.4663	45.5963	233	25	23.73
kisz–15b	Kamchatka-Kuril-Japan-Izu-Mariana-Yap	151.8144	45.2712	233	22	5
kisz–15y	Kamchatka-Kuril-Japan-Izu-Mariana-Yap	150.7619	46.2465	233	25	65.99
kisz–15z	Kamchatka-Kuril-Japan-Izu-Mariana-Yap	151.1151	45.9214	233	25	44.86
kisz–16a	Kamchatka-Kuril-Japan-Izu-Mariana-Yap	150.4572	45.0977	237	25	23.73
kisz–16b	Kamchatka-Kuril-Japan-Izu-Mariana-Yap	150.7694	44.7563	237	22	5
kisz–16y	Kamchatka-Kuril-Japan-Izu-Mariana-Yap	149.8253	45.7804	237	25	65.99
kisz–16z	Kamchatka-Kuril-Japan-Izu-Mariana-Yap	150.1422	45.4390	237	25	44.86
kisz–17a	Kamchatka-Kuril-Japan-Izu-Mariana-Yap	149.3989	44.6084	237	25	23.73
kisz–17b	Kamchatka-Kuril-Japan-Izu-Mariana-Yap	149.7085	44.2670	237	22	5
kisz–17y	Kamchatka-Kuril-Japan-Izu-Mariana-Yap	148.7723	45.2912	237	25	65.99
kisz–17z	Kamchatka-Kuril-Japan-Izu-Mariana-Yap	149.0865	44.9498	237	25	44.86
kisz–18a	Kamchatka-Kuril-Japan-Izu-Mariana-Yap	148.3454	44.0982	235	25	23.73
kisz–18b	Kamchatka-Kuril-Japan-Izu-Mariana-Yap	148.6687	43.7647	235	22	5
kisz–18y	Kamchatka-Kuril-Japan-Izu-Mariana-Yap	147.6915	44.7651	235	25	65.99
kisz–18z	Kamchatka-Kuril-Japan-Izu-Mariana-Yap	148.0194	44.4316	235	25	44.86
kisz–19a	Kamchatka-Kuril-Japan-Izu-Mariana-Yap	147.3262	43.5619	233	25	23.73
kisz–19b	Kamchatka-Kuril-Japan-Izu-Mariana-Yap	147.6625	43.2368	233	22	5
kisz–19y	Kamchatka-Kuril-Japan-Izu-Mariana-Yap	146.6463	44.2121	233	25	65.99
kisz–19z	Kamchatka-Kuril-Japan-Izu-Mariana-Yap	146.9872	43.8870	233	25	44.86
kisz–20a	Kamchatka-Kuril-Japan-Izu-Mariana-Yap	146.3513	43.0633	237	25	23.73
kisz–20b	Kamchatka-Kuril-Japan-Izu-Mariana-Yap	146.6531	42.7219	237	22	5
kisz–20y	Kamchatka-Kuril-Japan-Izu-Mariana-Yap	145.7410	43.7461	237	25	65.99
kisz–20z	Kamchatka-Kuril-Japan-Izu-Mariana-Yap	146.0470	43.4047	237	25	44.86
kisz–21a	Kamchatka-Kuril-Japan-Izu-Mariana-Yap	145.3331	42.5948	239	25	23.73
kisz–21b	Kamchatka-Kuril-Japan-Izu-Mariana-Yap	145.6163	42.2459	239	22	5
kisz–21y	Kamchatka-Kuril-Japan-Izu-Mariana-Yap	144.7603	43.2927	239	25	65.99
kisz–21z	Kamchatka-Kuril-Japan-Izu-Mariana-Yap	145.0475	42.9438	239	25	44.86
kisz–22a	Kamchatka-Kuril-Japan-Izu-Mariana-Yap	144.3041	42.1631	242	25	23.73
kisz–22b	Kamchatka-Kuril-Japan-Izu-Mariana-Yap	144.5605	41.8037	242	22	5
kisz–22y	Kamchatka-Kuril-Japan-Izu-Mariana-Yap	143.7854	42.8819	242	25	65.99
kisz–22z	Kamchatka-Kuril-Japan-Izu-Mariana-Yap	144.0455	42.5225	242	25	44.86
kisz–23a	Kamchatka-Kuril-Japan-Izu-Mariana-Yap	143.2863	41.3335	202	21	21.28
kisz–23b	Kamchatka-Kuril-Japan-Izu-Mariana-Yap	143.8028	41.1764	202	19	5
kisz–23v	Kamchatka-Kuril-Japan-Izu-Mariana-Yap	140.6816	42.1189	202	21	110.9
kisz–23w	Kamchatka-Kuril-Japan-Izu-Mariana-Yap	141.2050	41.9618	202	21	92.95
kisz–23x	Kamchatka-Kuril-Japan-Izu-Mariana-Yap	141.7273	41.8047	202	21	75.04
kisz–23y	Kamchatka-Kuril-Japan-Izu-Mariana-Yap	142.2482	41.6476	202	21	57.12
kisz–23z	Kamchatka-Kuril-Japan-Izu-Mariana-Yap	142.7679	41.4905	202	21	39.2
kisz–24a	Kamchatka-Kuril-Japan-Izu-Mariana-Yap	142.9795	40.3490	185	21	21.28
kisz–24b	Kamchatka-Kuril-Japan-Izu-Mariana-Yap	143.5273	40.3125	185	19	5
kisz–24x	Kamchatka-Kuril-Japan-Izu-Mariana-Yap	141.3339	40.4587	185	21	75.04
kisz–24y	Kamchatka-Kuril-Japan-Izu-Mariana-Yap	141.8827	40.4221	185	21	57.12
kisz–24z	Kamchatka-Kuril-Japan-Izu-Mariana-Yap	142.4312	40.3856	185	21	39.2
kisz–25a	Kamchatka-Kuril-Japan-Izu-Mariana-Yap	142.8839	39.4541	185	21	21.28
kisz–25b	Kamchatka-Kuril-Japan-Izu-Mariana-Yap	143.4246	39.4176	185	19	5
kisz–25y	Kamchatka-Kuril-Japan-Izu-Mariana-Yap	141.8012	39.5272	185	21	57.12
kisz–25z	Kamchatka-Kuril-Japan-Izu-Mariana-Yap	142.3426	39.4907	185	21	39.2
kisz–26a	Kamchatka-Kuril-Japan-Izu-Mariana-Yap	142.7622	38.5837	188	21	21.28
kisz–26b	Kamchatka-Kuril-Japan-Izu-Mariana-Yap	143.2930	38.5254	188	19	5
kisz–26x	Kamchatka-Kuril-Japan-Izu-Mariana-Yap	141.1667	38.7588	188	21	75.04
kisz–26y	Kamchatka-Kuril-Japan-Izu-Mariana-Yap	141.6990	38.7004	188	21	57.12
kisz–26z	Kamchatka-Kuril-Japan-Izu-Mariana-Yap	142.2308	38.6421	188	21	39.2

(continued on next page)

Table B4: (continued)

Segment	Description	Longitude (°E)	Latitude (°N)	Strike (°)	Dip (°)	Depth (km)
kisz–27a	Kamchatka-Kuril-Japan-Izu-Mariana-Yap	142.5320	37.7830	198	21	21.28
kisz–27b	Kamchatka-Kuril-Japan-Izu-Mariana-Yap	143.0357	37.6534	198	19	5
kisz–27x	Kamchatka-Kuril-Japan-Izu-Mariana-Yap	141.0142	38.1717	198	21	75.04
kisz–27y	Kamchatka-Kuril-Japan-Izu-Mariana-Yap	141.5210	38.0421	198	21	57.12
kisz–27z	Kamchatka-Kuril-Japan-Izu-Mariana-Yap	142.0269	37.9126	198	21	39.2
kisz–28a	Kamchatka-Kuril-Japan-Izu-Mariana-Yap	142.1315	37.0265	208	21	21.28
kisz–28b	Kamchatka-Kuril-Japan-Izu-Mariana-Yap	142.5941	36.8297	208	19	5
kisz–28x	Kamchatka-Kuril-Japan-Izu-Mariana-Yap	140.7348	37.6171	208	21	75.04
kisz–28y	Kamchatka-Kuril-Japan-Izu-Mariana-Yap	141.2016	37.4202	208	21	57.12
kisz–28z	Kamchatka-Kuril-Japan-Izu-Mariana-Yap	141.6671	37.2234	208	21	39.2
kisz–29a	Kamchatka-Kuril-Japan-Izu-Mariana-Yap	141.5970	36.2640	211	21	21.28
kisz–29b	Kamchatka-Kuril-Japan-Izu-Mariana-Yap	142.0416	36.0481	211	19	5
kisz–29y	Kamchatka-Kuril-Japan-Izu-Mariana-Yap	140.7029	36.6960	211	21	57.12
kisz–29z	Kamchatka-Kuril-Japan-Izu-Mariana-Yap	141.1506	36.4800	211	21	39.2
kisz–30a	Kamchatka-Kuril-Japan-Izu-Mariana-Yap	141.0553	35.4332	205	21	21.28
kisz–30b	Kamchatka-Kuril-Japan-Izu-Mariana-Yap	141.5207	35.2560	205	19	5
kisz–30y	Kamchatka-Kuril-Japan-Izu-Mariana-Yap	140.1204	35.7876	205	21	57.12
kisz–30z	Kamchatka-Kuril-Japan-Izu-Mariana-Yap	140.5883	35.6104	205	21	39.2
kisz–31a	Kamchatka-Kuril-Japan-Izu-Mariana-Yap	140.6956	34.4789	190	22	22.1
kisz–31b	Kamchatka-Kuril-Japan-Izu-Mariana-Yap	141.1927	34.4066	190	20	5
kisz–31v	Kamchatka-Kuril-Japan-Izu-Mariana-Yap	138.2025	34.8405	190	22	115.8
kisz–31w	Kamchatka-Kuril-Japan-Izu-Mariana-Yap	138.7021	34.7682	190	22	97.02
kisz–31x	Kamchatka-Kuril-Japan-Izu-Mariana-Yap	139.2012	34.6958	190	22	78.29
kisz–31y	Kamchatka-Kuril-Japan-Izu-Mariana-Yap	139.6997	34.6235	190	22	59.56
kisz–31z	Kamchatka-Kuril-Japan-Izu-Mariana-Yap	140.1979	34.5512	190	22	40.83
kisz–32a	Kamchatka-Kuril-Japan-Izu-Mariana-Yap	141.0551	33.0921	180	32	23.48
kisz–32b	Kamchatka-Kuril-Japan-Izu-Mariana-Yap	141.5098	33.0921	180	21.69	5
kisz–33a	Kamchatka-Kuril-Japan-Izu-Mariana-Yap	141.0924	32.1047	173.8	27.65	20.67
kisz–33b	Kamchatka-Kuril-Japan-Izu-Mariana-Yap	141.5596	32.1473	173.8	18.27	5
kisz–34a	Kamchatka-Kuril-Japan-Izu-Mariana-Yap	141.1869	31.1851	172.1	25	18.26
kisz–34b	Kamchatka-Kuril-Japan-Izu-Mariana-Yap	141.6585	31.2408	172.1	15.38	5
kisz–35a	Kamchatka-Kuril-Japan-Izu-Mariana-Yap	141.4154	30.1707	163	25	17.12
kisz–35b	Kamchatka-Kuril-Japan-Izu-Mariana-Yap	141.8662	30.2899	163	14.03	5
kisz–36a	Kamchatka-Kuril-Japan-Izu-Mariana-Yap	141.6261	29.2740	161.7	25.73	18.71
kisz–36b	Kamchatka-Kuril-Japan-Izu-Mariana-Yap	142.0670	29.4012	161.7	15.91	5
kisz–37a	Kamchatka-Kuril-Japan-Izu-Mariana-Yap	142.0120	28.3322	154.7	20	14.54
kisz–37b	Kamchatka-Kuril-Japan-Izu-Mariana-Yap	142.4463	28.5124	154.7	11	5
kisz–38a	Kamchatka-Kuril-Japan-Izu-Mariana-Yap	142.2254	27.6946	170.3	20	14.54
kisz–38b	Kamchatka-Kuril-Japan-Izu-Mariana-Yap	142.6955	27.7659	170.3	11	5
kisz–39a	Kamchatka-Kuril-Japan-Izu-Mariana-Yap	142.3085	26.9127	177.2	24.23	17.42
kisz–39b	Kamchatka-Kuril-Japan-Izu-Mariana-Yap	142.7674	26.9325	177.2	14.38	5
kisz–40a	Kamchatka-Kuril-Japan-Izu-Mariana-Yap	142.2673	26.1923	189.4	26.49	22.26
kisz–40b	Kamchatka-Kuril-Japan-Izu-Mariana-Yap	142.7090	26.1264	189.4	20.2	5
kisz–41a	Kamchatka-Kuril-Japan-Izu-Mariana-Yap	142.1595	25.0729	173.7	22.07	19.08
kisz–41b	Kamchatka-Kuril-Japan-Izu-Mariana-Yap	142.6165	25.1184	173.7	16.36	5
kisz–42a	Kamchatka-Kuril-Japan-Izu-Mariana-Yap	142.7641	23.8947	143.5	21.54	18.4
kisz–42b	Kamchatka-Kuril-Japan-Izu-Mariana-Yap	143.1321	24.1432	143.5	15.54	5
kisz–43a	Kamchatka-Kuril-Japan-Izu-Mariana-Yap	143.5281	23.0423	129.2	23.02	18.77
kisz–43b	Kamchatka-Kuril-Japan-Izu-Mariana-Yap	143.8128	23.3626	129.2	15.99	5
kisz–44a	Kamchatka-Kuril-Japan-Izu-Mariana-Yap	144.2230	22.5240	134.6	28.24	18.56
kisz–44b	Kamchatka-Kuril-Japan-Izu-Mariana-Yap	144.5246	22.8056	134.6	15.74	5
kisz–45a	Kamchatka-Kuril-Japan-Izu-Mariana-Yap	145.0895	21.8866	125.8	36.73	22.79
kisz–45b	Kamchatka-Kuril-Japan-Izu-Mariana-Yap	145.3171	22.1785	125.8	20.84	5
kisz–46a	Kamchatka-Kuril-Japan-Izu-Mariana-Yap	145.6972	21.3783	135.9	30.75	20.63
kisz–46b	Kamchatka-Kuril-Japan-Izu-Mariana-Yap	145.9954	21.6469	135.9	18.22	5

(continued on next page)

Table B4: (continued)

Segment	Description	Longitude (°E)	Latitude (°N)	Strike (°)	Dip (°)	Depth (km)
kisz–47a	Kamchatka-Kuril-Japan-Izu-Mariana-Yap	146.0406	20.9341	160.1	29.87	19.62
kisz–47b	Kamchatka-Kuril-Japan-Izu-Mariana-Yap	146.4330	21.0669	160.1	17	5
kisz–48a	Kamchatka-Kuril-Japan-Izu-Mariana-Yap	146.3836	20.0690	158	32.75	19.68
kisz–48b	Kamchatka-Kuril-Japan-Izu-Mariana-Yap	146.7567	20.2108	158	17.07	5
kisz–49a	Kamchatka-Kuril-Japan-Izu-Mariana-Yap	146.6689	19.3123	164.5	25.07	21.41
kisz–49b	Kamchatka-Kuril-Japan-Izu-Mariana-Yap	147.0846	19.4212	164.5	19.16	5
kisz–50a	Kamchatka-Kuril-Japan-Izu-Mariana-Yap	146.9297	18.5663	172.1	22	22.1
kisz–50b	Kamchatka-Kuril-Japan-Izu-Mariana-Yap	147.3650	18.6238	172.1	20	5
kisz–51a	Kamchatka-Kuril-Japan-Izu-Mariana-Yap	146.9495	17.7148	175.1	22.06	22.04
kisz–51b	Kamchatka-Kuril-Japan-Izu-Mariana-Yap	147.3850	17.7503	175.1	19.93	5
kisz–52a	Kamchatka-Kuril-Japan-Izu-Mariana-Yap	146.9447	16.8869	180	25.51	18.61
kisz–52b	Kamchatka-Kuril-Japan-Izu-Mariana-Yap	147.3683	16.8869	180	15.79	5
kisz–53a	Kamchatka-Kuril-Japan-Izu-Mariana-Yap	146.8626	16.0669	185.2	27.39	18.41
kisz–53b	Kamchatka-Kuril-Japan-Izu-Mariana-Yap	147.2758	16.0309	185.2	15.56	5
kisz–54a	Kamchatka-Kuril-Japan-Izu-Mariana-Yap	146.7068	15.3883	199.1	28.12	20.91
kisz–54b	Kamchatka-Kuril-Japan-Izu-Mariana-Yap	147.0949	15.2590	199.1	18.56	5
kisz–55a	Kamchatka-Kuril-Japan-Izu-Mariana-Yap	146.4717	14.6025	204.3	29.6	26.27
kisz–55b	Kamchatka-Kuril-Japan-Izu-Mariana-Yap	146.8391	14.4415	204.3	25.18	5
kisz–56a	Kamchatka-Kuril-Japan-Izu-Mariana-Yap	146.1678	13.9485	217.4	32.04	26.79
kisz–56b	Kamchatka-Kuril-Japan-Izu-Mariana-Yap	146.4789	13.7170	217.4	25.84	5
kisz–57a	Kamchatka-Kuril-Japan-Izu-Mariana-Yap	145.6515	13.5576	235.8	37	24.54
kisz–57b	Kamchatka-Kuril-Japan-Izu-Mariana-Yap	145.8586	13.2609	235.8	23	5
kisz–58a	Kamchatka-Kuril-Japan-Izu-Mariana-Yap	144.9648	12.9990	237.8	37.72	24.54
kisz–58b	Kamchatka-Kuril-Japan-Izu-Mariana-Yap	145.1589	12.6984	237.8	23	5
kisz–59a	Kamchatka-Kuril-Japan-Izu-Mariana-Yap	144.1799	12.6914	242.9	34.33	22.31
kisz–59b	Kamchatka-Kuril-Japan-Izu-Mariana-Yap	144.3531	12.3613	242.9	20.25	5
kisz–60a	Kamchatka-Kuril-Japan-Izu-Mariana-Yap	143.3687	12.3280	244.9	30.9	20.62
kisz–60b	Kamchatka-Kuril-Japan-Izu-Mariana-Yap	143.5355	11.9788	244.9	18.2	5
kisz–61a	Kamchatka-Kuril-Japan-Izu-Mariana-Yap	142.7051	12.1507	261.8	35.41	25.51
kisz–61b	Kamchatka-Kuril-Japan-Izu-Mariana-Yap	142.7582	11.7883	261.8	24.22	5
kisz–62a	Kamchatka-Kuril-Japan-Izu-Mariana-Yap	141.6301	11.8447	245.7	39.86	34.35
kisz–62b	Kamchatka-Kuril-Japan-Izu-Mariana-Yap	141.7750	11.5305	245.7	35.94	5
kisz–63a	Kamchatka-Kuril-Japan-Izu-Mariana-Yap	140.8923	11.5740	256.2	42	38.46
kisz–63b	Kamchatka-Kuril-Japan-Izu-Mariana-Yap	140.9735	11.2498	256.2	42	5
kisz–64a	Kamchatka-Kuril-Japan-Izu-Mariana-Yap	140.1387	11.6028	269.6	42.48	38.77
kisz–64b	Kamchatka-Kuril-Japan-Izu-Mariana-Yap	140.1410	11.2716	269.6	42.48	5
kisz–65a	Kamchatka-Kuril-Japan-Izu-Mariana-Yap	139.4595	11.5883	288.7	44.16	39.83
kisz–65b	Kamchatka-Kuril-Japan-Izu-Mariana-Yap	139.3541	11.2831	288.7	44.16	5
kisz–66a	Kamchatka-Kuril-Japan-Izu-Mariana-Yap	138.1823	11.2648	193.1	45	40.36
kisz–66b	Kamchatka-Kuril-Japan-Izu-Mariana-Yap	138.4977	11.1929	193.1	45	5
kisz–67a	Kamchatka-Kuril-Japan-Izu-Mariana-Yap	137.9923	10.3398	189.8	45	40.36
kisz–67b	Kamchatka-Kuril-Japan-Izu-Mariana-Yap	138.3104	10.2856	189.8	45	5
kisz–68a	Kamchatka-Kuril-Japan-Izu-Mariana-Yap	137.7607	9.6136	201.7	45	40.36
kisz–68b	Kamchatka-Kuril-Japan-Izu-Mariana-Yap	138.0599	9.4963	201.7	45	5
kisz–69a	Kamchatka-Kuril-Japan-Izu-Mariana-Yap	137.4537	8.8996	213.5	45	40.36
kisz–69b	Kamchatka-Kuril-Japan-Izu-Mariana-Yap	137.7215	8.7241	213.5	45	5
kisz–70a	Kamchatka-Kuril-Japan-Izu-Mariana-Yap	137.0191	8.2872	226.5	45	40.36
kisz–70b	Kamchatka-Kuril-Japan-Izu-Mariana-Yap	137.2400	8.0569	226.5	45	5
kisz–71a	Kamchatka-Kuril-Japan-Izu-Mariana-Yap	136.3863	7.9078	263.9	45	40.36
kisz–71b	Kamchatka-Kuril-Japan-Izu-Mariana-Yap	136.4202	7.5920	263.9	45	5
kisz–72a	Kamchatka-Kuril-Japan-Izu-Mariana-Yap	135.6310	7.9130	276.9	45	40.36
kisz–72b	Kamchatka-Kuril-Japan-Izu-Mariana-Yap	135.5926	7.5977	276.9	45	5
kisz–73a	Kamchatka-Kuril-Japan-Izu-Mariana-Yap	134.3296	7.4541	224	45	40.36
kisz–73b	Kamchatka-Kuril-Japan-Izu-Mariana-Yap	134.5600	7.2335	224	45	5
kisz–74a	Kamchatka-Kuril-Japan-Izu-Mariana-Yap	133.7125	6.8621	228.1	45	40.36

(continued on next page)

Table B4: (continued)

Segment	Description	Longitude (°E)	Latitude (°N)	Strike (°)	Dip (°)	Depth (km)
kisz–74b	Kamchatka-Kuril-Japan-Izu-Mariana-Yap	133.9263	6.6258	228.1	45	5
kisz–75a	Kamchatka-Kuril-Japan-Izu-Mariana-Yap	133.0224	6.1221	217.7	45	40.36
kisz–75b	Kamchatka-Kuril-Japan-Izu-Mariana-Yap	133.2751	5.9280	217.7	45	5

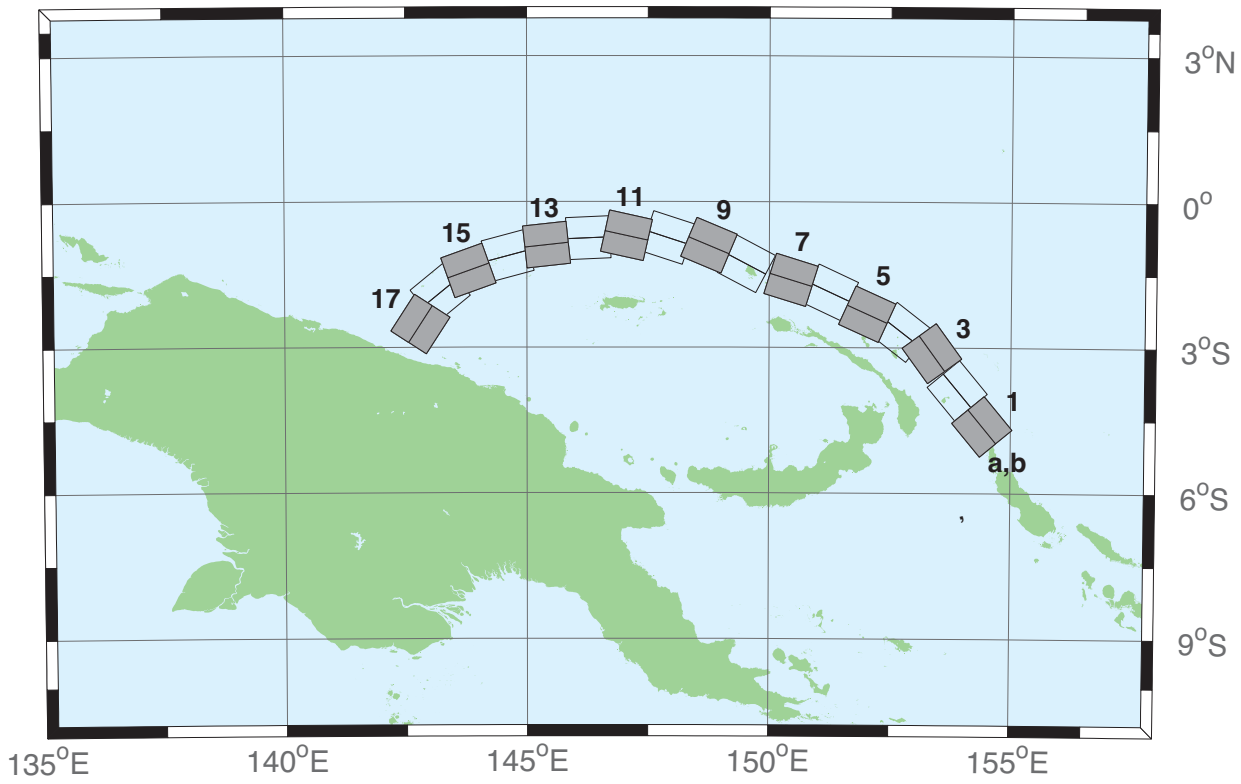

Figure B5: Manus–Oceanic Convergent Boundary Subduction Zone unit sources.

Table B5: Earthquake parameters for Manus–Oceanic Convergent Boundary Subduction Zone unit sources.

Segment	Description	Longitude (°E)	Latitude (°N)	Strike (°)	Dip (°)	Depth (km)
mosz–1a	Manus–Oceanic Convergent Boundary	154.0737	–4.8960	140.2	15	15.88
mosz–1b	Manus–Oceanic Convergent Boundary	154.4082	–4.6185	140.2	15	5
mosz–2a	Manus–Oceanic Convergent Boundary	153.5589	–4.1575	140.2	15	15.91
mosz–2b	Manus–Oceanic Convergent Boundary	153.8931	–3.8800	140.2	15	5.35
mosz–3a	Manus–Oceanic Convergent Boundary	153.0151	–3.3716	143.9	15	16.64
mosz–3b	Manus–Oceanic Convergent Boundary	153.3662	–3.1160	143.9	15	6.31
mosz–4a	Manus–Oceanic Convergent Boundary	152.4667	–3.0241	127.7	15	17.32
mosz–4b	Manus–Oceanic Convergent Boundary	152.7321	–2.6806	127.7	15	7.39
mosz–5a	Manus–Oceanic Convergent Boundary	151.8447	–2.7066	114.3	15	17.57
mosz–5b	Manus–Oceanic Convergent Boundary	152.0235	–2.3112	114.3	15	8.25
mosz–6a	Manus–Oceanic Convergent Boundary	151.0679	–2.2550	115	15	17.66
mosz–6b	Manus–Oceanic Convergent Boundary	151.2513	–1.8618	115	15	7.58
mosz–7a	Manus–Oceanic Convergent Boundary	150.3210	–2.0236	107.2	15	17.73
mosz–7b	Manus–Oceanic Convergent Boundary	150.4493	–1.6092	107.2	15	6.83
mosz–8a	Manus–Oceanic Convergent Boundary	149.3226	–1.6666	117.8	15	17.83
mosz–8b	Manus–Oceanic Convergent Boundary	149.5251	–1.2829	117.8	15	7.92
mosz–9a	Manus–Oceanic Convergent Boundary	148.5865	–1.3017	112.7	15	17.84
mosz–9b	Manus–Oceanic Convergent Boundary	148.7540	–0.9015	112.7	15	8.3
mosz–10a	Manus–Oceanic Convergent Boundary	147.7760	–1.1560	108	15	17.78
mosz–10b	Manus–Oceanic Convergent Boundary	147.9102	–0.7434	108	15	8.09
mosz–11a	Manus–Oceanic Convergent Boundary	146.9596	–1.1226	102.5	15	17.54
mosz–11b	Manus–Oceanic Convergent Boundary	147.0531	–0.6990	102.5	15	7.64
mosz–12a	Manus–Oceanic Convergent Boundary	146.2858	–1.1820	87.48	15	17.29
mosz–12b	Manus–Oceanic Convergent Boundary	146.2667	–0.7486	87.48	15	7.62
mosz–13a	Manus–Oceanic Convergent Boundary	145.4540	–1.3214	83.75	15	17.34
mosz–13b	Manus–Oceanic Convergent Boundary	145.4068	–0.8901	83.75	15	7.08
mosz–14a	Manus–Oceanic Convergent Boundary	144.7151	–1.5346	75.09	15	17.21
mosz–14b	Manus–Oceanic Convergent Boundary	144.6035	–1.1154	75.09	15	6.38
mosz–15a	Manus–Oceanic Convergent Boundary	143.9394	–1.8278	70.43	15	16.52
mosz–15b	Manus–Oceanic Convergent Boundary	143.7940	–1.4190	70.43	15	6.09
mosz–16a	Manus–Oceanic Convergent Boundary	143.4850	–2.2118	50.79	15	15.86
mosz–16b	Manus–Oceanic Convergent Boundary	143.2106	–1.8756	50.79	15	5
mosz–17a	Manus–Oceanic Convergent Boundary	143.1655	–2.7580	33	15	16.64
mosz–17b	Manus–Oceanic Convergent Boundary	142.8013	–2.5217	33	15	5

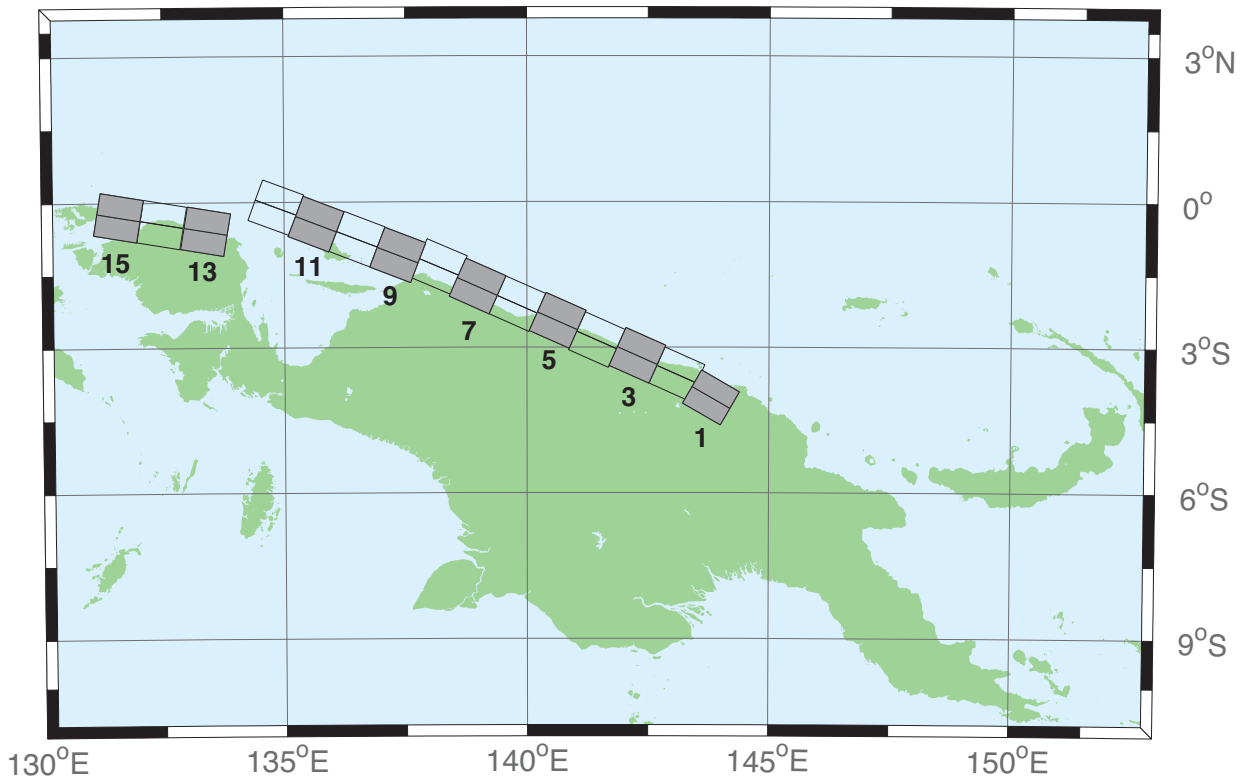

Figure B6: New Guinea Subduction Zone unit sources.

Table B6: Earthquake parameters for New Guinea Subduction Zone unit sources.

Segment	Description	Longitude (°E)	Latitude (°N)	Strike (°)	Dip (°)	Depth (km)
ngsz–1a	New Guinea	143.6063	–4.3804	120	29	25.64
ngsz–1b	New Guinea	143.8032	–4.0402	120	29	1.4
ngsz–2a	New Guinea	142.9310	–3.9263	114	27.63	20.1
ngsz–2b	New Guinea	143.0932	–3.5628	114	21.72	1.6
ngsz–3a	New Guinea	142.1076	–3.5632	114	20.06	18.73
ngsz–3b	New Guinea	142.2795	–3.1778	114	15.94	5
ngsz–4a	New Guinea	141.2681	–3.2376	114	21	17.76
ngsz–4b	New Guinea	141.4389	–2.8545	114	14.79	5
ngsz–5a	New Guinea	140.4592	–2.8429	114	21.26	16.14
ngsz–5b	New Guinea	140.6296	–2.4605	114	12.87	5
ngsz–6a	New Guinea	139.6288	–2.4960	114	22.72	15.4
ngsz–6b	New Guinea	139.7974	–2.1175	114	12	5
ngsz–7a	New Guinea	138.8074	–2.1312	114	21.39	15.4
ngsz–7b	New Guinea	138.9776	–1.7491	114	12	5
ngsz–8a	New Guinea	138.0185	–1.7353	113.1	18.79	15.14
ngsz–8b	New Guinea	138.1853	–1.3441	113.1	11.7	5
ngsz–9a	New Guinea	137.1805	–1.5037	111	15.24	13.23
ngsz–9b	New Guinea	137.3358	–1.0991	111	9.47	5
ngsz–10a	New Guinea	136.3418	–1.1774	111	13.51	11.09
ngsz–10b	New Guinea	136.4983	–0.7697	111	7	5
ngsz–11a	New Guinea	135.4984	–0.8641	111	11.38	12.49
ngsz–11b	New Guinea	135.6562	–0.4530	111	8.62	5
ngsz–12a	New Guinea	134.6759	–0.5216	110.5	10	13.68
ngsz–12b	New Guinea	134.8307	–0.1072	110.5	10	5
ngsz–13a	New Guinea	133.3065	–1.0298	99.5	10	13.68
ngsz–13b	New Guinea	133.3795	–0.5935	99.5	10	5
ngsz–14a	New Guinea	132.4048	–0.8816	99.5	10	13.68
ngsz–14b	New Guinea	132.4778	–0.4453	99.5	10	5
ngsz–15a	New Guinea	131.5141	–0.7353	99.5	10	13.68
ngsz–15b	New Guinea	131.5871	–0.2990	99.5	10	5

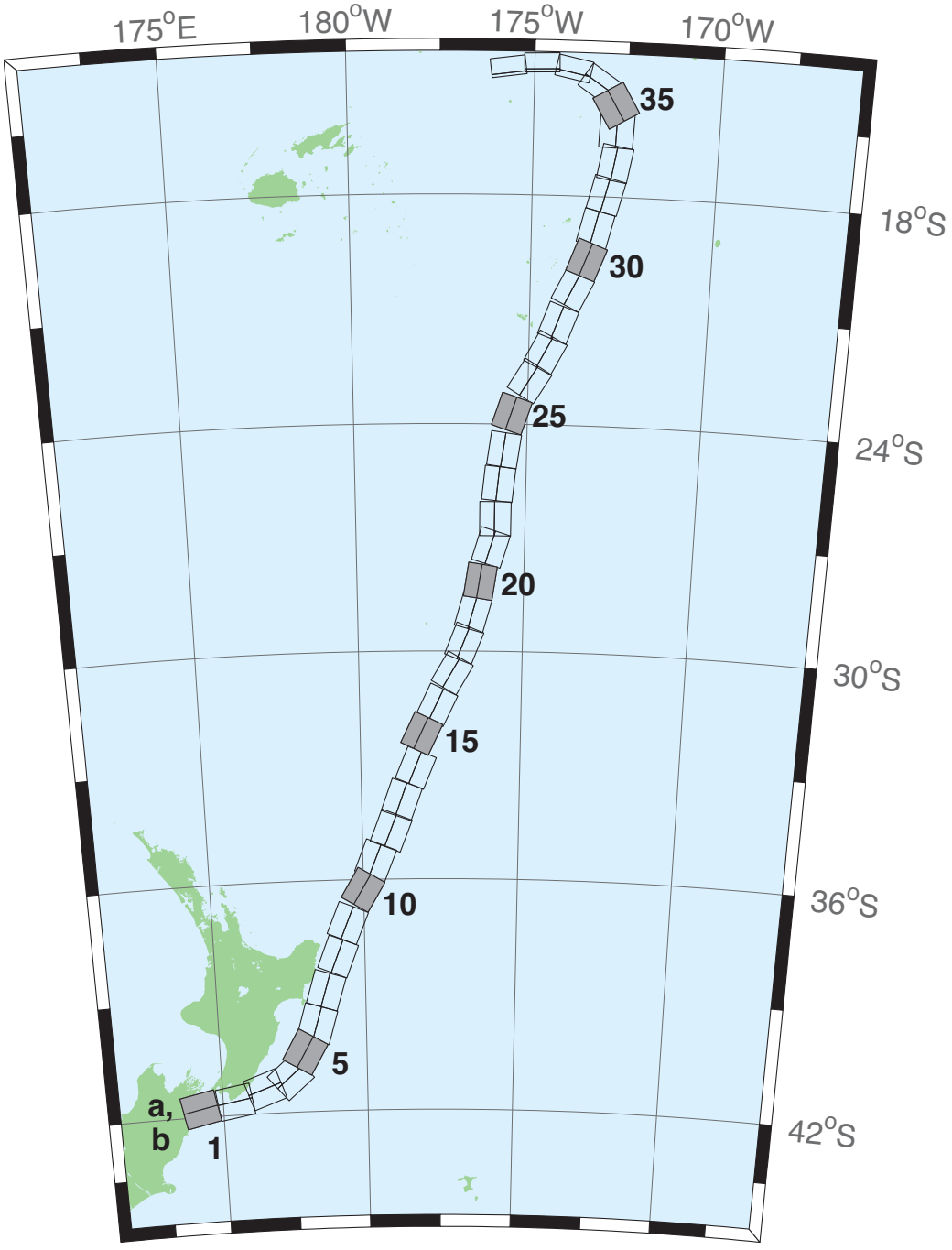

Figure B7: New Zealand–Keradec–Tonga Subduction Zone unit sources.

Table B7: Earthquake parameters for New Zealand–Keradec–Tonga Subduction Zone unit sources.

Segment	Description	Longitude (°E)	Latitude (°N)	Strike (°)	Dip (°)	Depth (km)
ntsz–1a	New Zealand–Keradec–Tonga	174.0985	–41.3951	258.6	24	25.34
ntsz–1b	New Zealand–Keradec–Tonga	174.2076	–41.7973	258.6	24	5
ntsz–2a	New Zealand–Keradec–Tonga	175.3289	–41.2592	260.6	29.38	23.17
ntsz–2b	New Zealand–Keradec–Tonga	175.4142	–41.6454	260.6	21.31	5
ntsz–3a	New Zealand–Keradec–Tonga	176.2855	–40.9950	250.7	29.54	21.74
ntsz–3b	New Zealand–Keradec–Tonga	176.4580	–41.3637	250.7	19.56	5
ntsz–4a	New Zealand–Keradec–Tonga	177.0023	–40.7679	229.4	24.43	18.87
ntsz–4b	New Zealand–Keradec–Tonga	177.3552	–41.0785	229.4	16.1	5
ntsz–5a	New Zealand–Keradec–Tonga	177.4114	–40.2396	210	18.8	19.29
ntsz–5b	New Zealand–Keradec–Tonga	177.8951	–40.4525	210	16.61	5
ntsz–6a	New Zealand–Keradec–Tonga	177.8036	–39.6085	196.7	18.17	15.8
ntsz–6b	New Zealand–Keradec–Tonga	178.3352	–39.7310	196.7	12.48	5
ntsz–7a	New Zealand–Keradec–Tonga	178.1676	–38.7480	197	28.1	17.85
ntsz–7b	New Zealand–Keradec–Tonga	178.6541	–38.8640	197	14.89	5
ntsz–8a	New Zealand–Keradec–Tonga	178.6263	–37.8501	201.4	31.47	18.78
ntsz–8b	New Zealand–Keradec–Tonga	179.0788	–37.9899	201.4	16	5
ntsz–9a	New Zealand–Keradec–Tonga	178.9833	–36.9770	202.2	29.58	20.02
ntsz–9b	New Zealand–Keradec–Tonga	179.4369	–37.1245	202.2	17.48	5
ntsz–10a	New Zealand–Keradec–Tonga	179.5534	–36.0655	210.6	32.1	20.72
ntsz–10b	New Zealand–Keradec–Tonga	179.9595	–36.2593	210.6	18.32	5
ntsz–11a	New Zealand–Keradec–Tonga	179.9267	–35.3538	201.7	25	16.09
ntsz–11b	New Zealand–Keradec–Tonga	180.3915	–35.5040	201.7	12.81	5
ntsz–12a	New Zealand–Keradec–Tonga	180.4433	–34.5759	201.2	25	15.46
ntsz–12b	New Zealand–Keradec–Tonga	180.9051	–34.7230	201.2	12.08	5
ntsz–13a	New Zealand–Keradec–Tonga	180.7990	–33.7707	199.8	25.87	19.06
ntsz–13b	New Zealand–Keradec–Tonga	181.2573	–33.9073	199.8	16.33	5
ntsz–14a	New Zealand–Keradec–Tonga	181.2828	–32.9288	202.4	31.28	22.73
ntsz–14b	New Zealand–Keradec–Tonga	181.7063	–33.0751	202.4	20.77	5
ntsz–15a	New Zealand–Keradec–Tonga	181.4918	–32.0035	205.4	32.33	22.64
ntsz–15b	New Zealand–Keradec–Tonga	181.8967	–32.1665	205.4	20.66	5
ntsz–16a	New Zealand–Keradec–Tonga	181.9781	–31.2535	205.5	34.29	23.59
ntsz–16b	New Zealand–Keradec–Tonga	182.3706	–31.4131	205.5	21.83	5
ntsz–17a	New Zealand–Keradec–Tonga	182.4819	–30.3859	210.3	37.6	25.58
ntsz–17b	New Zealand–Keradec–Tonga	182.8387	–30.5655	210.3	24.3	5
ntsz–18a	New Zealand–Keradec–Tonga	182.8176	–29.6545	201.6	37.65	26.13
ntsz–18b	New Zealand–Keradec–Tonga	183.1985	–29.7856	201.6	25	5
ntsz–19a	New Zealand–Keradec–Tonga	183.0622	–28.8739	195.7	34.41	26.13
ntsz–19b	New Zealand–Keradec–Tonga	183.4700	–28.9742	195.7	25	5
ntsz–20a	New Zealand–Keradec–Tonga	183.2724	–28.0967	188.8	38	26.13
ntsz–20b	New Zealand–Keradec–Tonga	183.6691	–28.1508	188.8	25	5
ntsz–21a	New Zealand–Keradec–Tonga	183.5747	–27.1402	197.1	32.29	24.83
ntsz–21b	New Zealand–Keradec–Tonga	183.9829	–27.2518	197.1	23.37	5
ntsz–22a	New Zealand–Keradec–Tonga	183.6608	–26.4975	180	29.56	18.63
ntsz–22b	New Zealand–Keradec–Tonga	184.0974	–26.4975	180	15.82	5
ntsz–23a	New Zealand–Keradec–Tonga	183.7599	–25.5371	185.8	32.42	20.56
ntsz–23b	New Zealand–Keradec–Tonga	184.1781	–25.5752	185.8	18.13	5
ntsz–24a	New Zealand–Keradec–Tonga	183.9139	–24.6201	188.2	33.31	23.73
ntsz–24b	New Zealand–Keradec–Tonga	184.3228	–24.6734	188.2	22	5
ntsz–25a	New Zealand–Keradec–Tonga	184.1266	–23.5922	198.5	29.34	19.64
ntsz–25b	New Zealand–Keradec–Tonga	184.5322	–23.7163	198.5	17.03	5
ntsz–26a	New Zealand–Keradec–Tonga	184.6613	–22.6460	211.7	30.26	19.43
ntsz–26b	New Zealand–Keradec–Tonga	185.0196	–22.8497	211.7	16.78	5
ntsz–27a	New Zealand–Keradec–Tonga	185.0879	–21.9139	207.9	31.73	20.67
ntsz–27b	New Zealand–Keradec–Tonga	185.4522	–22.0928	207.9	18.27	5
ntsz–28a	New Zealand–Keradec–Tonga	185.4037	–21.1758	200.5	32.44	21.76

(continued on next page)

Table B7: (continued)

Segment	Description	Longitude (°E)	Latitude (°N)	Strike (°)	Dip (°)	Depth (km)
ntsz–28b	New Zealand–Keradec–Tonga	185.7849	–21.3084	200.5	19.58	5
ntsz–29a	New Zealand–Keradec–Tonga	185.8087	–20.2629	206.4	32.47	20.4
ntsz–29b	New Zealand–Keradec–Tonga	186.1710	–20.4312	206.4	17.94	5
ntsz–30a	New Zealand–Keradec–Tonga	186.1499	–19.5087	200.9	32.98	22.46
ntsz–30b	New Zealand–Keradec–Tonga	186.5236	–19.6432	200.9	20.44	5
ntsz–31a	New Zealand–Keradec–Tonga	186.3538	–18.7332	193.9	34.41	21.19
ntsz–31b	New Zealand–Keradec–Tonga	186.7339	–18.8221	193.9	18.89	5
ntsz–32a	New Zealand–Keradec–Tonga	186.5949	–17.8587	194.1	30	19.12
ntsz–32b	New Zealand–Keradec–Tonga	186.9914	–17.9536	194.1	16.4	5
ntsz–33a	New Zealand–Keradec–Tonga	186.8172	–17.0581	190	33.15	23.34
ntsz–33b	New Zealand–Keradec–Tonga	187.2047	–17.1237	190	21.52	5
ntsz–34a	New Zealand–Keradec–Tonga	186.7814	–16.2598	182.1	15	13.41
ntsz–34b	New Zealand–Keradec–Tonga	187.2330	–16.2759	182.1	9.68	5
ntsz–35a	New Zealand–Keradec–Tonga	186.8000	–15.8563	149.8	15	12.17
ntsz–35b	New Zealand–Keradec–Tonga	187.1896	–15.6384	149.8	8.24	5
ntsz–36a	New Zealand–Keradec–Tonga	186.5406	–15.3862	123.9	40.44	36.72
ntsz–36b	New Zealand–Keradec–Tonga	186.7381	–15.1025	123.9	39.38	5
ntsz–37a	New Zealand–Keradec–Tonga	185.9883	–14.9861	102	68.94	30.99
ntsz–37b	New Zealand–Keradec–Tonga	186.0229	–14.8282	102	31.32	5
ntsz–38a	New Zealand–Keradec–Tonga	185.2067	–14.8259	88.4	80	26.13
ntsz–38b	New Zealand–Keradec–Tonga	185.2044	–14.7479	88.4	25	5
ntsz–39a	New Zealand–Keradec–Tonga	184.3412	–14.9409	82.55	80	26.13
ntsz–39b	New Zealand–Keradec–Tonga	184.3307	–14.8636	82.55	25	5

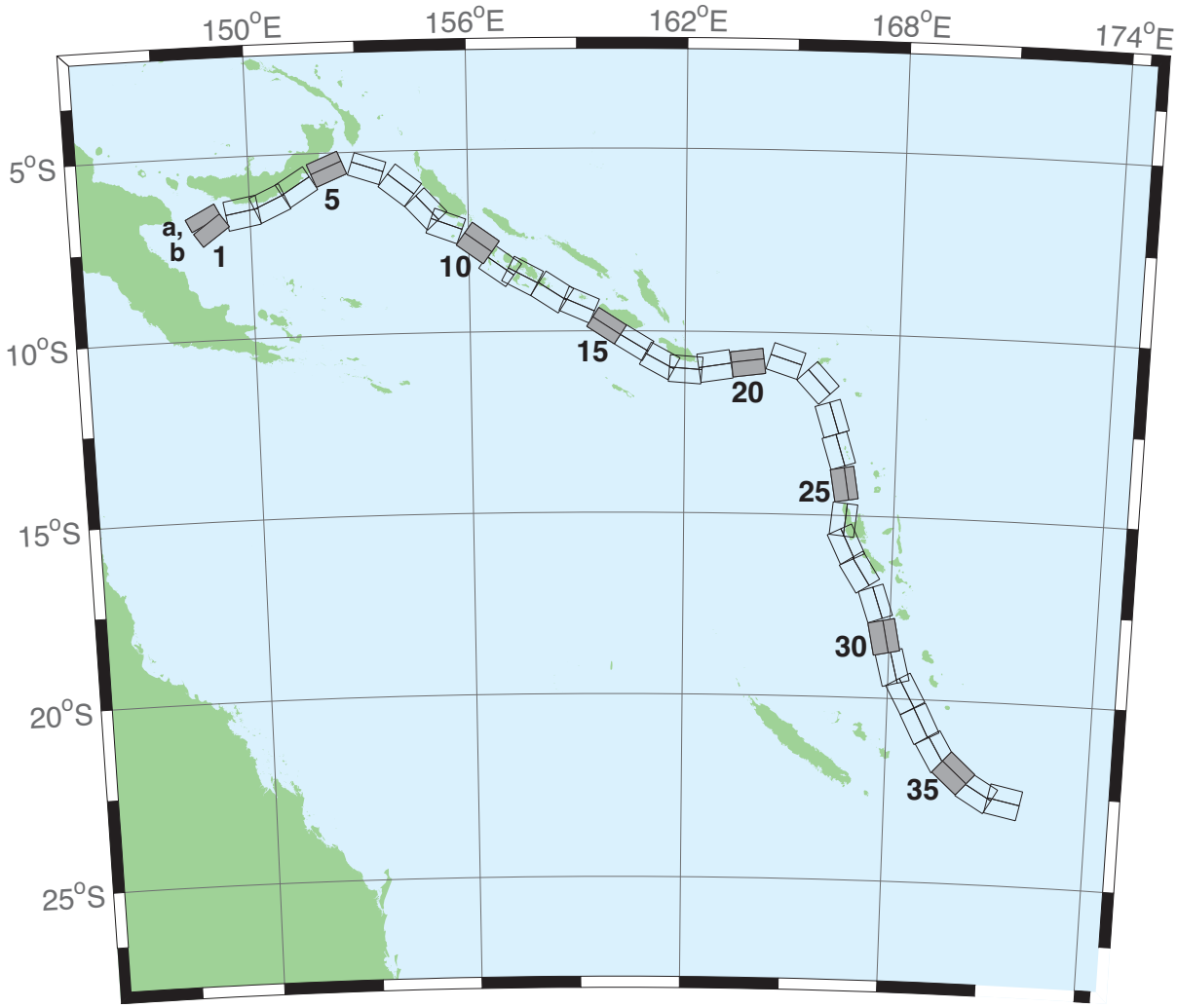

Figure B8: New Britain–Solomons–Vanuatu Zone unit sources.

Table B8: Earthquake parameters for New Britain–Solomons–Vanuatu Subduction Zone unit sources.

Segment	Description	Longitude (°E)	Latitude (°N)	Strike (°)	Dip (°)	Depth (km)
nvsz–1a	New Britain–Solomons–Vanuatu	148.6217	–6.4616	243.2	32.34	15.69
nvsz–1b	New Britain–Solomons–Vanuatu	148.7943	–6.8002	234.2	12.34	5
nvsz–2a	New Britain–Solomons–Vanuatu	149.7218	–6.1459	260.1	35.1	16.36
nvsz–2b	New Britain–Solomons–Vanuatu	149.7856	–6.5079	260.1	13.13	5
nvsz–3a	New Britain–Solomons–Vanuatu	150.4075	–5.9659	245.7	42.35	18.59
nvsz–3b	New Britain–Solomons–Vanuatu	150.5450	–6.2684	245.7	15.77	5
nvsz–4a	New Britain–Solomons–Vanuatu	151.1095	–5.5820	238.2	42.41	23.63
nvsz–4b	New Britain–Solomons–Vanuatu	151.2851	–5.8639	238.2	21.88	5
nvsz–5a	New Britain–Solomons–Vanuatu	152.0205	–5.1305	247.7	49.22	32.39
nvsz–5b	New Britain–Solomons–Vanuatu	152.1322	–5.4020	247.7	33.22	5
nvsz–6a	New Britain–Solomons–Vanuatu	153.3450	–5.1558	288.6	53.53	33.59
nvsz–6b	New Britain–Solomons–Vanuatu	153.2595	–5.4089	288.6	34.87	5
nvsz–7a	New Britain–Solomons–Vanuatu	154.3814	–5.6308	308.3	39.72	19.18
nvsz–7b	New Britain–Solomons–Vanuatu	154.1658	–5.9017	308.3	16.48	5
nvsz–8a	New Britain–Solomons–Vanuatu	155.1097	–6.3511	317.2	45.33	22.92
nvsz–8b	New Britain–Solomons–Vanuatu	154.8764	–6.5656	317.2	21	5
nvsz–9a	New Britain–Solomons–Vanuatu	155.5027	–6.7430	290.5	48.75	22.92
nvsz–9b	New Britain–Solomons–Vanuatu	155.3981	–7.0204	290.5	21	5
nvsz–10a	New Britain–Solomons–Vanuatu	156.4742	–7.2515	305.9	36.88	27.62
nvsz–10b	New Britain–Solomons–Vanuatu	156.2619	–7.5427	305.9	26.9	5
nvsz–11a	New Britain–Solomons–Vanuatu	157.0830	–7.8830	305.4	32.97	29.72
nvsz–11b	New Britain–Solomons–Vanuatu	156.8627	–8.1903	305.4	29.63	5
nvsz–12a	New Britain–Solomons–Vanuatu	157.6537	–8.1483	297.9	37.53	28.57
nvsz–12b	New Britain–Solomons–Vanuatu	157.4850	–8.4630	297.9	28.13	5
nvsz–13a	New Britain–Solomons–Vanuatu	158.5089	–8.5953	302.7	33.62	23.02
nvsz–13b	New Britain–Solomons–Vanuatu	158.3042	–8.9099	302.7	21.12	5
nvsz–14a	New Britain–Solomons–Vanuatu	159.1872	–8.9516	293.3	38.44	34.06
nvsz–14b	New Britain–Solomons–Vanuatu	159.0461	–9.2747	293.3	35.54	5
nvsz–15a	New Britain–Solomons–Vanuatu	159.9736	–9.5993	302.8	46.69	41.38
nvsz–15b	New Britain–Solomons–Vanuatu	159.8044	–9.8584	302.8	46.69	5
nvsz–16a	New Britain–Solomons–Vanuatu	160.7343	–10.0574	301	46.05	41
nvsz–16b	New Britain–Solomons–Vanuatu	160.5712	–10.3246	301	46.05	5
nvsz–17a	New Britain–Solomons–Vanuatu	161.4562	–10.5241	298.4	40.12	37.22
nvsz–17b	New Britain–Solomons–Vanuatu	161.2900	–10.8263	298.4	40.12	5
nvsz–18a	New Britain–Solomons–Vanuatu	162.0467	–10.6823	274.1	40.33	29.03
nvsz–18b	New Britain–Solomons–Vanuatu	162.0219	–11.0238	274.1	28.72	5
nvsz–19a	New Britain–Solomons–Vanuatu	162.7818	–10.5645	261.3	34.25	24.14
nvsz–19b	New Britain–Solomons–Vanuatu	162.8392	–10.9315	261.3	22.51	5
nvsz–20a	New Britain–Solomons–Vanuatu	163.7222	–10.5014	262.9	50.35	26.3
nvsz–20b	New Britain–Solomons–Vanuatu	163.7581	–10.7858	262.9	25.22	5
nvsz–21a	New Britain–Solomons–Vanuatu	164.9445	–10.4183	287.9	40.31	23.3
nvsz–21b	New Britain–Solomons–Vanuatu	164.8374	–10.7442	287.9	21.47	5
nvsz–22a	New Britain–Solomons–Vanuatu	166.0261	–11.1069	317.1	42.39	20.78
nvsz–22b	New Britain–Solomons–Vanuatu	165.7783	–11.3328	317.1	18.4	5
nvsz–23a	New Britain–Solomons–Vanuatu	166.5179	–12.2260	342.4	47.95	22.43
nvsz–23b	New Britain–Solomons–Vanuatu	166.2244	–12.3171	342.4	20.4	5
nvsz–24a	New Britain–Solomons–Vanuatu	166.7236	–13.1065	342.6	47.13	28.52
nvsz–24b	New Britain–Solomons–Vanuatu	166.4241	–13.1979	342.6	28.06	5
nvsz–25a	New Britain–Solomons–Vanuatu	166.8914	–14.0785	350.3	54.1	31.16
nvsz–25b	New Britain–Solomons–Vanuatu	166.6237	–14.1230	350.3	31.55	5
nvsz–26a	New Britain–Solomons–Vanuatu	166.9200	–15.1450	365.6	50.46	29.05
nvsz–26b	New Britain–Solomons–Vanuatu	166.6252	–15.1170	365.6	28.75	5
nvsz–27a	New Britain–Solomons–Vanuatu	167.0053	–15.6308	334.2	44.74	25.46
nvsz–27b	New Britain–Solomons–Vanuatu	166.7068	–15.7695	334.2	24.15	5
nvsz–28a	New Britain–Solomons–Vanuatu	167.4074	–16.3455	327.5	41.53	22.44

(continued on next page)

Table B8: (continued)

Segment	Description	Longitude (°E)	Latitude (°N)	Strike (°)	Dip (°)	Depth (km)
nvsz–28b	New Britain–Solomons–Vanuatu	167.1117	–16.5264	327.5	20.42	5
nvsz–29a	New Britain–Solomons–Vanuatu	167.9145	–17.2807	341.2	49.1	24.12
nvsz–29b	New Britain–Solomons–Vanuatu	167.6229	–17.3757	341.2	22.48	5
nvsz–30a	New Britain–Solomons–Vanuatu	168.2220	–18.2353	348.6	44.19	23.99
nvsz–30b	New Britain–Solomons–Vanuatu	167.8895	–18.2991	348.6	22.32	5
nvsz–31a	New Britain–Solomons–Vanuatu	168.5022	–19.0510	345.6	42.2	22.26
nvsz–31b	New Britain–Solomons–Vanuatu	168.1611	–19.1338	345.6	20.2	5
nvsz–32a	New Britain–Solomons–Vanuatu	168.8775	–19.6724	331.1	42.03	21.68
nvsz–32b	New Britain–Solomons–Vanuatu	168.5671	–19.8338	331.1	19.49	5
nvsz–33a	New Britain–Solomons–Vanuatu	169.3422	–20.4892	332.9	40.25	22.4
nvsz–33b	New Britain–Solomons–Vanuatu	169.0161	–20.6453	332.9	20.37	5
nvsz–34a	New Britain–Solomons–Vanuatu	169.8304	–21.2121	329.1	39	22.73
nvsz–34b	New Britain–Solomons–Vanuatu	169.5086	–21.3911	329.1	20.77	5
nvsz–35a	New Britain–Solomons–Vanuatu	170.3119	–21.6945	311.9	39	22.13
nvsz–35b	New Britain–Solomons–Vanuatu	170.0606	–21.9543	311.9	20.03	5
nvsz–36a	New Britain–Solomons–Vanuatu	170.9487	–22.1585	300.4	39.42	23.5
nvsz–36b	New Britain–Solomons–Vanuatu	170.7585	–22.4577	300.4	21.71	5
nvsz–37a	New Britain–Solomons–Vanuatu	171.6335	–22.3087	281.3	30	22.1
nvsz–37b	New Britain–Solomons–Vanuatu	171.5512	–22.6902	281.3	20	5

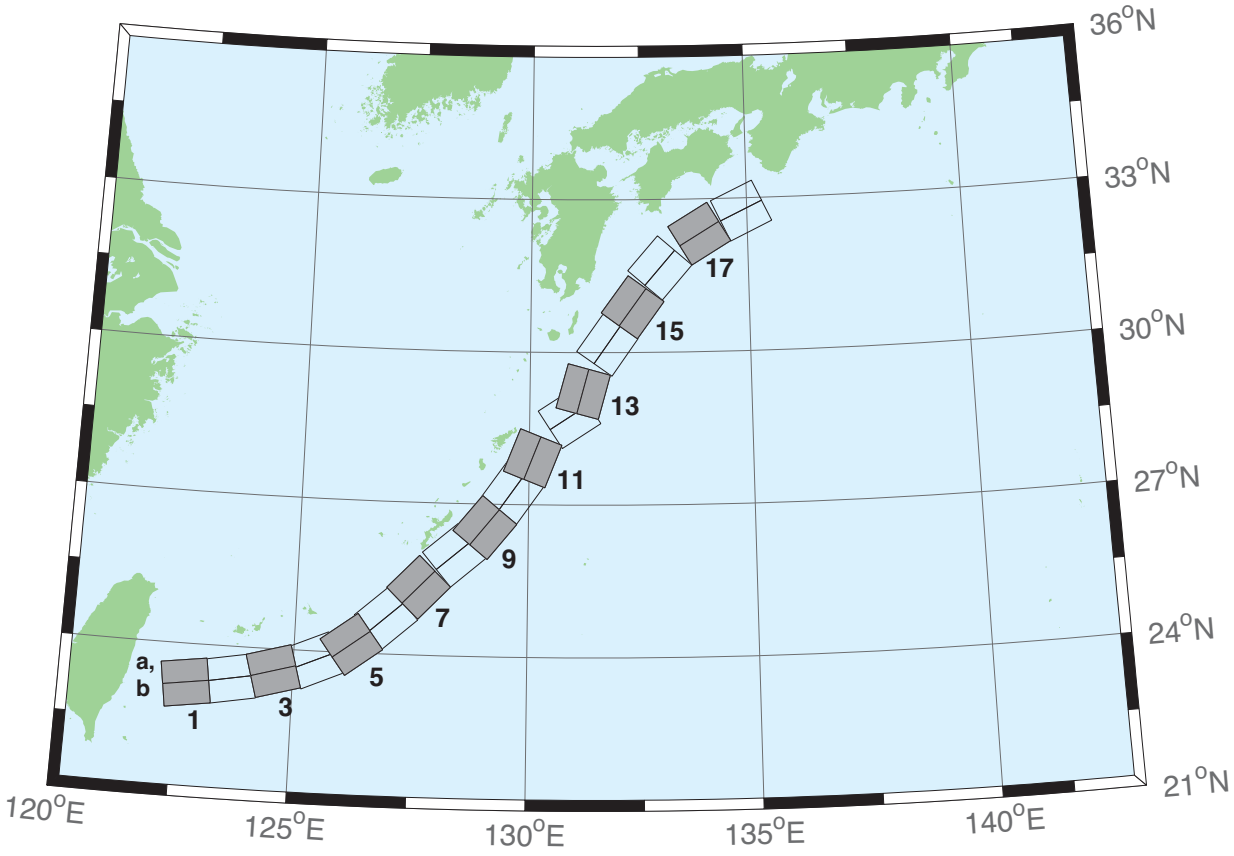

Figure B9: Ryukyu–Kyushu–Nankai Zone unit sources.

Table B9: Earthquake parameters for Ryukyu–Kyushu–Nankai Subduction Zone unit sources.

Segment	Description	Longitude (°E)	Latitude (°N)	Strike (°)	Dip (°)	Depth (km)
rnsz–1a	Ryukyu–Kyushu–Nankai	122.6672	23.6696	262	14	11.88
rnsz–1b	Ryukyu–Kyushu–Nankai	122.7332	23.2380	262	10	3.2
rnsz–2a	Ryukyu–Kyushu–Nankai	123.5939	23.7929	259.9	18.11	12.28
rnsz–2b	Ryukyu–Kyushu–Nankai	123.6751	23.3725	259.9	10	3.6
rnsz–3a	Ryukyu–Kyushu–Nankai	124.4604	23.9777	254.6	19.27	14.65
rnsz–3b	Ryukyu–Kyushu–Nankai	124.5830	23.5689	254.6	12.18	4.1
rnsz–4a	Ryukyu–Kyushu–Nankai	125.2720	24.2102	246.8	18	20.38
rnsz–4b	Ryukyu–Kyushu–Nankai	125.4563	23.8177	246.8	16	6.6
rnsz–5a	Ryukyu–Kyushu–Nankai	125.9465	24.5085	233.6	18	20.21
rnsz–5b	Ryukyu–Kyushu–Nankai	126.2241	24.1645	233.6	16	6.43
rnsz–6a	Ryukyu–Kyushu–Nankai	126.6349	25.0402	228.7	17.16	19.55
rnsz–6b	Ryukyu–Kyushu–Nankai	126.9465	24.7176	228.7	15.16	6.47
rnsz–7a	Ryukyu–Kyushu–Nankai	127.2867	25.6343	224	15.85	17.98
rnsz–7b	Ryukyu–Kyushu–Nankai	127.6303	25.3339	224	13.56	6.26
rnsz–8a	Ryukyu–Kyushu–Nankai	128.0725	26.3146	229.7	14.55	14.31
rnsz–8b	Ryukyu–Kyushu–Nankai	128.3854	25.9831	229.7	9.64	5.94
rnsz–9a	Ryukyu–Kyushu–Nankai	128.6642	26.8177	219.2	15.4	12.62
rnsz–9b	Ryukyu–Kyushu–Nankai	129.0391	26.5438	219.2	8	5.66
rnsz–10a	Ryukyu–Kyushu–Nankai	129.2286	27.4879	215.2	17	12.55
rnsz–10b	Ryukyu–Kyushu–Nankai	129.6233	27.2402	215.2	8.16	5.45
rnsz–11a	Ryukyu–Kyushu–Nankai	129.6169	28.0741	201.3	17	12.91
rnsz–11b	Ryukyu–Kyushu–Nankai	130.0698	27.9181	201.3	8.8	5.26
rnsz–12a	Ryukyu–Kyushu–Nankai	130.6175	29.0900	236.7	16.42	13.05
rnsz–12b	Ryukyu–Kyushu–Nankai	130.8873	28.7299	236.7	9.57	4.74
rnsz–13a	Ryukyu–Kyushu–Nankai	130.7223	29.3465	195.2	20.25	15.89
rnsz–13b	Ryukyu–Kyushu–Nankai	131.1884	29.2362	195.2	12.98	4.66
rnsz–14a	Ryukyu–Kyushu–Nankai	131.3467	30.3899	215.1	22.16	19.73
rnsz–14b	Ryukyu–Kyushu–Nankai	131.7402	30.1507	215.1	17.48	4.71
rnsz–15a	Ryukyu–Kyushu–Nankai	131.9149	31.1450	216	15.11	16.12
rnsz–15b	Ryukyu–Kyushu–Nankai	132.3235	30.8899	216	13.46	4.48
rnsz–16a	Ryukyu–Kyushu–Nankai	132.5628	31.9468	220.9	10.81	10.88
rnsz–16b	Ryukyu–Kyushu–Nankai	132.9546	31.6579	220.9	7.19	4.62
rnsz–17a	Ryukyu–Kyushu–Nankai	133.6125	32.6956	239	10.14	12.01
rnsz–17b	Ryukyu–Kyushu–Nankai	133.8823	32.3168	239	8.41	4.7
rnsz–18a	Ryukyu–Kyushu–Nankai	134.6416	33.1488	244.7	10.99	14.21
rnsz–18b	Ryukyu–Kyushu–Nankai	134.8656	32.7502	244.5	10.97	4.7

Glossary

Arrival Time The time when the first tsunami wave is observed at a particular location, typically given in local and/or universal time but also commonly noted in minutes or hours relative to time of earthquake.

Bathymetry The measurement of water depth of an undisturbed body of water.

Cascadia Subduction Zone Fault that extends from Cape Mendocino in Northern California northward to mid-Vancouver Island Canada. The fault marks the convergence boundary where the Juan de Fuca tectonic plate is being subducted under the margin of the North America plate.

Current Speed The scalar rate of water motion measured as distance/time.

Current Velocity Movement of water expressed as a vector quantity. Velocity is the distance of movement per time coupled with direction of motion.

Deep-ocean Assessment and Reporting of Tsunamis (DART®) Tsunami detection and transmission system that measures the pressure of an overlying column of water and detects the passage of a tsunami

Digital Elevation Model (DEM) A digital representation of bathymetry or topography based on regional survey data or satellite imagery. Data are arrays of regularly spaced elevations referenced to map projection of geographic coordinate system.

Epicenter The point on the surface of the earth that is directly above the focus of an earthquake.

Far-field Region outside of the source of a tsunami where no direct observations of the tsunami-generating event are evident, except for the tsunami waves themselves.

Focus The point beneath the surface of the earth where a rupture or energy release occurs due to a build up of stress or the movement of earth's tectonic plates relative to one another.

Inundation The horizontal inland extent of land that a tsunami penetrates, generally measured perpendicularly to a shoreline.

Marigram Tide gauge recording of wave level as a function of time at a particular location. The instrument used for recording is termed marigraph.

Moment Magnitude (MW) The magnitude of an earthquake on a logarithmic scale in terms of the energy released. Moment magnitude is based on the size and characteristics of a fault rupture as determined from long-period seismic waves.

Method of Splitting Tsunamis (MOST) A suite of numerical simulation codes used to provide estimates of the three processes of tsunami evolution: tsunami generation, propagation, and inundation.

Near-field Region of primary tsunami impact near the source of the tsunami. The near-field is defined as the region where non-tsunami effects of the tsunami-generating event have been observed, such as earth shaking from the earthquake, visible or measured ground deformation, or other direct (non-tsunami) evidences of the source of the tsunami wave.

Propagation database A basin-wide database of pre-computed water elevations and flow velocities at uniformly spaced grid points throughout the world Oceans. Values are computed from tsunamis generated by earthquakes with a fault rupture at any one of discrete 100 × 50 km unit sources along worldwide subduction zones.

Runup or Run-up Vertical difference between the elevation of tsunami inundation and the sea level at the time of a tsunami. Runup is the elevation of the highest point of land inundated by a tsunami as measured relative to a stated datum, such as mean sea level.

Short-term Inundation Forecasting for Tsunamis (SIFT) A tsunami forecast system that integrates tsunami observations in the deep-ocean with numerical models to provide an estimate of tsunami wave arrival, amplitude, at specific coastal locations while a tsunami propagates across an ocean basin.

Subduction zone A submarine region of the earth's crust at which two or more tectonic plates converge to cause one plate to sink under another, overriding plate. Subduction zones are regions of high seismic activity.

Synthetic event Hypothetical events based on computer simulations or theory of possible or even likely future scenarios.

Tidal wave Term frequently used incorrectly as a synonym for tsunami. A tsunami is unrelated to the predictable periodic rise and fall of sea level due to the gravitational attractions of the moon and sun: the tide.

Tide The predictable rise and fall of a body of water (ocean, sea, bay, etc.) due to the gravitational attractions of the moon and sun.

Tide Gauge An instrument for measuring the rise and fall of a column of water over time at a particular location.

Tele-tsunami or distant tsunami Most commonly, a tsunami originating from a source greater than 1000 km away from a particular location. In some contexts, a tele-tsunami is one that propagates through deep-ocean before reaching a particular location without regard to distance separation.

Travel time The time it takes for a tsunami to travel from the generating source to a particular location.

Tsunameter An oceanographic instrument used to detect and measure tsunamis in the deep-ocean. Tsunami measurements are typically transmitted acoustically to a surface buoy that in turn relays them in real-time to ground stations via satellite.

Tsunami A Japanese term that literally translates to "harbor wave." Tsunamis are a series of long period shallow water waves that are generated by the sudden displacement of water due to subsea disturbances such as earthquakes, submarine landslides, or volcanic eruptions. Less commonly, meteoric impact to the ocean or meteorological forcing can generate a tsunami.

Tsunami Hazard Assessment A systematic investigation of seismically active regions of the world oceans to determine their potential tsunami impact at a particular location. Numerical models are typically used to characterize tsunami generation, propagation, and inundation and to quantify the risk posed a particular community from tsunamis generated in each source region investigated.

Tsunami Magnitude A number that characterizes the strength of a tsunami based on the tsunami wave amplitudes. Several different tsunami magnitude determination methods have been proposed.

Tsunami Propagation The directional movement of a tsunami wave outward from the source of generation. The speed at which a tsunami propagates depends on the depth of the water column in which the wave is traveling. Tsunamis travel at a speed of 700 km/hr (450 mi/hr) over the average depth of 4000 m in the open deep Pacific Ocean.

Tsunami Source Abrupt deformation of the ocean surface that generates series of long gravity waves propagating outward from the source area. The deformation is typically produced by underwater earthquakes, landslide, volcano eruptions or other catastrophic geophysical processes.

Wave amplitude The maximum vertical rise or drop of a column of water as measured from wave crest (peak) or trough to a defined mean water level state.

Wave crest or peak The highest part of a wave or maximum rise above a defined mean water level state, such as mean lower low water.

Wave height The vertical difference between the highest part of a specific wave (crest) and it's corresponding lowest point (trough).

Wavelength The horizontal distance between two successive wave crests or troughs.

Wave period The length of time between the passage of two successive wave crests or troughs as measured at a fixed location.

Wave trough The lowest part of a wave or the maximum drop below a defined mean water level state, such as mean lower low water.

PMEL Tsunami Forecast Series Locations

Adak, AK
Apra Harbor, Guam — **Vol. 9**
Arecibo, PR
Arena Cove, CA
Atka, AK
Atlantic City, NJ
Bar Harbor, ME
Cape Hatteras, NC
Chignik, AK
Cordova, AK
Craig, AK
Crescent City, CA — **Vol. 2**
Daytona Beach, FL
Dutch Harbor, AK — **Vol. 10**
Elfin Cove, AK
Eureka, CA
Fajardo, PR
Florence, OR
Garibaldi, OR
Haleiwa, HI
Hilo, HI — **Vol. 1**
Homer, AK
Honolulu, HI
Jacksonville Beach, FL
Kahului, HI — **Vol. 7**
Kailua-Kona, HI
Kawaihae, HI
Keauhou, HI
Key West, FL
King Cove, AK
Kodiak, AK — **Vol. 4**
Lahaina, HI
La Push, WA
Los Angeles, CA — **Vol. 8**
Mayaguez, PR
Montauk, NY
Monterey, CA
Morehead City, NC
Myrtle Beach, SC
Nantucket, MA
Nawiliwili, HI
Neah Bay, WA
Newport, OR — **Vol. 5**
Nikolski, AK
Ocean City, MD
Pago Pago, American Samoa
Palm Beach, FL
Pearl Harbor, HI
Point Reyes, CA
Ponce, PR
Port Alexander, AK
Port Angeles, WA
Port Orford, OR
Port San Luis, CA
Port Townsend, WA
Portland, ME
Portsmouth, NH
San Diego, CA
San Francisco, CA — **Vol. 3**
San Juan, PR
Sand Island, Midway Islands
Sand Point, AK
Santa Barbara, CA
Santa Monica, CA
Savannah, GA
Seaside, OR — **Vol. 6**
Seward, AK
Shemya, AK
Sitka, AK
Toke Point, WA
U.S. Virgin Islands
Virginia Beach, VA
Wake Island, U.S. Territory
Westport, WA
Yakutat, AK

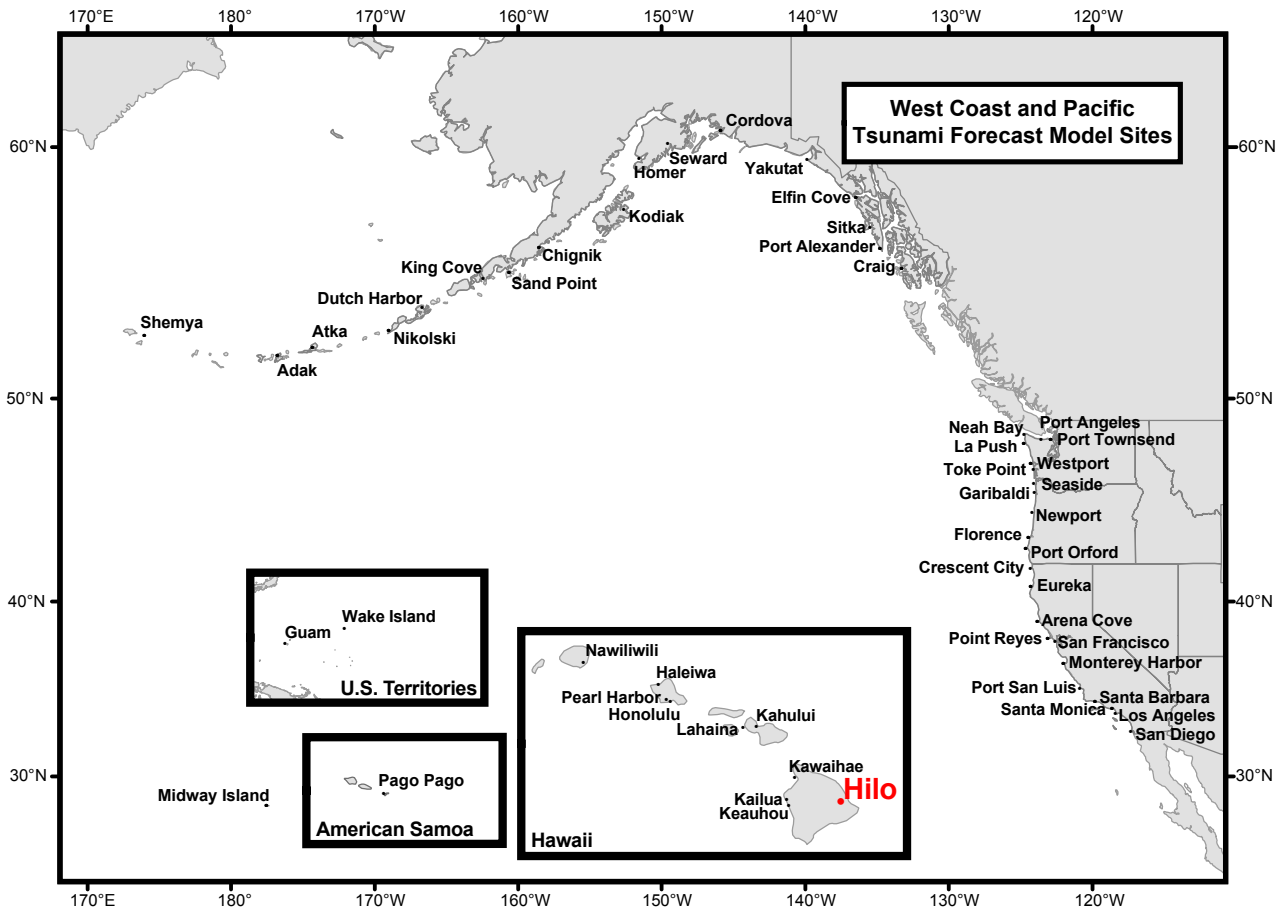
West Coast and Pacific
Tsunami Forecast Model Sites
170°E
180°
170°W
160°W
150°W
140°W
130°W
120°W
60°N
50°N
40°N
30°N
Cordova
Seward
Homer
Yakutat
Elfin Cove
Kodiak
Sitka
Port Alexander
Craig
Chignik
King Cove
Sand Point
Dutch Harbor
Shemya
Atka
Nikolski
Adak
Neah Bay
Port Angeles
La Push
Port Townsend
Toke Point
Westport
Seaside
Garibaldi
Newport
Florence
Port Orford
Crescent City
Eureka
Arena Cove
Point Reyes
San Francisco
Monterey Harbor
Port San Luis
Santa Barbara
Santa Monica
Los Angeles
San Diego
Guam
Wake Island
U.S. Territories
Nawiliwili
Haleiwa
Pearl Harbor
Honolulu
Kahului
Lahaina
Kawaihae
Hilo
Kailua
Keauhou
Hawaii
Midway Island
Pago Pago
American Samoa

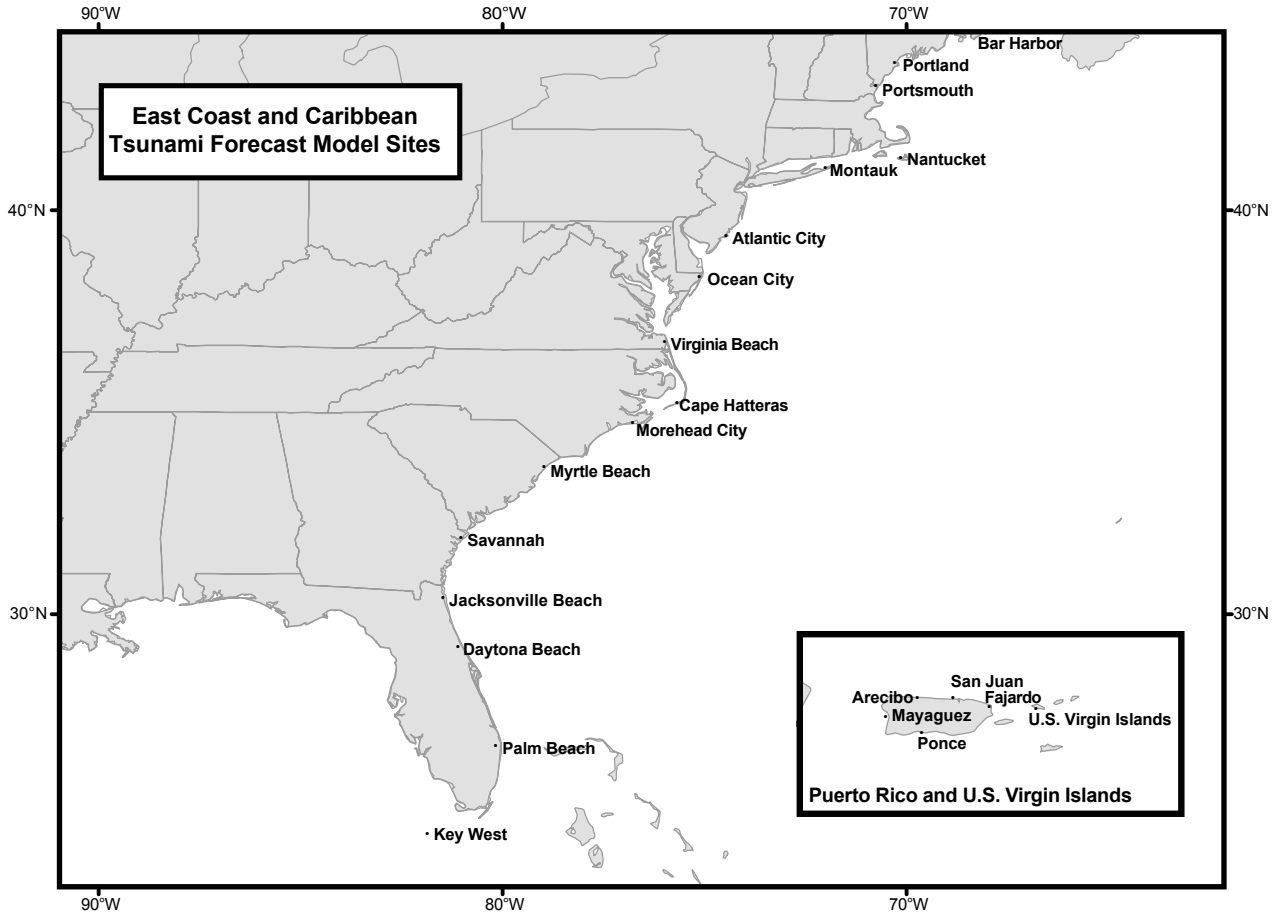
East Coast and Caribbean
Tsunami Forecast Model Sites
90°W
80°W
70°W
40°N
30°N
Bar Harbor
Portland
Portsmouth
Nantucket
Montauk
Atlantic City
Ocean City
Virginia Beach
Cape Hatteras
Morehead City
Myrtle Beach
Savannah
Jacksonville Beach
Daytona Beach
Palm Beach
Key West
San Juan
Arecibo
Fajardo
Mayaguez
U.S. Virgin Islands
Ponce
Puerto Rico and U.S. Virgin Islands